Technische Universität München

LEHRSTUHL FÜR HUMANBIOLOGIE

Sensitivity of enteric neurons to osmotic stimuli

Patrick Kollmann

Vollständiger Abdruck der von der Fakultät Wissenschaftszentrum Weihenstephan für Ernährung, Landnutzung und Umwelt der Technischen Universität München zur Erlangung des akademischen Grades eines

Doktors der Naturwissenschaften

genehmigten Dissertation

Vorsitzender:	Prof. Dr. Harald Luksch
Prüfer der Dissertation:	1. Prof. Dr. Michael Schemann
	2. Prof. Dr. Martin Klingenspor

Die Dissertation wurde am 21.07.2017 bei der Technischen Universität München eingereicht und durch die Fakultät Wissenschaftszentrum Weihenstephan für Ernährung, Landnutzung und Umwelt am 25.10.2017 angenommen.

“Problems that remain persistently insoluble should always be suspected as questions asked in the wrong way”

Alan Watts

für meine Eltern

FUNDING

This thesis was funded by German Research Foundation (Deutsche Forschungsgemeinschaft DFG) Graduiertenkolleg GRK 1482/3 – "Interface functions of the intestine between luminal factors and host signals.

TABLE OF CONTENTS

SUMMARY

Neurons of the enteric nervous system (ENS) are located inside the gut wall. This allows them to sense changes in their microenvironment. Amongst those changes are fluctuations in the concentration of osmotically active molecules during digestive and interdigestive periods. The hypothesis of this work was that enteric submucosal neurons, which are strategically located close to epithelial cells and blood vessels may sense and respond to shifts in osmolality. This study was aimed to investigate the osmosensitivity of submucosal neurons of the guinea pig.

To investigate neuronal activation after hypo- or hyperosmolar stimulation of freshly dissected guinea pig colonic preparations neuroimaging with a voltage sensitive dye was performed. In addition, the calcium imaging technique was used to investigate changes in intracellular calcium levels. Furthermore, volume changes of the neurons after the osmotic shifts were analysed. Stimulation of the neurons was achieved by exposing individual ganglia to hypo- or hyperosmolar stimuli ranging from 94 mOsm/kg to 494 mOsm/kg using a local perfusion system.

Hypo- and hyperosmolar stimuli resulted in action potential discharge in a subpopulation of enteric neurons. Noteworthy this activation took place with a delay of several seconds. Further application of a hypoosmolar solution also resulted in increase in intracellular calcium levels. Changes in cell volume were evident after hypoosmolar stimulation while they were not present after application of a hyperosmolar stimulus.

One of the most important channels in in regards to osmosensitivity is the transient receptor potential vanilloid 4 channel (TRPV4). Due to its expression in the peripheral nervous system it was the most promising candidate for being the responsible molecular structure for osmosensitivity in the ENS. Pharmacological experiments showed that the specific and potent TRPV4 agonist GSK1016790A activated enteric neurons. Intracellular calcium increase after osmotic shifts could be blocked by the TRP channel blocker ruthenium red and spike discharge was efficiently blocked by the specific TRPV4 blocker HC-067047. Furthermore, the presence of TRPV4 in the submucosal plexus was confirmed using qRT-PCR. The chemical coding of osmosensitive neurons was investigated using immunohistochemistry.

The conclusion of this study therefore is that osmosensitive neurons exist in the submucosal plexus (SMP). Furthermore, the majority of osmosensitive neurons are cholinergic. Pharmacological experiments strongly indicate the involvement of TRPV4 in sensing hypoosmolar stimuli.

ZUSAMMENFASSUNG

Neurone des enterischen Nervensystems (ENS) welches sich in der Wand des Gastrointestinaltraktes befindet besitzen die Fähigkeit kleinste Veränderungen im extrazellulären Milieu ihrer nahen Umgebung wahrzunehmen. Zu diesen Veränderungen zählen unter anderem auch Schwankungen in der Anzahl osmotisch wirksamer Teilchen, bedingt durch Nahrungs- und Flüssigkeitsaufnahme. Die Hypothese welche dieser Arbeit zu Grunde liegt ist, dass Neurone des submukosalen Plexus, welche in räumlicher Nähe sowohl zu Epithelzellen als auch zu Blutgefäßen liegen, in der Lage sind Veränderungen der Osmolalität zu detektieren und entsprechend darauf zu reagieren. Hierzu wurde die Osmosensitivität enterischer Neurone des submukosalen Plexus des Meerschweinchens untersucht.

Um neuronale Aktivierung nach Stimulation mit hypo- oder hyperosmolarer Lösung nachzuweisen wurden Bildgebende Verfahren mit spannungssensitiven Farbstoffen an Lebendpräparaten des Meerschweinchen Kolons angewendet. Des Weiteren fanden Kalzium sensitive Farbstoffe Anwendung, mit deren Hilfe Veränderungen der intrazellulären Kalziumkonzentration als Folge osmotischer Stimulation untersucht wurden. Darüber hinaus wurde die Veränderung des Zellvolumens nach osmotischer Stimulation analysiert. Die osmotischen Stimuli wurden mithilfe eines Mikro-perfusionssytems auf individuelle Ganglien appliziert wobei die Osmolalität der applizierten Lösungen zwischen 94 mOsm/kg und 494 mOsm/kg lag.

Hypo- und hyperosmolare Stimuli führten zu elektrischen Entladungen in einer Subpopulation enterischer Neurone, welche mit einer Verzögerung von mehreren Sekunden nach dem Stimulus auftrat. Die Perfusion mit einer hypoosmolaren Lösung führte darüber hinaus zu einem Anstieg der intrazellulären Kalziumkonzentration. Veränderungen des Zellvolumens konnten ebenfalls nach hypoosmolarer, nicht aber nach hyperosmolarer Stimulation beobachtet werden.

Einer der wichtigsten Ionenkanäle in Bezug auf Osmosensitivität ist der transient receptor potential vanilloid 4 Kanal (TRPV4). Aufgrund seiner Bedeutung für die Osmosensitivität in anderen Bereichen des peripheren Nervensystems ist er ein vielversprechender Kandidat für die osmosensitive molekulare Struktur im ENS. Pharmakologische Versuche zeigten, dass der TRPV4 Agonist GSK1016790A in enterischen Neuronen zur Entladung von Aktionspotentialen, sowie zu einer Kalziumantwort führt. Des Weiteren zeigten Experimente mit dem TRPV4 Inhibitor HC-067047, dass dieser die Antwort auf osmotische Stimuli signifikant reduzierte. Darüber hinaus konnte TRPV4 mit Hilfe von qRT-PCR auf mRNA Ebene im submukosalen Plexus des Meerschweinchens nachgewiesen werden. Zur neurochemischen Charakterisierung der osmosensitiven Neurone wurde Immunfluoreszenz verwendet.

Die Schlussfolgerung der vorliegenden Studie ist, dass osmosensitive Neurone im SMP existieren und daher das ENS in der Lage ist Änderungen der Osmolalität zu detektieren und entsprechend darauf zu reagieren. Die Mehrheit der osmosensitiven Neurone ist dem cholinergen Typ zuzuordnen. Die vorliegenden Ergebnisse deuten eine Beteiligung von TRPV4 an diesem Prozess an.

ABBREVIATIONS

5',6' – EET	5',6'- epoxyeicosatrienoic
$[Ca^{2+}]_i$	Intracellular calcium concentration
ADH	Antidiuretic hormone / vasopressin
ANNA-1	Anti neuronal nuclear autoantibody
Anti-Hu	autoantibody against RNA binding protein Hu (see ANNA-1)
AQP1	Aquaporine 1
AQP2	Aquaporine 2
AQP3	Aquaporine 3
AQP4	Aquaporine 4
ATP	Adenosine triphosphate
BLAST	Basic local alignment search tool
cDNA	complementary deoxyribonucleic acid
ChAT	Choline acetyltransferase
CHO	Chinese hamster ovary
CNS	Central nervous system
Di-8-ANEPPS	(1-(3-sulfanato-propyl-4-[β-[2-(di-n-octylamino)-6-naphthyl]vinyl]pyridinium betaine
DMSO	Dimethylsulfoxid
DRG	Dorsal root ganglion
EAA	Excitatory amino acid
ECF	Extracellular fluid
ENS	Enteric nervous system
EPSP	Excitatory postsynaptic potential
ER	Endoplasmatic reticulum
GPCR	G-protein coupled receptor
HEPES	4-(2-hydroxyethyl)-1-piperazineethanesulfonic acid
IHC	Immunohistochemistry
IP_3	inositol-(1,4,5)-trisphosphate
IPAN	Intrinsic primary afferent neuron
MEN	Mechanosensitive enteric neurons
MNC	Magnocellular neurosecretory cell
MP	Myenteric plexus
mRNA	messenger RNA
MSORT	Multi-site optical recording technique
NMDA	N-Methyl-D-aspartatic acid
OSM9	Osmotic avoidance abnormal family member 9
OTRPC4	OSM9-like transient receptor potential channel member 4
OVLT	Organum vasculosum lamina terminalis
PBS	Phosphate buffered saline
PACAP	Pituitary adenylyl cyclase activating peptide
PCR	Polymerase chain reaction
PLA_2	Phospholipase A_2
PVN	Paraventricular nucleus
qPCR	Quantitative real-time PCR
RAMEN	Rapidly adapting mechanosensitive enteric neurons
RIN	RNA integrity number
RLI	Resting light intensity
RNA	Ribonucleic acid
ROS	Reactive oxygen species
RVD	Regulatory volume decrease

RVI	Regulatory volume increase
SAC	Stretch activated channel
SAMEN	Slowly adapting mechanosensitive enteric neurons
SIC	Stretch inhibited channel
SMP	Submucosal plexus
SON	Supraoptic nucleus
TRP	Transient receptor potential
TRPA	Transient receptor potential Ankyrin
TRPC	Transient receptor potential canonical
TRPM	Transient receptor potential melastin
TRPML	Transient receptor potential mucolipin
TRPP	Transient receptor potential polycistin
TRPV	Transient receptor potential vanilloid
TTX	Tetrodotoxin
USAMEN	Ultra-slowly adapting mechanosensitive enteric neurons
VIP	Vasoactive intestinal peptide
VR-OAC	Vanilloid receptor-related osmotically activated channel
VSD	Voltage sensitive dye

1. INTRODUCTION

1.1 The systemic and cellular osmotic homoeostasis

1.1.1 Mechanism of water flow through the cell membrane

The main function of the lipid bilayer that forms the cell membrane is separating the cytoplasm from the extracellular fluid. One of the main characteristics of the cell membrane is its semi permeability. Small hydrophobic molecules (e.g. steroids, fatty acids), gases and small uncharged particles can move freely between the cytoplasm and the extracellular fluid, while macromolecules and ions cannot pass the membrane directly (for detailed description see: Boujard et al. 2014). Water, which is undoubtedly the most important solvent for all organisms, can only diffuse through lipid bilayers to a very low extent. Nevertheless, for a very long period of time it was thought that no specialized water-channels are needed to facilitate water transport through the cell membrane. This widely held misconception was disposed not long ago when the group of Peter Agre described the first specialized water channel, Aquaporine1 (AQP1) (Borgnia et al., 1999; Denker et al., 1988). For his discovery Agre was honoured in 2003 with the Nobel Prize for chemistry (Nobelprize.org, 2017). Since this finding at least nine more aquaporines have been discovered. Aquaporines are not equally distributed throughout the different tissues of the organism. They can be found for example in epithelial cells, microvascular endothelial cells, the epidermis, immune cells, adipocytes and skeletal muscle (Papadopoulos and Verkman, 2013). In particular, the kidney alone harbours seven different types of aquaporines (Nielsen et al., 2002). While it may seem only logical that the kidney is equipped with molecules specialized in water transport, also tissues with a less obvious relationship to water transport do express aquaporines. One of those tissues is the nervous system. Aquaporines can be found both in the central and in the peripheral nervous system. Although central nervous expression of aquaporines is better understood than their peripheral expression, this will not be discussed further within the present work, as this study was entirely focused on the enteric nervous system (ENS). In the ENS glia cells express AQP1 while AQP4 is present in glia cells as well as in neurons of the submucosal and the myenteric plexus (Figure 1) (Nagahama et al., 2006; Papadopoulos and Verkman, 2013; Thi et al., 2008).

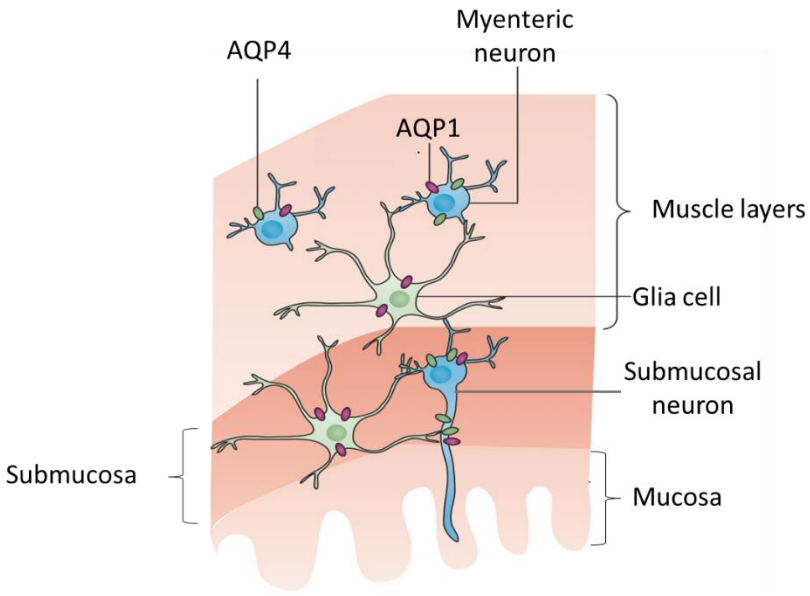

Figure 1: distribution of aquaporines in the ENS. AQP1 and 4 are both present in the ENS. While AQP4 is only expressed in enteric neurons, AQP1 is expressed in enteric neurons as well as enteric glia cells. (Modified from Papadopoulos and Verkman 2013)

1.1.2 Consequence of the water flow through the cell membrane

The word osmosis refers to movement of fluid across a membrane in response to differing concentrations of solutes on the two sides of the membrane (Sperelakis 2012). One osmole is defined as one mole of osmotic active particles. Osmotic active particles are defined as particles that are soluble in a certain solvent (in biological terms mostly water) and cannot pass a certain membrane while the solvent can (Mortimer and Müller, 2003). According to the International Union of Pure and Applied Chemistry (IUPAC) osmolality or the osmotic concentration is defined as the product of the osmolality and the mass density of water and has the unit Osm/L (IUPAC compedium 2009) while osmolality is defined as the number of osmoles per kg of solvent. The osmotic concentration is the driving force of the water flow across the membrane that is facilitated by the channels described above. The osmotic pressure Δπ depends on the effective concentration difference across the cell membrane (Δc) and the osmotic coefficient (Φ), which describes the permeability of the membrane for a certain substance under certain conditions. It therefore is described for each solute *i* by

$$\Delta\pi = RT \sum \phi_i \Delta c_i$$

where *R* and *T* are the gas constant and the absolute temperature. This equation is basically an extension of van´t Hoff's law, taking into account the non-ideal behaviour of solutions, by including the osmotic coefficient. When more than one solute is present in the solution, interactions between the

solutes can appear which make the osmotic pressure described by the equation above, rather an approximation than an exact calculation. The osmotic pressure is defined as the hydrostatic pressure necessary to stop the osmotic flow across a barrier. Therefore, osmotic pressure can only be measured at the equilibrium, when the pressure driven flow balances the osmotic driven flow. By this definition fluid movement always occurs from the compartment of lower osmotic pressure to the one with higher osmotic pressure (Sperelakis 2012). Amount of water moving across the cell membrane (J_v) in a certain time period is described by

$$J_v = L_p\,(\Delta\pi - \Delta p)$$

depending on the difference between osmotic pressure ($\Delta\pi$) and hydrostatic pressure (Δp) and on ΔL_p, which is the conductivity of the cell membrane for water. This conductivity is highly dependent on the presence of aquaporines (Lang et al., 1998a). The lowering of extracellular osmolality therefore, leads to an inflow of water into the cytoplasm and in consequence to swelling of the cell. On the other hand, an increase in extracellular osmolality leads to an enhanced outflow of water and consequently, to cell shrinkage. These processes continue until the hydrostatic pressure and the osmotic pressure are equal and J_v becomes zero. However excessive changes in cell volume interfere with integrity of cell membrane and cytoskeletal architecture. In addition to that, even small changes in intracellular water content have a profound influence on protein function and cellular performance by disturbing the complex intracellular communication network through dilution of messenger molecules (Lang, 2007; Pasantes-Morales et al., 2006). Not only on a cellular, but also on a systemic level, changes in cell volume can have severe consequences for organ function. Cell volume changes in particular have dramatic consequences in the brain where the rigid skull limits its possibilities to expand. Expansion of brain tissue therefore leads to a rise in intracranial pressure, which often results in ischemia, infarct, excitotoxicity and neuronal death (Pasantes-Morales et al., 2006).

The physiological set points of plasma osmolality in mammals cluster around the value of 300 mOsm/kg with physiological fluctuations of 1-3% (Baylis, 1983; Bourque, 2008). Although in health osmolality is tightly controlled by sophisticated homeostatic mechanisms, changes in plasma osmolality can occur within a certain range (Gill et al., 1985). For example, 40 minutes of exercise under warm conditions or 24 h of water deprivation causes plasma osmolality to rise by more than 10 mOsm/kg in healthy humans. On the other hand drinking of 850 ml of water lowers the plasma osmolality of a dehydrated individual by approximately 6 mOsm/kg within 30 minutes (Bourque, 2008). Further a decrease in extracellular osmolality is an accessory syndrome in hyponatremia, which can result from a number of pathological conditions (e.g. congestive heart failure, nephrotic syndrome or hepatic cirrhosis) (Fisher et al., 2008).

1.1.3 Mechanisms of cell volume regulation

To avoid the consequences of extracellular plasma changes described above, cells are equipped with a whole number of mechanisms for cell volume regulation. The processes by which swollen or shrunken cells return to a normal volume are called regulatory volume decrease (RVD) and regulatory volume increase (RVI) respectively (McManus et al., 1995). RVD is achieved by excretion of organic and inorganic osmolytes from the cytoplasm together with osmotically obliged water (Pasantes-Morales et al., 2006).

Inorganic ions: the main intracellular electrolytes that contribute to cellular volume regulation are K^+ and Cl^-. In response to swelling most animal cells activate K^+ and Cl^- channels (McManus et al., 1995). The activation of K^+ channels is only effective for volume regulation if the anion channels are operating in parallel. Otherwise the cell would simply hyperpolarize up to the K^+ equilibrium potential without significant net loss of ions (Lang et al., 1998b). Cell volume regulatory ion channels include the voltage gated K^+ channels of the shaker-related subfamily member 3 and 5 (Kv1.3, Kv1.5), member 1 of the E family (KCNE1), member one of the subfamily Q (KCNQ1) as well as the anion channels chloride channel protein 2 and 3 (ClC-2 and ClC-3) (Lang, 2007). In addition to that the K^+/Cl^- co-transporter is an electroneutral system that contributes to RVD in red blood cells and some types of epithelial cells with a high intracellular Cl^- content (Mongin and Orlov, 2001).

RVI is achieved through the uptake of both KCl and NaCl. The intracellular concentration of these salts is increased through activation of Na^+/H^+ and Cl^-/HCO_3^- exchangers and the $Na^+/K^+/2Cl^-$ cotransporter. Volume regulation via electrolytes is a process that is initiated within seconds after a perturbation in cell volume. Such a fast response is possible because the channels and transporters which mediate electrolyte transport reside already in the plasma membrane or are stored in submembrane cytoplasmatic vesicles (McManus et al., 1995).

Organic osmolytes: in contrast to electrolytes organic osmolytes are so called “compatible” or “nonperturbing” solutes. This implies that cells can accumulate high concentrations of them or withstand large shifts in their concentration without having to face harmful side effects (Yancey, 2004). In contrast, perturbing solutes, such as electrolytes, can interfere with membrane potential or disrupt metabolic processes when they are present at high concentrations. Organic osmolytes of animal cells can be grouped into three distinct classes: polyols (e.g., sorbitol and myo-inositol), amino acids and their derivatives (e.g., taurine, alanine, and proline) and methylamines (e.g., betaine, glycerylphosphorylcholine) (McManus et al., 1995).

In response to cell swelling organic osmolytes are degraded or released from the cytoplasm (Kimelberg et al., 1990). The release of organic osmolytes is mediated by the same channels that are also

responsible for volume dependent Cl^- release from the cytoplasm (Strange and Jackson, 1995). In a second, slower step mechanisms controlling the synthesis and the uptake of organic osmolytes are down- regulated (McManus et al., 1995).

RVI by organic osmolytes is achieved by cellular uptake and generation of organic osmolytes (Friedrich et al., 2006). The disadvantage of organic osmolytes, despite their high metabolic cost, is their delayed effect on cell volume compared to ions (McManus et al., 1995). For instance, the formation of sorbitol from glucose is catalysed by aldose reductase, which is expressed following osmotic cell shrinkage. Therefore, an appropriate increase of sorbitol concentration in the cytoplasm requires several hours (Lang, 2007). In contrast to sorbitol the organic osmolytes myoinositol, betaine and taurine are taken up by specific Na^+ coupled transporters which in parallel to organic osmolytes also mediate the uptake of NaCl (Friedrich et al., 2006). Again, expression of these transporters first has to be upregulated and full adaptation requires hours to days (Lang, 2007).

The response of neuronal tissues to changes in extracellular osmolality is of special interest. Firstly, because reductions in intracellular ion concentration may have a direct impact on neural excitability by inducing changes to the membrane potential. Secondly, because several organic osmolytes are neuroactive (e.g. taurine) (Fisher et al., 2008). Organic osmolytes are not only released by neurons themselves but also by glia cells, which make the major contribution to volume regulation in the CNS *in vivo* (Kimelberg, 1995; Pasantes-Morales et al., 1990).

1.1.4 Mechanisms of systemic osmoregulation

Despite substantially changing environmental conditions, animal cells experience a relatively consistent environment (Randall, 1997). To keep fluctuations of osmolality of the extracellular fluid (ECF) in the narrow range described above, systemic regulatory mechanisms are necessary. In mammals systemic fluid homeostasis is achieved by behavioural regulation of water intake and control of renal water excretion.

The most important hormone in the regulation of diuresis is vasopressin or antidiuretic hormone (ADH). In the kidney ADH leads to increased water reabsorption in the loop of Henle, which is facilitated by increased expression and insertion of aquaporine 2 water channels (AQP2) (Nielsen et al., 2002). ADH is synthesized by magnocellular neurosecretory cells (MNCs) of the supraoptic (SON) and paraventricular nuclei. The axon terminals of those neurons lie in the posterior part of the pituitary gland and release ADH into the bloodstream (Silverman and Zimmerman, 1983). The rate of action-potential discharge by MNCs varies as a positive function of the ECF osmolality. Although MNCs are intrinsically osmosensitive (Brimble and Dyball, 1977), they are not the primary sensor for osmotic shifts in the central nervous system (CNS). This sensor is located in the organum vasculosum lamina

terminalis (OVLT). Cells of the OVLT project to the MNCs and respond to an increase in extracellular osmolality with an increase in action potential frequency (Ciura and Bourque, 2006). OVLT neurons also send processes to thalamic areas where signals are further processed and relayed to brain areas where sensation of thirst takes place and behavioural responses are coordinated (Bourque, 2008).

Nevertheless, sensors that influence systemic osmoregulation are not only found in the CNS. Peripheral osmoreceptors have been described in the oropharyngeal cavity (Kuramochi and Kobayashi, 2000), the splanchnic nerves (Choi-Kwon and Baertschi, 1991), the hepatic portal vein (Baertschi and Vallet, 1981), the liver (Adachi, 1984) and the gastrointestinal tract (Baertschi and Pence, 1995; Carlson et al., 1997). A potential function of peripheral osmoreceptors could be the detection of the osmotic strength of ingested materials and thus the induction anticipatory responses that might buffer the potential impact of food related shifts in osmolality (Bourque, 2008).

1.1.5 The molecular basis of osmotransduction

Although the existence of central and peripheral osmoreceptors in mammals has been acknowledged for many years, their molecular identity had been an enigma until October 2000 when two groups, one around Rainer Strotmann (Strotmann et al., 2000), and the other around Wolfgang Liedtke (Liedtke et al., 2000), identified an osmosensitive cation channel that they called "OSM9-like transient receptor potential channel member 4" (OTRPC4) or Vanilloid receptor-related osmotically activated channel (VR-OAC) respectively. The channel, later named TRPV4, had been identified due to structural similarities to "Osmotic avoidance abnormal family member 9" (OSM9), the osmosensitive channel of *C. elegans* (Colbert et al., 1997). Later the relevance of TRPV4 for osmoregulation was further confirmed by showing that TRPV4$^{-/-}$ mice express impaired response to hyper- as well to hypoosmolar stimuli (Liedtke and Friedman, 2003). This channel has been shown to be an important peripheral osmoreceptor, detecting hypoosmolar stimuli in hepatic blood vessels (Lechner et al., 2011).

While TRPV4 might have been the first osmosensitive channel investigated, it certainly is not the only one. Within the TRPV family alone two additional members appear to have osmosensitive properties (Liedtke, 2006). One is a capsaicin insensitive N-terminal splice variant of TRPV1, which has been shown to be the responsible osmotransducer in SON and PVN MNCs in mice (Sharif Naeini et al., 2006), as well as in the primary osmosensory neurons in the OVLT (Ciura and Bourque, 2006). The other one, TRPV2, is involved in the regulation of vascular tone by functioning as a mechano-transducer in aortic myocytes and in addition exhibits osmosensitive properties (Muraki et al., 2003). The only mammalian member of the TRPA family, TRPA1 is primarily activated by noxious cold and different chemical stimuli (e.g. isothiocyanates and allicin) (Bandell et al., 2004). It has been described in vagal, splanchnic and pelvic visceral afferents. In addition to its chemosensory properties it also expresses mechanosensory and probably osmosensory properties (Brierley et al., 2009). Mechanosensitive properties of TRPA1

have been described in mouse DRG (Vilceanu and Stucky, 2010). Although it is expressed in peripheral sensory neurons (Brierley et al., 2009) evidence for its expression in submucosal neurons of the ENS is lacking (Boesmans et al., 2011; Holzer, 2011). Another TRP channel whose mechano- and osmosensitive properties are well investigated is TRPV1. This channel plays a major role in sensing hyperosmolality in the CNS (Zaelzer et al., 2015). One of the members of the TRP family, which is expressed in neurons of the SMP as well as of the MP is TRPC6 (Liu et al., 2008). Hypoosmolar stimulation as well as pressure induced cell membrane stretch led to a TRPC6 mediated increase in $[Ca^{2+}]_{in}$ (Gomis et al., 2008). This marks TRPC6 as one candidate in the search for an osmosensitive structure in the ENS. Cultured cells overexpressing TRPM3, which has been identified in the kidney and in the brain, show an intracellular Ca^{2+} increase in response to a decrease in extracellular osmolality (Grimm et al., 2003). Nevertheless, the most important member of the TRP family in terms of osmo- and mechanosensitivity is TRPV4. Its expression in sensory afferents in combination with its osmosensitive properties make it the most promising candidate for the osmosensitive structure in the ENS (Alessandri-Haber et al., 2005; Lechner et al., 2011; Liedtke, 2006).

Despite the knowledge of the existence and relevance of these channels, knowledge about their activation mechanism is rather incomplete. There are several possibilities how changes in osmolality could be transduced into an increased or decreased channel opening probability. The first one is dilution or concentration of a certain, still unknown intracellular solute. Another one would be the change in intracellular ionic strength, which has a direct effect on the membrane potential. The third one is a direct mechanical effect that shrinking or swelling of the cell membrane could have on ion channels (Bourque, 2008). As a matter of fact, osmosensitivity is closely linked to mechanosensitivity. Indeed, a wide overlap between osmosensitive and mechanosensitive channels exists (Gomis et al., 2008; Liedtke, 2007; Prager-Khoutorsky and Bourque, 2015). This connection is not very surprising concerning the fact that changes in osmolality are transduced into membrane stretch or shrinkage. In 1993 Oliet and Bourque showed that a negative pressure, applied to the inside of a cell in a patch-clamp experiment, had the same effect on the action potential frequency as a hyperosmolar stimulation of the cell with an equally high osmotic pressure. The other way round the effect of a hypoosmolar stimulation could be reversed by applying a negative hydrostatic pressure to the inside of the cell (Oliet and Bourque, 1993). Three years later the same group provided more evidence for the connection between osmosensitivity and mechanosensitivity by showing that Gadolinium (Gd^{3+}), a blocker of stretch sensitive ion channels, blocks the response of MNCs to hypertonic stimulation (Oliet and Bourque, 1996). Responses, that are evoked by swelling or shrinking of a cell, occur without simultaneous changes in intracellular ionic strength or change in the concentration of intracellular solutes, suggesting that osmotransduction in the examined cells is indeed a mechanical process

(Bourque, 2008). In addition the importance of f-actin for the activation of TRPV1 under hyperosmolar conditions has been shown, also linking its activation to mechanical events (Zhang et al., 2007).

Because TRPV1 is inhibited by cell stretch and activated by cell shrinking, it is a so-called stretch inhibited channel (SIC). TRPV4 is activated by the opposite stimulus quality and is therefore a so-called stretch activated channel (SAC). The activation of TRPV4 by hypoosmolar stimuli is dependent on the activation of cytosolic phospholipase A_2 (PLA_2) (Vriens et al., 2004), an enzyme that catalyses the hydrolysis of phospholipids and thereby synthesizes arachidonic acid (Pedersen et al., 2000). Arachidonic acid is subsequently metabolised to 5',6'- epoxyeicosatrienoic acid (5',6' – EET) by cytochrome P450 which then activates TRPV4 (Watanabe et al., 2003).

1.1.6 Hypothesis: existence of a local osmoregulatory pathway in the gastrointestinal tract

All the osmosensors in different organs mentioned above have one common property: via vagal afferents (Adachi, 1984) or spinal pathways (Vallet and Baertschi, 1982) they all project to the CNS in the SON and the PVN where the effector neurons that control the release of ADH are located. This route of action, which includes the humoral pathway, leads to an inevitable delay between detected osmotic shift and homeostatic response (Bourque, 2008). Thus, the existence of local regulatory mechanisms in distinct organs would be reasonable for speeding up local responses to osmotic shifts. The gastrointestinal tract is the system that seems to be predestined to harbour such an intrinsic regulatory mechanism. First of all, the gut is the primary site where osmotic perturbations related to nutrient and water ingestion take place. Secondly, the gut is equipped with all components needed for an intrinsic reflex pathway: sensors, an integrating centre (the ENS), and effectors, which are the smooth muscles of the gut wall and the secretory glands.

For quite some time it is known that changes in the intraluminal osmolality after food-intake are able to change the gastrointestinal motility, independent from the caloric load of the meal (Keinke et al., 1984). In 1926 Apperly wrote that "the stomach remains its content until suitable osmotic pressure roughly isotonic with plasma is reached" (Apperly, 1926). In 1951 another group confirmed parts of this hypothesis by testing the effects of different osmotic loads on gastric emptying and secretion. They found that a high osmotic load delayed gastric emptying and reduced secretion which lead them to the assumption of a presumed osmo-receptor that is activated by fluid withdrawal through a semi permeable membrane (Hunt et al., 1951). More evidence that osmolality of the intestinal content may be linked to changes in motility patterns came from a group at the University of Hohenheim in 1986, when they found that the increased osmolality of a non-caloric mannitol meal altered the jejunal motor activity in dogs (Schemann and Ehrlein, 1986). In 1994 another group found that the changes in jejunal motility patterns after intraluminal infusion of a hyperosmolar solution were dependent on local

osmoreceptors control (Lin et al., 1994). These findings were confirmed and refined when another group of researchers found that high osmotic loads inhibit small intestinal motility independent from their caloric load (Seidl et al., 2013). Surprisingly all of the studies mentioned above only investigated the effects of hyperosmolar solutions infused into the gut lumen while neglecting hypoosmolar conditions to the largest extent.

The ENS is the structure responsible for the control of the gastrointestinal motility. Nevertheless, the question of what role the ENS plays in the physiological responses mentioned above still remains unresolved. The same applies to the question of whether enteric neurons are osmosensitive.

1.2 The enteric nervous system

1.2.1 The discovery of the enteric nervous system

The gastrointestinal tract is the only organ that contains an intrinsic nervous system able to mediate reflexes in the complete absence of input from the CNS (Bayliss and Starling, 1899; Trendelenburg, 1917; for a detailed review see Blackshaw et al., 2007). This intrinsic nervous system is called the enteric nervous system (ENS). One may wonder what caused evolution to create a structure as sophisticated as the ENS and not concentrate all the neuronal capacity in the CNS. As Michael Gershon suggested in his book "The Second Brain" (Gershon, 1999) the most likely answer might be that our progenitors simply could spend more brain volume on higher cognitive tasks, with their guts working on their own. Stunningly, structures similar to the ENS can be found throughout the animal kingdom, for example in insects (Ganfornina et al., 1996), molluscs (Campbell and Burnstock, 1968) and even in the marine polyp *hydra* (Shimizu et al., 2004).

The first anatomical description of the ENS came in 1857 from the German scientist Georg Meissner, who found a neuronal structure just beneath the mucosa of the gut, which was later called the submucosal plexus (SMP) (Meissner, 1857). Only a few years later, Leopold Auerbach described a second neuronal plexus within the gut wall, lying in between the circular and the longitudinal muscle layers (Auerbach, 1862). This structure became later known as the myenteric plexus (MP). However, these were just anatomical descriptions without any functional insights. True founders of neurogastroenterology, the science that studies the ENS, can be identified in Ernest Henry Starling and William Maddock Bayliss. In 1899 they published their work about what they called "The law of the intestine" (Bayliss and Starling, 1899). They found that an increase in internal pressure of the intestine resulted in a muscular movement propelling the luminal content in an anal direction (Bayliss and Starling, 1899). They already proposed that this action had to be nerve mediated. By severing the nerves that connected the investigated loop of gut they deprived it from all central nervous inputs. Surprisingly the "law of the intestine" still applied for this denervated piece of gut. In 1917 Ulrich Trendelenburg went one step further. He investigated isolated pieces of guinea pig gut in an organ bath and still was able to see the peristaltic reflex. With this experiment he provided evidence that the whole reflex circuit is contained inside every segment of intestine: detection of distention, integration of the information and activation of the effectors (Trendelenburg, 1917). The ability of the ENS to work as an integrative centre, that collects information, processes it and forwards it to the effectors, is what makes the gut such a unique organ.

1.2.2 The anatomy of the ENS

The anatomy and physiology of the guinea pig ENS is described below. The guinea pig is the best studied animal model of neurogastroenterology. Most of the data on single neuronal types concerning function, chemical coding and electrophysiological behaviour have been obtained from experiments in guinea pigs. In general, the enteric nervous system has similar functions in all mammalian species, and all species have more or less the same functionally defined neurons. Nevertheless, interspecies differences have to be taken into account. One example is the organisation of the SMP. In larger animals (e.g. pigs and humans) the SMP consists of three distinct but interconnected plexuses, while in smaller animals, such as the guinea pig, only one layer can be found (Furness, 2006).

Generally, the ENS consists of ganglia, which are organized in two distinct plexuses (Figure 2). Ganglia are connected with each other and with effector systems through primary interganglionic fibre tracts and secondary and tertiary fibre tracts (Hansen, 2003). There is still unclarity about the number of neurons in the ENS. In literature numbers from 100 million (Epstein et al., 1996) up to 500 (Furness, 2006) million neurons can be found. In addition to these neurons a comparable number of enteric glia cells is present in the ENS, neighbouring the neurons (Rühl, 2005).

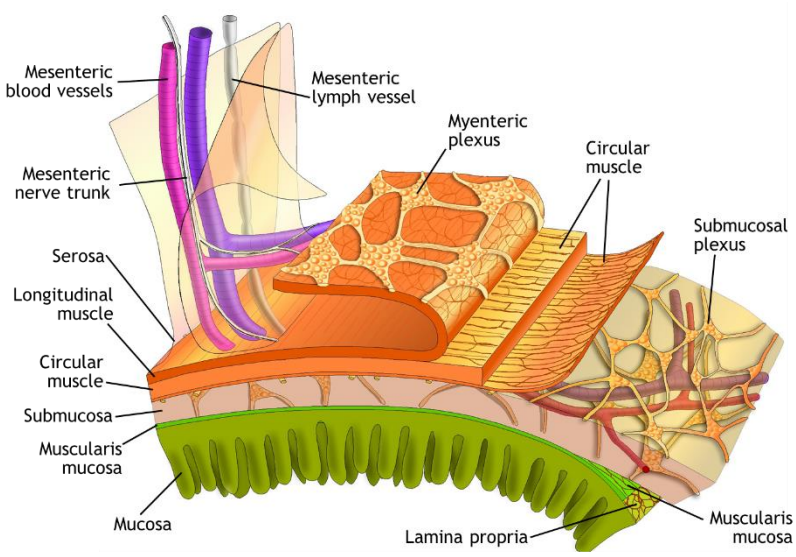

Figure 2: layers of the intestine. Copyright: Simon Brooks

The MP is present alongside the whole gut, starting from the upper esophagus and reaching up to the internal anal sphincter, whereas the SMP is only present in the small and large intestine (Auerbach, 1862; Furness, 2006; Meissner, 1857; Schabadasch, 1930; Schofield, 1960). The two networks also differ in the size of their ganglia. Ganglia in the SMP are usually smaller and their interganglionic strands are finer compared to the ones of the MP (Furness, 2006). Historically, enteric neurons have

been classified using their morphological, functional, electrophysiological and neurochemical properties (Hansen, 2003).

Morphological classification of enteric neurons

The first to distinguish enteric neurons by means of their shape was the Russian histologist Alexander Dogiel in 1895. Dogiel described three different types of neurons, known as Dogiel type I, II and III and defined by the length and morphology of their processes (Dogiel, 1895). Although over the years this concept has seen many modifications and revisions it still bears some significance as the morphological structure of the neurons correlates with their physiological function. Dogiel Type I neurons mostly have a stellate outline with 4-20 lamellar dendrites and a long axonal process. Dogiel Type II neurons in contrast have round or oval somata, 3-10 long dendrites and are nowadays believed to be multiaxonal (Stach, 1981). Dogiel type III neurons are described as having between two and ten relatively short dendrites, ending within the ganglion of origin (Dogiel, 1895).

Electrophysiological classification of enteric neurons

By means of electrophysiological properties enteric neurons can be classified into AH neurons and S neurons. AH is the abbreviation for after-hyperpolarization, while the S stands for synaptic (Hirst et al., 1974). The action potential of AH neurons has a larger amplitude and a longer duration than S neurons. These neurons are named after the long hyperpolarization after an action potential (lasting up to 10 seconds) observed in intracellular recording experiments. Furthermore, AH neurons display a characteristic Ca^{2+} - hump in the repolarization phase because part of their spike component is driven by Ca^{2+} influx (Hirst et al., 1974). The depolarizing phase of the action potential consists of a tetrodotoxin (TTX) sensitive Na^{+} component and a TTX insensitive Ca^{2+} component (North, 1973). AH neurons usually do not exhibit fast excitatory postsynaptic potentials (EPSPs) while slow EPSPs in these neurons often trigger action potentials. In the MP of the guinea pig ileum all AH neurons have a Dogiel type II morphology (Furness, 2006).

S neurons in contrast fire short, TTX sensitive action potentials followed by a brief after hyperpolarization. Typically they show a Dogiel type I morphology with a single axon (Hirst et al., 1974).

Functional classification of enteric neurons

Functionally neurons of the ENS have been grouped into sensory, interneurons, motoneurons and intestinofugal neurons (Furness, 2000) (Figure 3: schematic organization of the ENS. LM: Longitudinal muscle; MP: Myenteric plexus; CM: Circular muscle; SM: Submucous plexus; MU: Mucosa. Motor neurons are displayed in blue; IPANs are displayed in red; secretomotor neurons are displayed in black and interneurons are displayed in orange. (modified from Furness, 2006). Sensory neurons have been historically defined as intrinsic primary afferent neurons (IPANs) (Furness et al., 2004).

Sensory neurons: around 20% of all enteric neurons are IPANs (Furness et al., 2004). Cell bodies of IPANs are located in submucosal as well as in myenteric ganglia with their nerve endings projecting to the mucosa. In the SMP around 11 % of the neurons can be assigned to this class (Furness, 2000). The term "sensory" is generally avoided for describing IPANs for two reasons: although IPANs may be the first neurons in the pathway, they may be activated by other cells (e.g. enterochromaffin cells) and should therefore not be called sensory neurons. The second reason simply is that activation of IPANs does not trigger any sensation (Furness et al., 2004). Sensory neurons can be activated by various stimuli, such as mechanical deformation and intraluminal chemical stimuli (Schemann et al. 2002; Neunlist, Peters, and Schemann 1999; Jänig 2006; Mazzuoli and Schemann 2009; Bertrand et al. 1997). Effective stimuli include acidic pH, alkaline solution and 5-HT (Furness, 2000). Blocking of synaptic transmission by lowering the Ca^{2+} concentration of the bathing solution did not lead to decreased sensitivity to the stimuli (Furness, 2000). Therefore, the response of IPANs to stimuli is not the consequence of synaptic activation by other neurons. By means of electrophysiology IPANs are AH neurons with a Dogiel type II morphology (Furness, 2000). The main neurotransmitter of IPANs is the neuropeptide Substance P with acetylcholine being the most important co-transmitter (Furness et al., 2004)

Motoneurons: they are the effector neurons of the ENS. They can be subdivided into muscle motorneurons and secreto motorneurons. Excitatory muscle motorneurons are located in the MP from where they project to the longitudinal and circular muscle layers. Their excitatory effect on smooth muscle cells is based on the release of acetylcholine which acts on the muscarinic acetylcholine receptors of the smooth muscle cells (Furness, 2000). While acetylcholine undoubtedly is the most important neurotransmitter activating smooth muscle, it is certainly not the only one. Tachykinins such as substance P and neuropeptide K and γ also have a contributory effect on smooth muscle activation by excitatory muscle motorneurons in the gut (Lippi et al., 1998). All three substances are neuropeptides and act via G-protein coupled receptors (GPCRs) (Maggi, 1995). Inhibitory muscle motoneurons are also present in the MP. Their main neurotransmitter is nitric oxide (NO) which has a relaxing effect on smooth muscle by activating the cytosolic guanylate cyclase and thereby increasing intracellular cGMP levels (Furness and Costa, 1973) (pathway described in Allgemeine und spezielle Pharmakologie und Toxikologie 1984). Nevertheless it became clear from knockout experiments that NO is not the only transmitter that plays a role in the inhibition of smooth muscle cells by enteric neurons (Huang et al., 1993). Other important transmitters are the vasoactive intestinal peptide VIP, which is expressed by all inhibitory muscle motoneurons of the ENS (Fahrenkrug, 1979), as well as adenosine triphosphate (ATP) (Burnstock, 1972), pituitary adenylyl cyclase activating peptide (PACAP) (McConalogue et al., 1995) and carbon monoxide (Rattan and Chakder, 1993). Another class of motoneurons are the secretomotor / vasodilator neurons which are located solely in the SMP (Furness,

2000). The function of these neurons is to regulate secretion of the mucosal epithelium and the local blood flow. Secretomotor neurons can be subdivided into cholinergic and non-cholinergic groups. Cholinergic secretomotor neurons can on occasion act as vasodilators in addition to their secretomotor activity. The acetylcholine released from the cholinergic neurons activates the muscarinic receptors of the mucosal epithelium and by doing so stimulates secretion of mucus. The non-cholinergic group uses VIP as the main transmitter and also causes vasodilatory effects (Furness, 2006; Hansen, 2003). The vast majority of neurons in the SMP (89%) are secretomotor neurons (Furness, 2000). In terms of electrophysiological and morphological properties motoneurons are S neurons with a Dogiel type I morphology (Hansen, 2003).

Enteric interneurons: interneurons are only present in the MP. In the guinea pig one type of ascending and three types of descending interneurons can be found. All ascending interneurons are cholinergic and are part of the pathway of the propulsive reflexes of the gut. Also, all descending neurons are cholinergic but can be grouped into three different classes dependent from their co- transmitters. The first group, which expresses choline acetyltransferase (ChAT), nitric oxide synthase (NOS) and VIP, is involved in local motility reflexes. The second descending group is characterised by their expression of ChAT and somatostatin and is involved in the conduction of migrating myoelectric complexes. The last group is characterised by co-expression of ChAT and 5-HT. These neurons are involved mainly in secretomotor reflexes (Furness, 2000; Pompolo and Furness, 1998). Interneurons can be defined electrophysiologically either as AH or S neurons (Hansen, 2003).

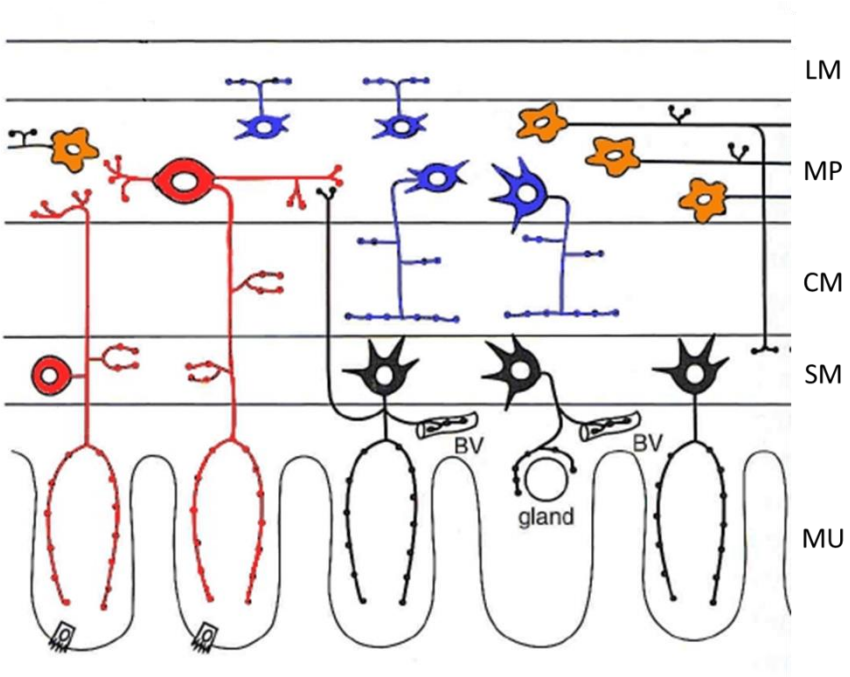

Figure 3: schematic organization of the ENS. LM: Longitudinal muscle; MP: Myenteric plexus; CM: Circular muscle; SM: Submucous plexus; MU: Mucosa. Motor neurons are displayed in blue; IPANs are displayed in red; secretomotor neurons are displayed in black and interneurons are displayed in orange. (modified from Furness, 2006)

It has to be mentioned that, although this simplified functional classification of enteric neurons still bears relevance, it has become revised over the last years. The finding that not only IPANs show sensitivity to mechanical stimuli, but also many motor and interneurons has a major impact on the field of enteric neuroscience (Mazzuoli and Schemann, 2009).

Mechanosensitive enteric neurons were described in 2008 in the myenteric plexus of guinea pig ileum (Mazzuoli et al., 2008). They found that mechanosensitive enteric neurons belong to different functional classes of neurons and that 31% of enteric interneurons and 47% of the motor neurons could be classified as so called rapidly adapting mechanosensitive enteric neurons (RAMEN) (Mazzuoli and Schemann, 2009). Later RAMEN also have been described in the MP of mouse small and large intestine (Mazzuoli and Schemann, 2012). In contrast to RAMEN, slowly adapting mechanosensitive enteric neurons (SAMEN) continued firing throughout a sustained mechanical deformation.

1.3 Neuroimaging in the ENS

Until the development of optical methods for the recording of neuronal excitability, intracellular methods were the only way to study electrical, synaptic and neuropharmacological properties of enteric neurons. Intracellular neurophysiological methods, such as patch-clamp recordings have been used to characterise the neurophysiological and neuropharmacological properties of enteric neurons (Bornstein et al., 1994). In addition immunohistochemistry has helped understanding species-, region- and target-specific neurochemical coding of populations of enteric neurons (Neunlist et al., 1999b). Unfortunately, both methods fail to show how activity patterns are integrated in more complex systems. The main advantage of optical recording techniques over single cell recording techniques is their ability to record activity in many cells simultaneously. This offers the possibility to investigate how integrated neuronal circuits are linked (Vanden Berghe et al., 2001). In addition, optical methods allow recordings from cells that would be challenging to access with conventional methods, e.g. because they grow in three dimensional structures. Another general advantage of optical methods is that they are less invasive compared to intracellular recording techniques, and do not alter ion concentration and integrity of the cell membrane (Schemann et al., 2002). Of course, for the purpose of studying osmosensitivity the advantage of not altering ion concentration is of great importance.

Voltage Sensitive Dye (VSD) Imaging: dyes of the ANEP family (e.g. Di-8-ANEPPS) have been synthesized by the group around Leslie Loew starting in 1985 (Fluhler et al., 1985). Due to their chemical structure, these probes integrate into the cell membrane (Figure 4). In response to changes in membrane potential a shift of absorption and emission spectra occurs within sub-millisecond time range (Robinson et al., 2011). The changes in resting light intensity (RLI) measured in this study arise from a shift of the emission and excitation spectra of the dye in response to shifts in the electric potential.

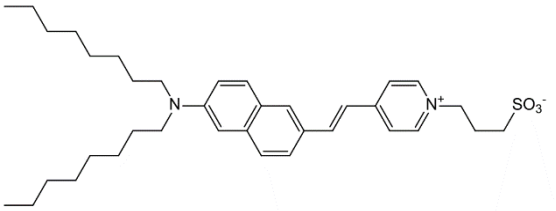

Figure 4: molecular structure of Di-8-ANEPPS, the voltage sensitive probe used for this study

Since action potentials are rather short events, special recording techniques had to be developed to provide a framerate sufficient to visualize events in the temporal range of milliseconds. In addition, these techniques had to be sensitive enough to detect RLI changes in the single digit percentage range (Grinvald et al., 1988). The method mostly used nowadays is known as the multisite optical recording technique (MSORT). It utilizes arrays of photodiodes or a CCD chip for signal detection (Grinvald et al.,

1988). The method of recording neuronal events with the help of VSD was initially developed in invertebrates (Cohen et al., 1978; Salzberg et al., 1977) but soon also applied to vertebrate nervous systems (Obaid et al., 1999). It is noteworthy that the first vertebrate neuronal cells where VSD was applied were SMP neurons of the guinea pig (Obaid et al., 1999). The MSORT technique combines a high temporal resolution of up to 2 kHz framerates with a single cell spatial resolution. These advantages make the MSORT technique useful for studying the response of intact enteric networks to different stimuli (Neunlist, Peters, and Schemann 1999). Despite its value certain limitations in using VSD have to be mentioned. The signal to noise ratio is crucial for the detection of electrical activity. If the signal to noise ratio therefore is too low, small changes in membrane potential are not detected. This is in particular relevant for subthreshold excitatory postsynaptic potentials (EPSPs) with low signal amplitudes (Neunlist, Peters, and Schemann 1999). Another limiting aspect of the method are the possible phototoxic effects of VSDs which arise from the formation of reactive oxygen species (ROS) during long-term illumination (Obaid et al., 1999). The easiest way to prevent the formation of ROS is the restriction of the duration of illumination to a few seconds.

Ca^{2+}- imaging: Ca^{2+} is an important second messenger molecule and involved in many different intracellular processes (e.g. release of synaptic vesicles, binding to calmodulin etc.) (Berridge, 1998; Kandel, 1996). Ca^{2+} enters the cytoplasm either through voltage gated, ligand gated or mechanically gated Ca^{2+}- channels. The reservoirs for Ca^{2+} ions are the extracellular space and the endoplasmatic reticulum (ER). Ca^{2+}- release from the ER is achieved by the activation of ryanodine receptors or inositol-(1,4,5)-trisphosphate (IP_3) receptors. Both, IP_3 and ryanodine receptors display the phenomenon of Ca^{2+} induced Ca^{2+} release. High concentrations of $[Ca^{2+}]_{in}$ lead to activation of a variety of kinases, phosphatases and channels (e.g. Ca^{2+} - activated Cl^- or K^+ - channels) (Berridge, 1998; Vanden Berghe et al., 2001). Although Ca^{2+} signals do not represent action potential events directly, membrane-potential events have been shown to be closely related to changes in $[Ca^{2+}]_{in}$ levels (Michel et al., 2011). As described above, part of the repolarising component in AH-neurons is a rise in $[Ca^{2+}]_{in}$ leading to the opening of Ca^{2+} activated K^+ channels and the afterhyperpolarisation (Vanden Berghe et al., 2001). With recording frequencies of >200 Hz $[Ca^{2+}]_{in}$ peaks associated with action potentials can be detected (Michel et al., 2011) makeing the Ca^{2+} imaging technique a valuable method for measuring neuronal activity. In this study Ca^{2+} imaging was used to detect slow long lasting Ca^{2+} responses following the stimulation of enteric neurons. Therefore, a rather low framerate of 2 Hz was chosen, allowing recording times of up to 90 seconds without significant bleaching of the dye. In addition, this approach greatly reduced phototoxic effects of the dye. One of the advantages of the Ca^{2+} imaging technique is that investigation of activity is not limited to neurons, but can also reveal Ca^{2+} events for example in enteric glia cells or immune cells (Boesmans et al., 2013). Ca^{2+} imaging is a valuable method in investigating the possible role of enteric glia in osmosensitivity in the ENS. Ca^{2+} indicators are

chelators that act as Ca^{2+} buffering molecules. Nevertheless their sensitivity is so high that disturbance of intracellular Ca^{2+} signalling due to the buffering effect of the dye seems highly unlikely (Vanden Berghe et al., 2001). Upon binding of Ca^{2+} the dye molecules undergo an increase in fluorescence due to a change in conformation. The dye used for the present study was Fluo-4AM, which is the membrane soluble (acetoxymethyl) ester form of the probe (Gee et al., 2000).

1.4 Aim

The aim of this work was to identify and characterise osmosensitive neurons in the SMP of the guinea pig. Cells of the SMP were exposed to iso-, hypo-, and hyperosmolar stimuli of different strength while their activity was recorded using ultrafast neuroimaging techniques with VSDs and Ca^{2+} sensitive dyes. These osmosensitive responses were then analysed and characterised. For the application of the stimuli a new experimental approach with a short term and local application of chemical substances was developed and tested for feasibility. In addition, changes in cell volume after application of the osmotic stimulus were assessed.

After osmosensitive enteric neurons were identified, the question for the molecular basis of osmotransduction was addressed. In a first step, pharmacological experiments were conducted to test the effect of two channel blockers. The presence of TRPV4 in submucosal neurons was demonstrated by applying a highly specific and potent activator of TRPV4. The expression of TRPV4 in the SMP was investigated at the protein and RNA levels using immunohistochemical methods, as well as quantitative PCR (qPCR). Immunohistochemistry was also used to study the chemical coding of the enteric neurons identified as osmosensitive in the imaging experiments.

2. MATERIAL AND METHODS

2.1 Buffers and solutions

If not stated otherwise all substances for the preparation of the following solutions were obtained from Sigma- Aldrich (Schnelldorf, Germany).

Krebs solution for preparation:

Substance	mmol/l
$MgCl_2.6H_2O$	1.2
$CaCl_2.2H_2O$	2.5
NaH_2PO_4	1.2
NaCl	117
$NaHCO_3$	25
Glucose	11
KCl	4.7

Krebs solution for experiment:

Substance	mmol/l
$MgCl_2.6H_2O$	1.2
$CaCl_2.2H_2O$	2.5
NaH_2PO_4	1.2
NaCl	117
$NaHCO_3$	20
Glucose	11
KCl	4.7

The osmolality of the Krebs solution for experiments was 296 mOsm/kg and the pH was adjusted to 7.4 at a temperature of 37.0°C

HEPES perfusion buffer for experiment:

Substance	mM
$MgCl_2$	1.2
$CaCl_2$	2.5
NaCl	136
HEPES	10
Glucose	10
KCl	5

The osmolality of the HEPES buffer was 296 mOsm/kg and the pH was adjusted to 7.4 at a temperature of 37.0°C

194 mOsm/kg HEPES (reduced NaCl):

Substance	mM
$MgCl_2$	1.2
$CaCl_2$	2.5
NaCl	83
HEPES	10
Glucose	10
KCl	5

This solution was used as a hypoosmolar stimulus in the experiments. Decrease in osmolality was achieved by reducing the NaCl content of the solution. The osmolality was 194 mOsm/Kg and the pH was adjusted to 7.4 at a temperature of 37°C.

144 mOsm/kg HEPES (reduced NaCl):

Substance	mM
$MgCl_2$	1.2
$CaCl_2$	2.5
NaCl	58
HEPES	10
Glucose	10
KCl	5

This solution was used as a hypoosmolar stimulus in the experiments. Decrease in osmolality was achieved by reducing the NaCl content of the solution. The osmolality was 144 mOsm/kg and the pH was adjusted to 7.4 at a temperature of 37°C

94 mOsm/kg HEPES (reduced NaCl):

Substance	mM
$MgCl_2$	1.2
$CaCl_2$	2.5
NaCl	33
HEPES	10
Glucose	10
KCl	5

This solution was used as a hypoosmolar stimulus in the experiments. Decrease in osmolality was achieved by reducing the NaCl content of the solution. The osmolality was 94 mOsm/kg and the pH was adjusted to 7.4 at a temperature of 37°C

Hyperosmolar HEPES:

Substance	mM
$MgCl_2$	1.2
$CaCl_2$	2.5
NaCl	136
HEPES	10
Glucose	10
KCl	5
D-Mannitol	100 / 200

The addition of D-Mannitol resulted in an increased osmolality of the solution to 394 mOsm/kg or 494 mOsm/kg. The pH was adjusted to 7.4 at a temperature of 37.0°C

4% Paraformaldehyd solution "Fix":

Substance	Amount
Phosphate Buffer (0.1 M)	50 ml
Paraformaldehyde	2 g
Picric acid (1.2%)	100 µl

Phosphate Buffer (0.1 M):

Substance	Amount
H_2O bidest.	800 ml
$NaH_2PO_4 H_2O$	3.0 g
$Na_2HPO_4 7H_2O$	32.68 g

pH was adjusted to 7.44 using NaOH (1M) and H_3PO_4 (1M) and the volume of the solution was adjusted to 1 l with bidestilled water.

Phosphate buffered saline (PBS):

Substance	Amount
H_2O bidest.	800 ml
NaCl	8.8 g
Phosphate Buffer	116 ml

Volume was adjusted to 1 l with bidestilled H_2O after the substances were mixed.

Sucrose solution:

Substance	Amount
Saccharose	3 g
PBS/NaN_3 buffer	7 ml

Blockingserum:

Substance	Amount
PBS/NaN_3	48 ml
Horse serum	2 ml
Triton X-100	250 µl

PBS/NaN_3 buffer:

Substance	Amount
NaN_3	1 g
PBS	1 l

2.2 Animals and tissue preparation

All tissue samples were obtained from male “Dunkin Hartley” guinea pigs (Envigo RMS GmbH, Horst, Netherlands). The weight of the animals at the time of arrival at our lab was 200 to 250g. The animals were kept under standardised conditions at the institute for at least one week (20-24°C room temperature, 60% humidity and a day: night cycle of 12:12 h) in an isolation cabinet, (UniProtect, Ehret, Emmendingen). Per cage two animals were housed. Animals received a standard diet (Altromin Spezialfutter GmbH & Co. KG, Lage, Germany) and drinking water ad libitum. Animal weight at time of experiments was 353.6 ± 6.3 g (mean ± SEM). Guinea pigs were killed by cervical dislocation followed by exsanguination in accordance with the local animal ethical committee and according to the German guidelines for animal protection and animal welfare.

The abdomen was opened using surgical scissors and tissue forceps (Dumont #5, Fine Science Tools (FST), Heidelberg, Germany). Approximately 2 cm of the proximal part of the distal colon were removed from the animal and used for further preparation. Tissue preparation was performed under constant perfusion with ice cold, carbogenated (95% CO_2, 5% O_2; Andeldinger, Freising, Germany) Krebs- solution and under a binocular microscope (SZ51, Olympus, Hamburg, Germany). The colonic tissue was opened along the mesenteric border, content was removed and the specimen was pinned to a Sylgard® coated Petri dish (Sylgard® 184, Down Corning GmbH, Wiesbaden, Germany) with the mucosal side facing upward. The mucosa was removed by peeling it gently off with rounded forceps (Dumont #7, FST) to avoid damage to the plexus lying beneath. After incisions were made on three sides of the plexus using a fine spring scissor (15370-52, FST) the submucosal plexus was carefully pulled off the subjacent circular muscle layer and pinned over the rectangular opening (2×1 cm) of a Sylgard® ring with the mucosal side facing upwards. In a final step remaining muscle pieces as well as connective tissue, covering the submucous ganglia, were removed using a spring scissor (15370-52, FST).

2.3 Experimental setup for neuroimaging

For the neuro imaging experiments the Sylgard® ring with the tissue pinned was then placed in a self-made acrylic glass recording chamber with a 42 mm glass bottom which had a thickness of 130 µM (Sauer, Reutlingen, Germany). This chamber was then connected to a peristaltic perfusion pump (Minipuls3, Gilson Inc., Middleton, USA) that circulated the perfusion buffer from a heated reservoir placed in a water bath (WiseCircu®; Witeg, Wertheim, Germany) through plastic tubes (Tygon®R3603, Ø 2.79mm) to the recording chamber and back. To maintain a temperature of 37°C in the recording chamber the perfusion buffer was led through a glass heat exchanger placed several centimetres before the recording chamber.

During the imaging experiments the recording chamber rested on top of an inverted microscope (Zeiss Axio Observer.D1; Carl Zeiss Microscopy GmbH, Göttingen, Germany). Due to the high light intensity needed for a feasible signal to noise ratio oil immersion objectives with a high numerical aperture were used (Olympus UApo 40x OI3/340 Oil NA 1.35-0.5 and Olympus UPlanApo 100x Oil NA 1.35-0.5 Olympus Corporation, Tokyo, Japan). To position micro-pipettes, electrodes and tissue retainers, for preventing movement, micromanipulators of the type M 3333 were used (Narishige International Limited; London, UK). For signal detection in ultrafast neuroimaging experiments a cooled charge coupled device (CCD) camera was used (NeuroCCD-SMQ imaging system, RedShirtImaging LLC, Decatur, GA, USA). In combination with the x100 objective the resulting spatial resolution was 2.0 µm per pixel. Light source for the voltage sensitive dye (VSD) imaging experiments was a 3W green LED (LE T A2A true green (521 nm) 700mA; OSRAM GmbH, Munich, Germany). Calcium imaging experiments were carried out using a 3W blue LED (LE B A2A blue (460 nm) 700mA; OSRAM). The filter set used for VSD imaging contained a dichroic mirror with a separation wavelength of 565 nm, an excitation filter with a spectrum of 530- 560 nm and a barrier filter with a 575 – 645 nm spectrum (AHF Analysetechnik AG; Tübingen, Germany). For calcium imaging experiments a dichroic mirror with a separation wavelength of 660 nm was used. The excitation filter had its maximum transition at 620 nm and a bandwidth of 60 nm while the emission filter had its maximum transition at 700 nm with a bandwidth of 75 nm. For high resolution images of the ganglia an Axio Cam ICm1 in combination with the Axio Vision software was used (Zeiss). The microscope as well as the NeuroCCD camera was mounted on a vibration isolated table (TMC Technical Manufacturing Corporation, Peabody, USA) to prevent mechanical disturbances causing experimental artefacts (Figure 6).

Application of drugs as well as staining of ganglia with the VSD was achieved by local pressure application (PDES-2L, npi electronic GmbH, Tamm, Germany) via a glass microejection pipette (Science products, Hofheim, Germany). The tips of the pipettes were pulled with a Flaming/Brown micropipette puller (Sutter instrument Co., Novato, CA, USA) to a diameter of approximately 5 µm. Electrical

stimulation of neurons was achieved with a Teflon™ coated platinum electrode with a diameter of 25 µm (Science products GmbH, Hofheim, Germany) connected to a constant current stimulus isolator (A360, WPI; Berlin, Germany).

Application of larger fluid quantities (10 – 50 µl) was carried out with two electrically driven programmable syringe pumps (UltraMicroPump III, WPI) which were connected to a self-manufactured two channel application device. This device was made from two stainless steel tubes with an inner diameter of 0.2 mm and an outer diameter of 0.4 mm that were placed inside Teflon™ tubes with the same diameter. Both tubes were then glued to a pipette holder with their openings aiming at the same point. Preliminary tests with Fast Green confirmed that both channels of the device perfused the exact same region of the specimen, which was crucial for paired experiments (Figure 5).

For the exact timing of the stimuli the Pulse Pal v2 an open source pulse train generator was used (Sanders and Kepecs, 2014) (Sanworks LLC, Sound Beach, NY, USA).

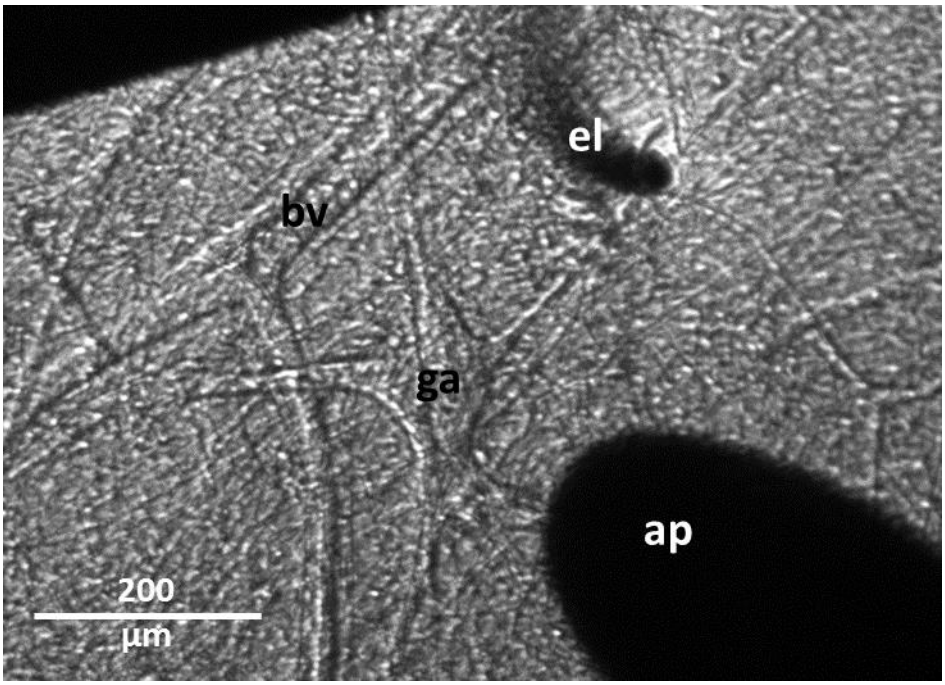

Figure 5: brightfield image of the submucosal layer in the experimental chamber: ga = ganglion, bv = blood vessel, el = point electrode used for viability testing, ap = tip of the application device used for larger fluid quantities.

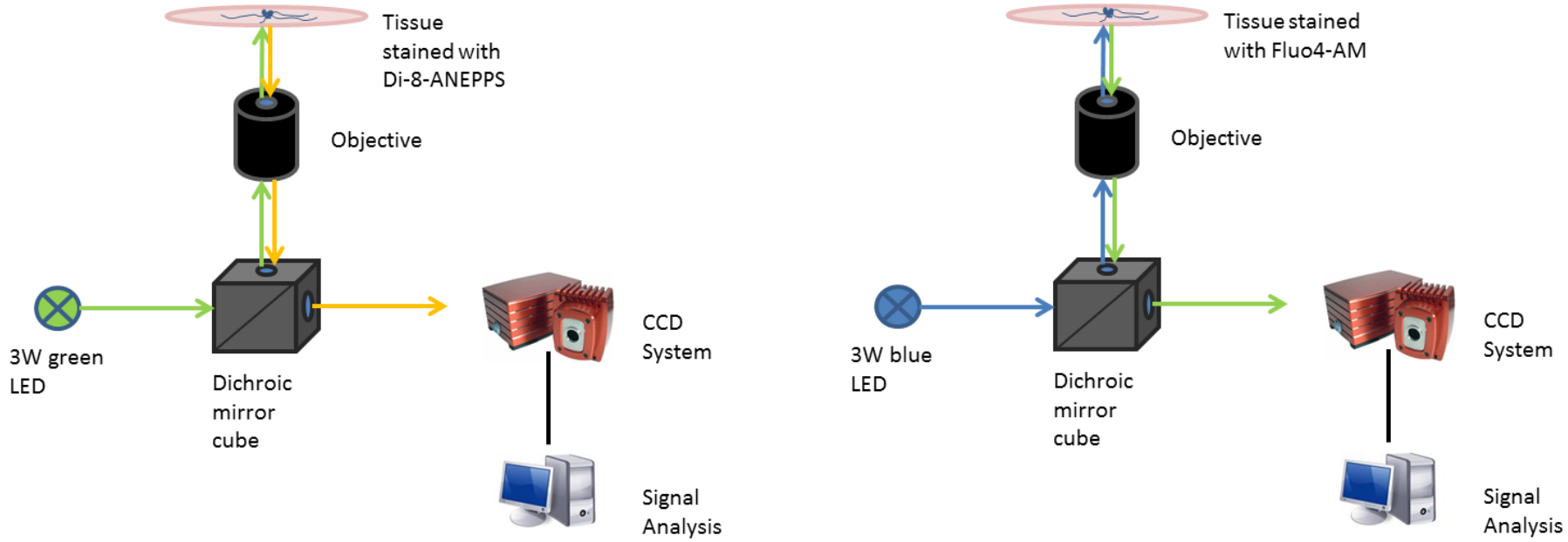

Figure 6: Left: experimental setup for VSD imaging; Right: experimental setup for Ca^{2+} - imaging

2.4 Experimental techniques

2.4.1 Voltage Sensitive Dye imaging

During these experiments, the specimen was continuously perfused with 37°C HEPES- solution that was constantly fumigated with normal air to ensure O_2 saturation of the tissue. For pharmacological experiments on the other hand 37°C Krebs- solution, saturated with carbogen was used. In contrast to the pH of Krebs- solution the pH of HEPES- solution is independent from fumigation with carbogen. To avoid experimental artefacts caused by a change in pH HEPES buffered solution was used in all experiments in which application of larger fluid quantities was needed. This was the case in all experiments where the reactions to different osmotic shifts were tested. For VSD- imaging experiments 1-(3-sulfonatopropyl)-4-[beta[2-(din-octylamino)-6-naphthyl]vinyl]pyridinium betaine (Di-8-ANEPPS Invitrogen, Carlsbad, CA, USA) was used. The dye was used in a concentration of 20 µM dissolved in Krebs- solution containing 0.0135% Pluronic F-127 (Invitrogen) and 0.135% DMSO (Acros Organics, Geel, Belgium). Di-8-ANEPPS was injected selectively into the submucous ganglia of choice. This approach, in comparison with incubation of the whole tissue sample, allowed us to massively reduce background fluorescence and therefore to increase the signal to noise ratio. Dye injection was performed by gently placing a pulled glass micro-pipette (tip ⌀ ca. 5µm) on the surface of the ganglion and delivering 5-10 pressure pulses of 0.5 – 1.0 bar, each lasting 300 ms. Between staining and the first recording an interval of at least 15 minutes was adhered to allow the dye to properly incorporate into the membrane.

2.4.2 Calcium - imaging

For the Ca^{2+}- imaging experiments the same perfusion buffers as described above were used. The only modification was the addition of 500 µM probenecid, an inhibitor of organic anion transporters. This ensured a neuronal staining that was stable for several hours. As a calcium reporter Fluo-4 AM (Invitrogen) was used. The specimen was incubated for 45 minutes in a ⌀ 2cm petri dish filled with 10µM Fluo-4 AM dissolved in 2 ml carbogen fumigated Krebs- solution containing 500 µM probenecid and 1% DMSO. After the incubation period, the tissue was washed for 20 minutes in probenecid containing Krebs- solution.

2.5 Experimental protocols for neuroimaging experiments

2.5.1 Hypo- and hyperosmolar stimulation of enteric neurons

In these experiments solutions hypo- and hyperosmolar relatively to the regular perfusion buffer were applied locally onto submucous ganglia of interest. Application was performed using the self-manufactured device for application of larger fluid quantities described above in combination with two electrically driven syringe pumps (UMPIII, WPI). The total volume of each application was 20 µl and the application rate was 4 µl/s resulting in a total application time of 5 seconds. The different osmotic shifts tested were -200 mOsm/kg, -150 mOsm/kg, -100 mOsm/kg, +100 mOsm/kg and +200 mOsm/kg relative to the regular perfusion buffer.

Hyperosmolality of the applied HEPES solution was established by adding defined amounts of mannitol. By doing so the solution was either adjusted to an osmolality of 394 mOsm/kg or 494 mOsm/kg which is approximately 100 and 200 mOsm/kg above the physiological plasma osmolality of the guinea pig. To exclude unspecific effects also the response to application of isoosmolar solution was investigated. During the whole acquisition, the perfusion pump was stopped to keep the osmotic shift presented to the ganglion constant. Preliminary experiments showed that stopping the perfusion for up to 1 minute had no effect on neuronal activity.

In the experiments using the VSD technique two different acquisition approaches were carried out. One was to record continuously for 12 seconds from one ganglion while the stimulus was delivered with a delay of 2 seconds from the beginning of the recording period. The first two seconds of each recording therefore represent the basal activity of the neurons in the ganglion of interest. Because of possible phototoxic effects of the relatively long recording time of 12 seconds it was decided to use another approach that allowed an even longer overall recording time. For each recording four consecutive acquisitions, each with duration of two seconds, were conducted. The interval between the acquisitions was set to 8 seconds. Therefore, the overall recording time was 40 seconds with a total illumination time of 8 seconds (Figure 7). In this setting, the stimulus was delivered during the second acquisition period. Therefore, the first acquisition period represented the basal activity of the neurons, while the following three acquisition periods represented the response to the stimulus. The number of action potentials was measured in three different periods after application of either an isoosmolar HEPES solution or a HEPES solution with an altered osmolality. The first recording period ranged from 0-2 seconds after the start of the application, the second one from 10-12 seconds and the third from 20-22 seconds. Hypoosmolality in these experiments was either achieved by lowering the NaCl concentration of the HEPES solution or diluting the HEPES solution with distilled water. This solution

was then applied using the self-made application device described above. The order of applications of the two solutions was switched randomly.

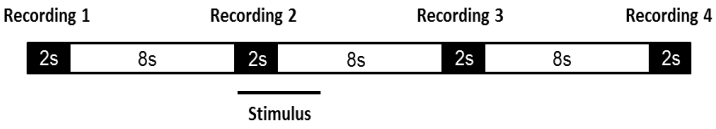

Figure 7: schematic illustration of the interval recording protocol

To keep the overall illumination duration as low as possible while gaining as much information as possible a total recording duration of 1 minute with a framerate of 2 Hz has proven feasible in the Ca^{2+}-imaging experiments.

2.5.3 Reproducibility test

To determine the reproducibility of the neuronal responses to osmotic shifts the same hypo- or hyperosmolar stimulus was applied twice onto the same ganglion consecutively. Between both stimulations a time period of 20 minutes was adhered. During this time, the tissue was perfused with standard perfusion HEPES.

2.5.4 Investigation of the influence of NaCl on the response to osmotic shifts

The goal of this set of experiments was to investigate whether the neuronal response to a hypoosmolar HEPES solution was triggered by the general reduction of solutes in the solution or specifically by the reduction of the concentration of Na^+ and Cl^- ions. Individual ganglia were treated with the hypoosmolar low NaCl HEPES as well as with a HEPES solution where the osmolality was reduced by dilution with distilled water. Both solutions were applied onto the same ganglia consecutively. In between the applications, a 20-minute interval was adhered. For these experiments, the continuous recording paradigm was used.

2.5.2 Pharmacological experiments

Ruthenium red

Ruthenium red (Figure 8) is described as a broad-spectrum blocker of TRP channels (Ramsey et al., 2006). The blocking effect of ruthenium red on the responses to osmotic stimuli in neuronal tissues has been described by other groups (Kamakura et al., 2016). Therefore, the effect of 10 µM ruthenium red on neuronal responses in the ENS after applying 94 mOsm/kg HEPES solution was investigated using the Ca^{2+}-imaging method. Due to the fact that the emission spectrum of ruthenium red overlaps with that of Di-8-ANEPPS, the effect of ruthenium red was not tested using VSD -imaging. Ruthenium red was added to the perfusion HEPES solution and the hypoosmolar stimulus was applied as described above. Experiments were performed in a paired design.

Ruthenium red (Sigma-Aldrich) was delivered as desiccated powder, dissolved in H_2O to a 100 mM stock solution. The drug was applied by adding stock solution to the reservoir of the perfusion HEPES solution. The final concentration was 10 µM. Before testing the drug effects a wash-in period of at least 20 minutes was adhered.

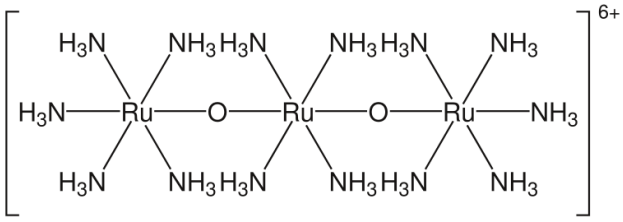

Figure 8: structural formula of ruthenium red (obtained from the manufacturers website)

TRPV4 blocker HC-067047

HC-067047 (Figure 9)(Sigma-Aldrich) is a highly specific and potent blocker of the TRPV4 cation channel (Everaerts et al., 2010). The blocker was delivered as desiccated powder, dissolved in DMSO to a stock solution of 10 mM and aliquoted immediately. Application was done by adding the drug to the perfusion Krebs solution. The final working concentration here was 150 nM. Prior to testing drug effects, a period of at least 20 minutes was adhered to allow proper binding of the blocker.

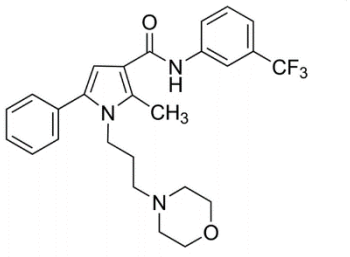

Figure 9: structural formula of HC-067047 (obtained from the manufacturers website)

TRPV4 activator GSK1016790A

GSK1016790A (Figure 10) (Sigma-Aldrich) is described as a potent and specific activator of TRPV4 (Thorneloe et al., 2008). GSK1016790A was delivered as a dry powder, dissolved in DMSO to a stock solution of 10 mM and aliquoted immediately. To obtain the final working concentration of 20 µM, 1 µl of the stock solution was diluted in 500 µl Krebs solution. Application was carried out using the local pressure application device described above. The drug was ejected for a period of 4 seconds with a pressure of 0.5 bar.

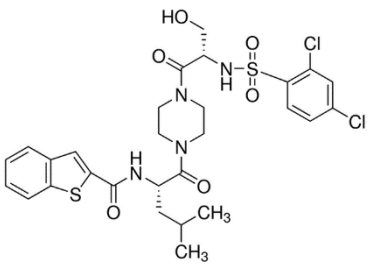

Figure 10: structural formula of GSK1016790A (obtained from the manufacturers website)

ω-conotoxin GVIA

To block synaptic transmission in the VSD imaging experiments the neurotoxic peptide ω-conotoxin GVIA (Alomone Labs, Jerusalem, Israel) was used. ω-conotoxin GVIA is a specific blocker of the N-type voltage dependent Ca^{2+} channel (Cruz and Olivera, 1986). Due to its irreversible action (Cunningham et al., 1998), experiments were performed in an unpaired design. The drug was delivered as dry powder and dissolved to a 100 µM stock solution in deionized water. The final concentration was achieved by dissolving the stock solution in the HEPES solution used to perfuse the tissue during the

imaging experiments to a final concentration of 200 nM. Before testing the drug effects, a wash-in period of at least 20 minutes was adhered.

2.5.3 Viability test

Before applying osmotic shifts onto ganglia or performing pharmacological experiments the viability of the ganglion of interest was tested. Electrical stimulation with a monopolar point electrode delivering rectangular pulses of 20 to 90 µA and a duration of 600 µs was the method of choice. In case of viable cells this resulted in fast EPSPs (fEPSPs) in the postsynaptic neurons. It has to be taken into account that the number of neurons responding in this test does not necessarily resemble the number of vital neurons in the ganglion. Usually the number of neurons responding to electrical stimulation is an underestimation based on two factors. First of all, only a subpopulation of all axons running towards the ganglion is stimulated with this method. Secondly, most but not all neurons of the SMP receive fEPSPs. Despite those disadvantages, electrical stimulation is a quick and efficient way to test the overall viability of the ganglion and essential for investigating sensitivity of enteric neurons and drug actions.

To evaluate the effect of HC-067047 on the electric excitability of the neurons, ganglia were stimulated electrically before and after a 20-minute perfusion with 150 nM HC-067047 with the same electric stimulus as described above. The amplitude of the EPSPs before and after the perfusion with the blocker was measured.

2.6 Measurement of changes in visible cytoplasmic area

Application of osmotic shifts to cells can lead to changes in cell volume. Unfortunately, it is not possible to measure 3 dimensional changes with the used imaging technique. Nevertheless, a rough estimation about cell volume changes can be made measuring the visible cytoplasmic area of neurons stained with Di-8-ANEPPS. Due to the fact that Di-8-ANEPPS incorporates into the cell membrane it allows measuring the cytoplasmic area easily. To measure those changes, a high-resolution image of the investigated ganglion was obtained using the Axio Cam ICm1 (Zeiss GmbH) before the hypoosmolar stimulus was applied. The hypoosmolar stimulus was applied and 10 additional high resolution images were taken over the next 10 seconds. The visible cytoplasmic areas of the cells of interest were then encircled and measured in the Axio Vision software (Zeiss GmbH). This outline of the cells was copied on to the image of the same cell, which was taken at the time point of maximum deformation. The outline was adjusted to fit onto the deformed cells, the area was measured again and compared to the visible area before the stimulus.

2.7 Validation of stimulation method

As described above a self-manufactured device was used to test the sensitivity of enteric neurons to osmotic changes in a paired experimental design. To gain knowledge about the actual osmotic shift delivered to the ganglion of interest preliminary experiments had to be carried out. In these experiments, the fluorescence intensity of a known concentration of Fast Green (Sigma- Aldrich) was compared to the fluorescence intensity of the same concentration of Fast Green applied into the recording chamber with the self-manufactured device. The first step of this process was to establish a calibration curve. Fast Green concentrations of 0.050 mM, 0.100 mM, 0.125 mM 0.250 mM and 0.500 were filled into the recording chamber. The resulting fluorescence intensity measured with the CCD camera was then plotted against the Fast Green concentration. Due to unspecific background fluorescence, the light intensity of the chamber filled just with pure H_2O had to be subtracted from the fluorescence intensities measured for the different Fast Green concentrations.

In a second step the same concentrations of Fast Green were administered into the water filled chamber using the application device described above. The position of the tip, applied volumes as well as application speed were set to the exact same values as in the later experiments. Here again fluorescence intensity was measured and plotted against the used Fast Green concentrations. The similarity of the two resulting curves can be used as an indicator for the degree of saturation of the perfusion buffer with the applied substance in the region of interest.

2.8 Measurement of the guinea pig plasma osmolality

During exsanguination of the animal, approximately 1 ml of arterial blood was collected from the carotids using Li- Heparin containing vacutainers (Sarstedt AG & Co, Nürmbrecht, Germany). The vacutainer was gently inverted 10 times to mix the blood with the granules. According to the guidelines for blood probe handling provided by the manufacturer, blood samples were centrifuged for 10 minutes at 2000 RCF. After centrifugation 3 bands were visible in the sample tube being from low to high plasma, leucocytes and erythrocytes. The supernatant (plasma) was transferred to an Eppendorf cup and checked for turbidity. Only clear plasma samples free from turbidity were used for osmolality measurement. Subsequently measurement of the plasma osmolality was conducted using a freezing point osmometer (Osmomat 030, Gonotec GmbH, Berlin, Germany). The device was calibrated with a 300 mOsm/kg calibration solution provided by the manufacturer. Each sample was measured three times and the sensor was cleaned after every measurement. The mean of the three values was the final result for each animal. The protocol for plasma osmolality measurement was established according to the method described by Bohnen et al. (Bohnen et al., 1992).

2.9 Immunohistochemistry

2.9.1 Staining protocol

Tissue was fixated over night with the fixative solution described above either immediately after the experiment or directly after preparation. Following the fixation, the specimen was washed three times in PBS. For Long term storage, the tissue was stored in PBS containing NaN_3 (0.1%) as preservative and kept at 4°C. The whole staining procedure was performed at room temperature. Preincubation in blocking serum for reduction of unspecific antibody binding was performed for one hour followed by three 10-minute washing steps with PBS. The primary antibody was diluted in blocking serum. Incubation with the primary antibody took 16 hours under continuous agitation, again followed by three washing steps with PBS. The secondary antibody also was diluted in blocking serum. Incubation with the secondary antibody took two hours under continuous agitation. The last step of the staining protocol was to wash the tissue three times in PBS. The stained specimen was mounted on a microscope slide (Superfrost Plus, Thermo Scientific), using a fine forceps and lint-free paper to spread the tissue out. One drop of Dianova IS Mounting Media without hardener, Dianova, Hamburg, Germany) was placed on the tissue to reduce bleaching during illumination and covered with a cover slide (Menzel, Braunschweig, Germany). For some tissues Antifading Mounting Medium DAPI (Dianova) was used to mount the specimen on the microscope slide in order to visualise nuclei.

2.9.2 Image acquisition

Analysis of the stained specimen was carried out using an Olympus BX61WI microscope (Olympus GmbH) equipped with a 100 W mercury- vapor lamp and appropriate filter blocks. Image acquisition was performed using the F-View Soft Imaging System and image analysis software Cell^P (Olympus GmbH).

2.9.3 Antibodies

Complete list of primary antibodies used for immunofluorescence:

Antibody	**Dilution**	**Supplier**
Rabbit anti VIP	1:1000	Peninsula Laboratories (CA, USA)
Goat anti ChAT	1:100	Merck KGaA (Darmstadt, Germany)
Rabbit anti TRPV4	1:500	OriGene Technologies Inc. (Rockville, MD, USA)
Human anti HuD	1:10.000	serum of patient #27 see (Li et al. 2016)

Complete list of secondary antibodies used for immunofluorescence:

Antibody	Dilution	Supplier
Donkey anti Rabbit Cy3	1:500	Dianova (Hamburg, Germany)
Donkey anti goat Cy2	1:500	Dianova
Donkey anti human DL488	1:500	Dianova

According to the manufacturer, the used antibody against TRPV4 was only validated in human, mouse and rat tissue. Therefore, the peptide sequence of the immunogen detected by the antibody was compared to the corresponding sequence in *homo sapiens, rattus norvegicus, mus musculus* and *cavia porcellus* using the BLAST algorithm of the National Center for Biotechnology Information. The highest sequence identity was found for rat TRV4 with 88%, followed by murine and human TRPV4 with 81% and 69% sequence identity. The guinea pig TRPV4 sequence only showed a sequence identity of 63% to the immunogen peptide sequence of the used TRPV4 antibody. Therefore, more unspecific binding of the antibody was expected in guinea pig preparations. Nevertheless, it was decided to test the antibody on guinea pig tissue independently from the rather low sequence homology.

To further validate the quality and specificity of the immunofluorescent staining in guinea pig SMP preparations a test staining with the same antibody concentration was performed in human SMP. In addition, the whole staining procedure was performed in one guinea pig SMP preparation without the primary antibody for TRPV4. This was done to make sure that the fluorescence signal was not due to unspecific binding of the secondary antibody.

2.10 Quantitative real-time PCR

2.10.1 Tissue collection

For qPCR applications samples of guinea pig submucosal plexus were collected. Tissue dissection was performed as described above. Special care was taken to remove all muscular residues on the tissue in order to avoid contamination of the SMP samples with muscle cells. As positive controls for TRPV4 expression pieces of the bladder wall including all tissue layers, as well as pieces of the kidney were removed from the animals. As a negative control for TRPV4 expression pieces of the femoral extensor muscle were collected. Immediately after the preparation the tissue was snap-frozen in liquid nitrogen and stored at -80°C until further use.

2.10.2 RNA isolation and cDNA synthesis

Frozen tissue samples were homogenized in 1 ml TRIsure (Bioline, London, UK) using a dispersing instrument (Ultra-Turrax D-1, Miccra GmbH, Mühlheim, Germany). After addition of chloroform and agitation for several seconds the mixture was centrifuged at 12,000 g for 15 minutes at 4°C and the aqueous phase containing the ribonucleic acid (RNA) was extracted. After precipitation with 75% ethanol 700 µl of the solution was added to a spin column of a commercial RNA isolation kit (SV Total RNA Isolation System, Promega, Fitchburg, WI, USA). The column was centrifuged for 15 s at 8,000 g at room temperature. The residual volume of the aqueous phase was added to the column and centrifuged for 1 min at 12,000 g at room temperature. Further processing, which included several washing steps and the incubation with DNase, was performed according to the instructions of the kit manufacturer. RNA was eluted in 50 µl of nuclease-free water and stored at -80°C upon further processing. RNA concentration was determined spectrophotometrically at 260 nm using a plate reader (Infinite® 200 PRO NanoQuant, Tecan Group Ltd., Männedorf, Switzerland). RNA integrity of random samples was validated using a bioanalyzer system (2100, Agilent Technologies, Santa Clara, CA, USA). This method of evaluating RNA integrity is based on a conventional gel electrophoresis transferred to a chip-format in order to reduce separation time and sample consumption. Eukaryotic 18S and 28S ribosomal RNA fragments within the electrophoretic trace are detected by laser-induced fluorescence. Using the number and size of these fragments a dimensionless RNA integrity number (RIN) is calculated which allows the evaluation of RNA integrity. The RIN ranges from 0 (completely degraded) to 10 (perfectly intact). For the analysis samples were diluted in nuclease-free water to a concentration of 30 ng/µl and denaturated for 2 min at 70°C. The RIN was determined according to the manufacturer´s protocol (Agilent RNA 6000 Nano Kit). All samples had RIN values ranging from 6.6 to 10, which was considered as sufficiently intact for the synthesis of complementary DNA (cDNA). Synthesis of cDNA was conducted using a commercial kit (SensiFAST™ cDNA Synthesis Kit, Bioline GmbH, Luckenwalde, Germany) containing poly-deoxythymidine oligonucleotides and random hexamer primers that allow

subsequent amplification of messenger RNAs (mRNA) using PCR primers targeting the coding sequence or untranslated regions. For the reverse transcription, which was conducted according to the manufacturer´s protocol, 500 ng of RNA template were used. The final reaction volume of 10µl was processed in a thermal cycler (FlexCycler, Analytik Jena AG, Jena, Germany) (see appendix for thermal cycler protocol).

2.10.3 Quantitative real-time PCR (qRT-PCR)

In order to determine the relative expression of TRPV4, mRNA- levels of TRPV4 were measured in 6 samples of SMP and compared to the mRNA- levels in tissues were a high TRPV4 expression has been proven. Expression of TRPV4 has been shown in the kidney (Tian, 2004), as well as in the bladder (Birder et al., 2007). Therefore 3 samples of whole- wall bladder tissue and kidney cross sections from 3 animals served as positive controls for TRPV4 expression. According to "The Human Protein Atlas" (http://www.proteinatlas.org) (Uhlén et al., 2015), TRPV4 expression is low in skeletal muscle. Therefore 2 samples from the femoral extensor muscle of guinea pigs served as negative control.

Quantitative real-time PCR was conducted on 384-well plates with well sizes of 12.5 µl. Each well contained 6.25 µl 2x SensiMix SYBR No-ROX (Bioline), 250 nM forward and reverse primers and 1 µl template cDNA in a dilution of 1:10. To ensure comparability and reproducibility all samples of the same experiment were run in triplicates on the same plate. Primers for qRT-PCR were designed to create products spanning at least one intron to exclude quantification of PCR products derived from genomic DNA. Specificity of the primers as well as the length of the PCR products were validated using *in silico* PCR (https://genome.ucsc.edu/) See appendix for primer sequences and product length. Expression levels of target genes were quantified by a standard curve, consisting of pooled cDNA diluted by the factor 2 in at least 8 steps. A SYBR-green based detection of PCR products was conducted during 45 PCR cycles using a LightCycler® 480 Instrument II (Roche, Basel, Switzerland). After 45 PCR cycles a temperature ramp was run through to establish a melting curve in order to screen for unspecific PCR products. See appendix for detailed description of PCR program parameters. As β-actin is an established an well proven housekeeping gene (Kreuzer et al., 1999) expression levels of target mRNAs were normalized to the expression level of β-actin in each tissue investigated.

2.11 Data analysis and statistics

Primary data from neuroimaging experiments was analysed using the Neuroplex (RedShirtImaging) software. Data was collected in Microsoft Office Excel 2016 (Microsoft Corp., Redmont, WA, USA). All statistical analysis was preformed using either Sigmaplot 9.0 (Systat Software Inc., Erkrath, Germany) or GraphPad Prism 6 (GraphPad Software Inc., La Jolla, CA, USA). If not stated otherwise data is presented as mean ± standard deviation or median and [$Q_{0.25}$/$Q_{0.75}$] in case of non-gaussian distribution. Data was tested for normal distribution using Shapiro-Wilk test. In case of normally distributed data a standard t-test was performed for experiments with no pairing. Data which was obtained in a paired experimental design was analysed using a paired t-test. In case of not normally distributed data Mann-Whitney rank sum test was performed to detect differences between two groups. In case of not normally distributed data and paired experimental design, Wilcoxon rank sum test was used to compare the data sets. For the comparison of more than two groups, one way analysis of variance, or Kruskal-Wallis repeated measures analysis of variance on ranks was performed in cases the data was not normally distributed. For all analysis, the difference between data groups was defined significant for P-values below 0.05. Neuroindex was calculated by multiplying the percentage of responding neurons per ganglion with the mean or median response frequency (Buhner et al., 2014).

3. RESULTS

3.1 Plasma osmolality of the guinea pig

No exact value for the plasma osmolality of the guinea pig could be found screening the literature (PubMed). Therefore, plasma osmolality of four animals was measured after they were sacrificed. The mean plasma osmolality was found to be 293.5 ± 2.1 mOsm/kg (Figure 11).

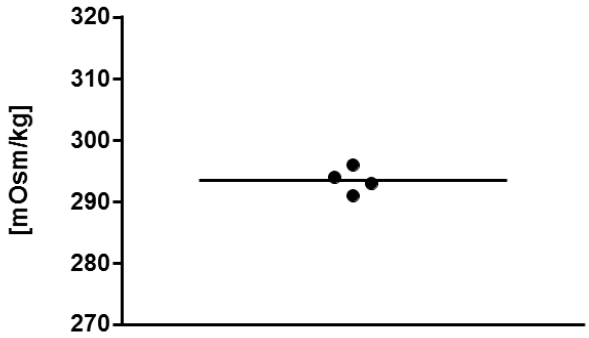

Figure 11: plasma osmolality of the guinea pig.

3.2 Method validation with Fast Green

To test the newly developed application method for large fluid quantities, the fluorescence intensity of a series of known Fast Green concentrations was measured and compared to the fluorescence intensity of the same concentration of Fast Green, applied in the same way as the osmotic stimulus in the experiments studying osmosensitivity. By doing so, the dilution of an applied substance at the site of application could be evaluated. The fluorescence intensity of each concentration was measured 5 times and compared to the fluorescence intensity of the known concentration. The mean accordance of the two curves was 91.0 ± 1.2%. Higher concentrations showed a higher accordance than lower concentrations (Figure 12).

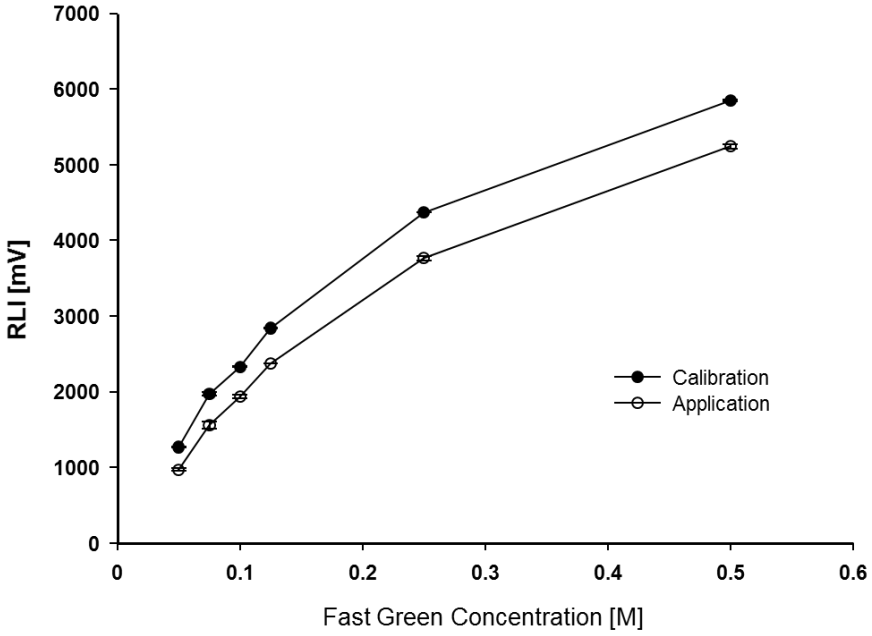

Figure 12: comparison of fluorescence levels of known Fast Green concentrations to Fast Green of the same concentrations applied through the application system.

3.3 Spontaneous activity of SMP neurons

In the experiments testing the effects of a hypoosmolar compared to an isoosmolar solution, spontaneous activity of the cells was measured. On every cell the effect of both solutions was tested in randomised order. Every cell that showed action potential discharge during the first 2 seconds recording period was considered to be spontaneously active, independent from whether the applied solution was hypoosmolar or isoosmolar. Out of all 294 neurons investigated in this series of experiments 31 neurons showed spontaneous activity when the first solution was applied (Figure 13). In median, this was 1.0 [0.0/2.0] cells per ganglion. These neurons fired action potentials with a median frequency of 1.0 [0.5/ 3.0] Hz. When the second solution was applied 25 cells showed spontaneous activity. This was in median 0.0 [0.0/2.0] cells per ganglion. These numbers were not significantly different from application of the first solution. The spontaneous action potential frequency nevertheless was 0.0 [0.0/2.0] Hz before the application of the second solution and significantly lower than before the application of the first solution (Figure 14).

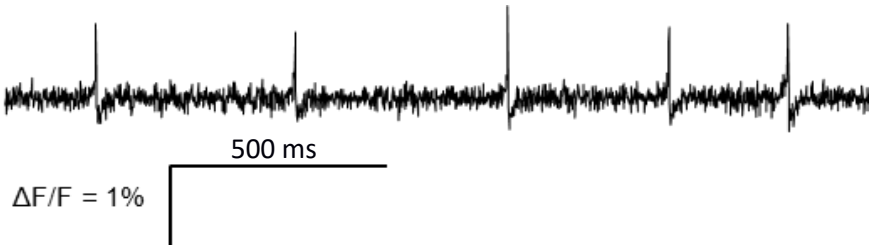

Figure 13: example of spontaneous action potential discharge in a neuron under baseline conditions. Data filtered with highpass filter at 9.9 Hz.

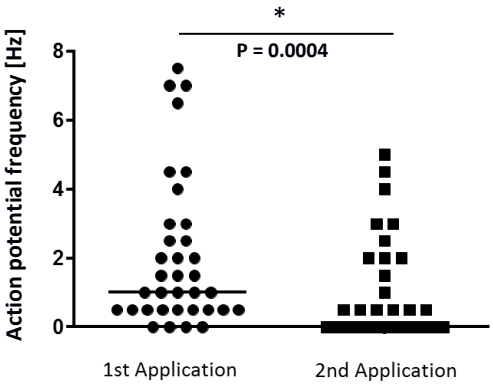

Figure 14: spontaneous action potential frequency in the baseline recording period during the first and the second application. In this analysis, all spontaneously active neurons were analysed. Shapiro-Wilk test revealed a non-Gaussian distribution. Wilcoxon signed rank test revealed a significant difference between the action potential frequencies (P = 0.0004). Each dot represents one neuron.

3.4 Percentage of neurons responding to different osmotic stimuli

In these experiments the percentage of neurons, showing a frequency increase after application of an isoosmolar HEPES solution was compared to the percentage of neurons showing a frequency increase after application of different osmotic stimuli. This was done in a paired experimental design.

94 mOsm/kg: in this set of experiments 294 neurons in 21 ganglia originating from 7 tissues were investigated. 69 of those cells showed action potential discharge after either the isoosmolar or the hypoosmolar solution was applied. After application of the isoosmolar solution per ganglion 7.0 [0.0/15.0] % of the cells showed an increased action potential frequency, while after the application of the hypoosmolar HEPES solution 11.0 [7.0/17.0] % displayed an increase in action potential firing frequency. With a p-value of 0.0642 the values were not significantly different (Figure 15 left).

144 mOsm/kg: here a total of 123 neurons in 9 ganglia originating from 4 tissues were investigated. Per ganglion 18.0 [0.0/41.0] % of the neurons displayed an increase in action potential firing frequency.

This percentage was not significantly different from the percentage of neurons with increased action potential firing frequency after the 94 mOsm/kg hypoosmolar stimulus (P = 0.6470)

394 mOsm/kg: in this set of experiments 102 neurons in 6 ganglia originating from 3 tissues were investigated. 17 of those cells showed action potential discharge after either the isoosmolar or the hyperosmolar solution was applied. After application of the isoosmolar solution per ganglion 6.3 [3.8/19.5] % of the neurons showed an increased action potential frequency. After the application of the hyperosmolar solution 2.4 [0.0/8.3] % of the neurons showed an increase in action potential frequency. Also, these numbers were not significantly different with a p-value of 0.3125 (Figure 15 middle).

494 mOsm/kg: here 190 neurons in 10 ganglia originating from 4 tissues were investigated. 46 of these neurons showed activity either after the isoosmolar or the hyperosmolar solution was applied. After application of the isoosmolar solution per ganglion 3.6 [0.0/13.0] % of the neurons had an increased action potential firing frequency while after the application of the hyperosmolar solution 7.7 [5.9/16.9] % of the neurons displayed an increased action potential frequency. The numbers were not significantly different showing a p-value of 0.0742 (Figure 15 right).

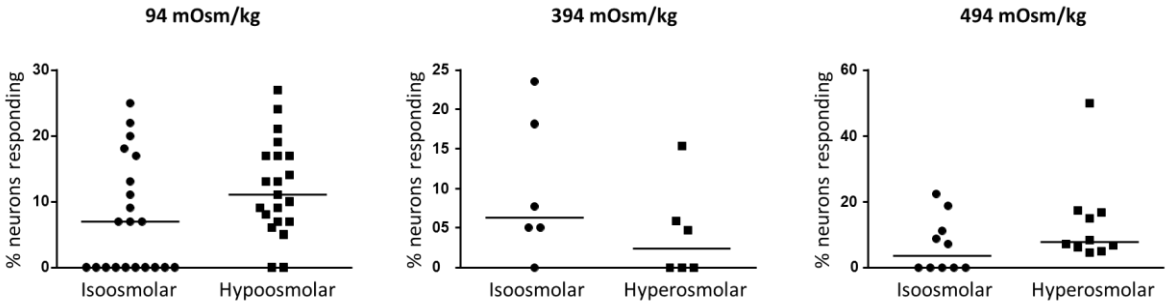

Figure 15: percent of neurons per ganglion showing an increase in action potential firing frequency after application of an isoosmolar, hypoosmolar or hyperosmolar HEPES solution. Shapiro-Wilk test revealed a non-Gaussian distribution for all datasets. Wilcoxon rank sum test revealed no significant difference between % of neurons showing an increase in action potential frequency after isoosmolar HEPES was applied and the % of neurons showing an increase in action potential frequency after an hypoosmolar or hyperosmolar HEPES solution was applied.

3.5 Action potential frequencies after different osmotic stimuli

The action potential frequencies after the application of an isoosmolar HEPES solution were compared to the action potential frequencies after the application of either a hypoosmolar or hyperosmolar solutions in a paired experimental design. Action potential frequencies of all cells that fired at least one action potential were taken into account.

94 mOsm/kg: 69 cells in 21 ganglia originating from 7 tissues showed action potential discharge either after application of the isoosmolar HEPES solution or the hypoosmolar HEPES solution. The action potential firing frequency was 0.0 [0.0/0.3] Hz after the isoosmolar solution was applied and significantly higher with 0.2 [0.0/2.3] after the hypoosmolar HEPES solution was applied. Wilcoxon rank sum test resulted in a p-value of 0.0003 (Figure 16 left).

144 mOsm/kg: 48 cells in 9 ganglia originating from 4 tissues showed action potential discharge either during the first or the second application of a hypoosmolar stimulus. The action potential frequency was 0.7 [0.0/2.7] Hz after the first hypoosmolar stimulation. This was not significantly different from the action potential frequency after the application of the 94 mOsm/kg stimulus (P = 0.1042).

394 mOsm/kg: 17 cells in 6 ganglia originating from 3 tissues showed action potential discharge either after application of the isoosmolar HEPES solution or the hyperosmolar HEPES solution. The action potential firing frequency was 0.5 [0.0/1.3] Hz after the isoosmolar HEPES solution was applied. After application of the hyperosmolar HEPES solution the firing frequency was significantly lower with 0.0 [0.0/0.3] Hz. Wilcoxon rank sum test resulted in a p-value of 0.0342 (Figure 16 middle).

494 mOsm/kg: 46 cells in 10 ganglia originating from 4 tissues showed action potential discharge either after application of the isoosmolar HEPES solution or the hyperosmolar HEPES solution. The action potential firing frequency was 0.0 [0.0/0.4] Hz after the application of the isoosmolar HEPES solution and 0.5 [0.0/1.0] Hz after the application of the hyperosmolar HEPES solution. This difference was significant with a p-value of 0.0009 (Figure 16 right).

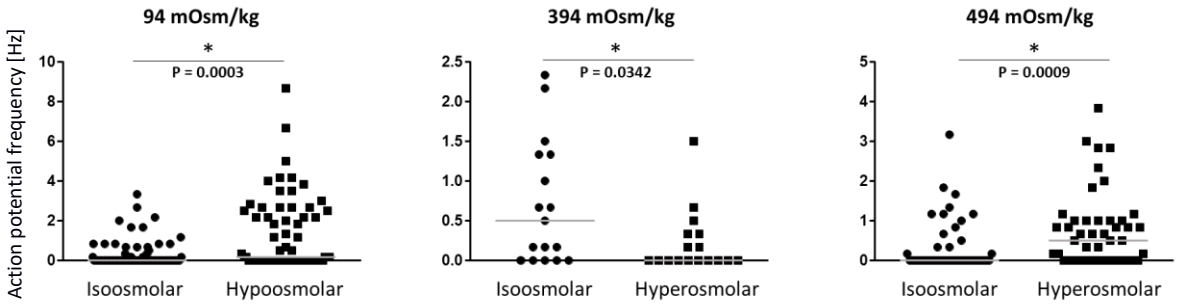

Figure 16: action potential frequency after application of an isoosmolar, hypoosmolar or hyperosmolar HEPES solution. Shapiro-Wilk test revealed a non-Gaussian distribution for all datasets. Wilcoxon rank sum test showed significant differences between the isoosmolar HEPES solution and the hypo- or hyperosmolar HEPES solution for all 3 datasets with p-values of 0.0003, 0.0342 and 0.0009.

Due to the lack of reproducibility of the response (see 3.10 Reproducibility of the neuronal response to osmotic shifts) a paired comparison of action potential frequencies after different osmotic stimuli was not possible. Therefore, the action potential frequencies of the response to a 144 mOsm/kg HEPES solution of 13 cells in 4 ganglia originating from 4 tissues were compared to the action potential frequencies of the response to a 94 mOsm/kg HEPES solution of 40 cells in 12 ganglia coming from 4 tissues. The median action potential frequency after application of the 144 mOsm/kg HEPES solution was 2.7 [0.9/4.3] Hz while it was not significantly different after application of the 94 mOsm/kg HEPES solution being 2.5 [1.0/4.3] Hz (Figure 17).

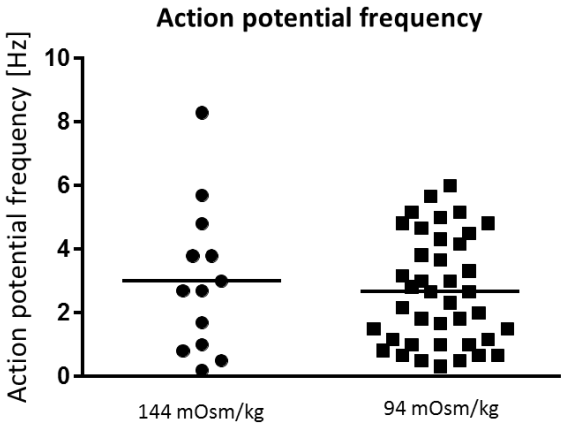

Figure 17: comparison of firing frequencies after application of 144 mOsm/kg HEPES solution and 94 mOsm/kg HEPES solution. Shapiro-Wilk normality test revealed non-Gaussian distribution. Mann Whitney test resulted in a p-value of 0.8823.

3.6 Neuroindex after different osmotic stimuli

The neuroindex per ganglion after the application of isoosmolar HEPES solution was compared to the neuroindex after application of hypoosmolar or hyperosmolar HEPES solution in a paired experimental design.

94 mOsm/kg: the neuroindex after the application of isoosmolar HEPES solution as well as after application of hypoosmolar solution was calculated for 21 ganglia originating from 7 tissues. After application of the isoosmolar HEPES solution the neuroindex was 1.1 [0.0/9.9] while it was 21.7 [3.8/ 40.1] after application of the hypoosmolar HEPES solution onto the same ganglia. With a p-value of 0.0010 this difference was significant (Figure 18 left).

144 mOsm/kg: the neuroindex after the first application of a 144 mOsm/kg HEPES solution was 0.0 [0.0/85.6]. This was not significantly different from the neuroindex after the application of the 94 mOsm/kg HEPES solution (P = 0.7149).

394 mOsm/kg: the neuroindex after the application of isoosmolar HEPES solution as well as after application of hyperosmolar solution was calculated for 6 ganglia originating from 3 tissues. After the application of the isoosmolar HEPES solution the neuroindex for these ganglia was 8.3 [1.2/23.6] while it was 1.2 [0.0/6.0] after the application of the hyperosmolar solution. Nevertheless, this difference was not significant with a p-value of 0.3125 (Figure 18 middle).

494 mOsm/kg: the neuroindex after the application of isoosmolar HEPES solution as well as after application of hyperosmolar solution was calculated for 10 ganglia originating from 4 different tissues. After the application of the isoosmolar HEPES solution the neuroindex of these ganglia was 3.5 [0.0/19.0] while it was 7.7 [3.3/18.7] after the application of the hyperosmolar solution. Nevertheless, also this difference was not statistically significant with a p-value of 0.1055 (Figure 18 right).

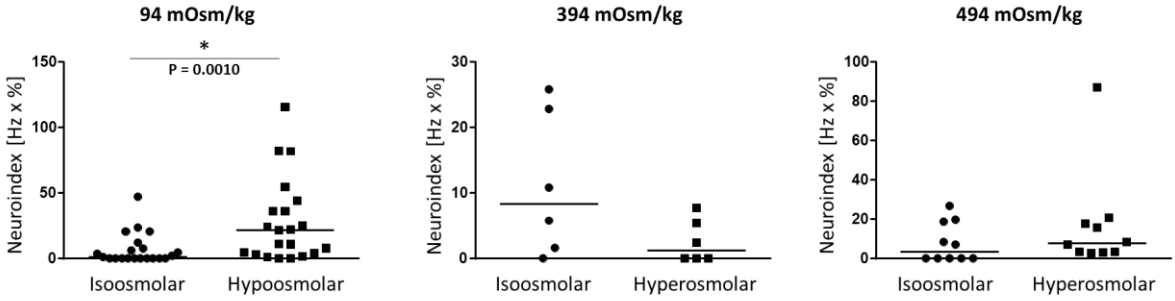

Figure 18: neuroindex after the application of an isoosmolar, hypoosmolar and hyperosmolar solution. Shapiro-Wilk test revealed a non-Gaussian distribution for all datasets. Wilcoxon rank sum test showed a significant difference in neuroindex only for the application of the hypoosmolar solution compared to the neuroindex after the isoosmolar solution (p = 0.0010). For both hyperosmolar stimuli, the difference in neuroindex after isoosmolar and stimulus application was not significant with p-values of 0.3125 and 0.1055 respectively.

3.7 Investigation of inhibitory effect of hyperosmolar solutions

Due to the contradictory results concerning the activating effect of hyperosmolar solutions on submucosal neurons it was tested, whether the application of the hyperosmolar solution had any inhibitory effect on the neurons. To do so, changes in action potential frequency of 10 spontaneously active cells in 4 ganglia originating from 2 guinea pigs were analysed after a hyperosmolar solution with an osmolality of 394 mOsm/kg was applied (Figure 19 left). The same procedure was performed for 13 neurons in 3 ganglia originating from 2 animals which were treated with a 494 mOsm/kg HEPES solution (Figure 19 right).

The spontaneous action potential frequency before the application of the 394 mOsm/kg HEPES was 1.5 ± 0.7 Hz and was not significantly changed after the hyperosmolar solution was applied (1.4 ± 1.3 Hz) (P = 0.8648). Interestingly the application of the 494 mOsm/kg HEPES solution led to a significant increase in action potential firing frequency in spontaneously active neurons from 1.5 ± 0.9 Hz before the application to 3.0 ± 1.5 Hz after the application (P = 0.0007).

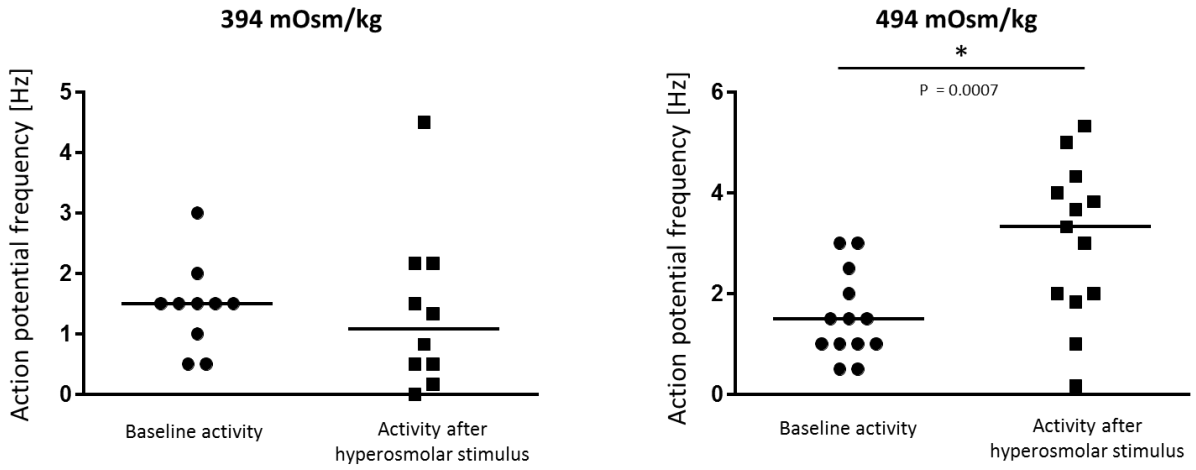

Figure 19: comparison of action potential firing frequencies of spontaneously active cells before and after the application of a hyperosmolar stimulus. Shapiro-Wilk test showed a Gaussian distribution of the data in all datasets. Left: effect of a 394 mOsm/kg HEPES solution on the action potential frequency of spontaneously active neurons. Paired t-test showed no difference (p = 0.8648). Right: effect of a 494 mOsm/kg HEPES solution on the action potential frequency of spontaneously active neurons. Paired t-test revealed a significant difference (P = 0.0007).

3.8 Latency of action potential discharges after osmotic shifts

After a hypoosmolar or hyperosmolar HEPES solution was applied, the latency of the first action potential discharge was measured. This was done for two different hypoosmolar and one hyperosmolar stimulus in experiments using the continuous recording paradigm. In order to be able to make a clear statement about the latency of the response only cells that showed no spontaneous activity whatsoever were included in this analysis.

The latency of the response of 27 neurons in 10 ganglia originating from 7 animals after application of 94 mOsm/kg HEPES was analysed (Figure 20). The period between application of the hypoosmolar solution and the first action potential fired was found to be 6.1 [4.7/7.8] seconds. For 27 neurons in 10 ganglia coming from 3 tissues the latency of the response to a hypoosmolar HEPES solution with an osmolality of 144 mOsm/kg was investigated and found to be 4.6 [1.9/7.2] seconds which was not significantly different from the more extreme stimulus ($p = 0.1317$). After application of a hyperosmolar stimulus with an osmolality of 394 mOsm/kg the latency to the first action potential discharge was 4.4 [1.5/6.5] seconds. This was not significantly different from the latency after application of the mild hypoosmolar stimulus ($p = 1$) but significantly different from the application of the strong hypoosmolar stimulus ($p = 0.0174$) (Figure 21).

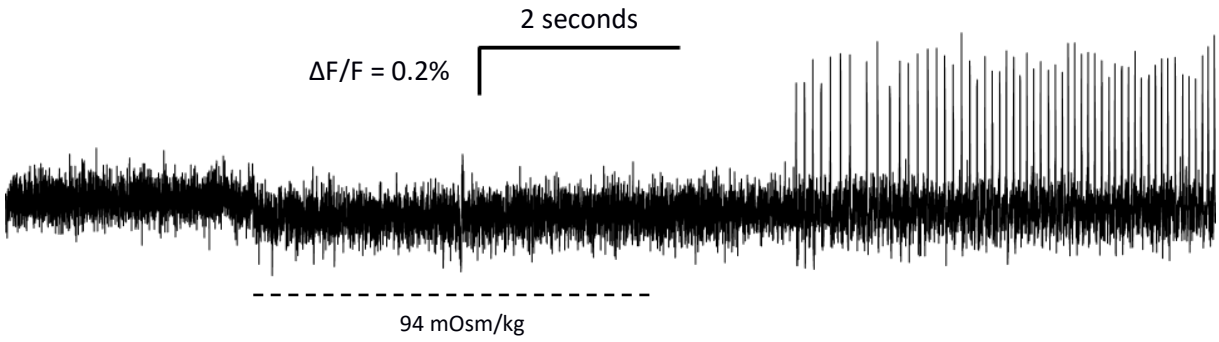

Figure 20: action potential discharge after hypoosmolar stimulation. The cell starts firing action potentials around two seconds after the hypoosmolar solution was applied.

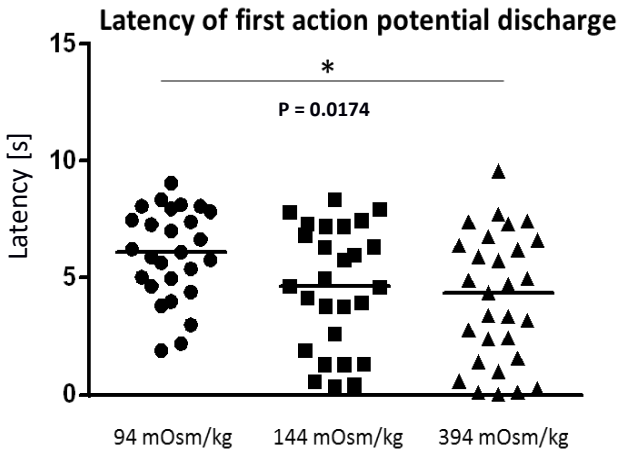

Figure 21: comparison of the latency of action potential discharge after application of different osmotic stimuli. Shapiro-Wilk test showed a non-Gaussian distribution for all datasets. Kruskall-Wallis test showed a significant difference in response latency only between the 94 mOsm/kg stimulus and the 394 mOsm/kg stimulus (P = 0.0174). For this analysis, only cells that showed no spontaneous action potential discharge were considered.

Table 1: comparison of main findings in response to different osmotic stimuli

	94 mOsm/kg	**144 mOsm/kg**	**394 mOsm/kg**	**494 mOsm/kg**
% neurons responding	11.0 [7.0/17.0]	18.0 [0.0/41.0]	2.4 [0.0/8.3]	7.7 [5.9/16.9]
Spike frequency [Hz]	0.2 [0.0/2.3]	0.7 [0.0/2.7]	0.0 [0.0/0.3]	0.5 [0.0/1.0]
Neuroindex	21.7 [3.8/40.1]	0.0 [0.0/85.6]	1.2 [0.0/6.0]	7.7 [3.3/18.7]
Latency [s]	6.1 [4.7/7.8]	4.6 [1.9/7.2]	4.4 [1.5/6.5]	
Reproducibility	32.5 %	44.8 %		

3.9 Kinetics of neuronal responses to osmotic shifts

Criteria for the classification of cells as osmosensitive

The interval recording paradigm was used to investigate the kinetics of the responses to hypoosmolar and hyperosmolar stimuli. Since a significant number of neurons showed spontaneous action potential discharge it was decided to establish criteria by which one could distinguish responders from non-responders.

1) An increase in action potential firing frequency after the application of an osmotic shift.
2) A higher variance of action potential frequency across the four recording periods of the osmotic shift compared to the four recording periods of the isoosmolar application

Response kinetics after application of 94 mOsm/kg HEPES solution

Out of a total number of 294 neurons, 30 neurons (10.2 %) fulfilled both criteria and therefore were defined as osmosensitive enteric neurons. Per ganglion 11.4 ± 7.5 % of all cells responded to the hypoosmolar stimulus. Out of 21 investigated ganglia 17 contained at least one cell that was sensitive to the hypoosmolar stimulus. The action potential frequency averaged over the three recording periods in cells classified as responders after application of an isotonic solution was 0.0 [0.0/0.17] Hz and 2.6 [1.8/3.6] Hz after hypoosmolar stimulation (Figure 22).

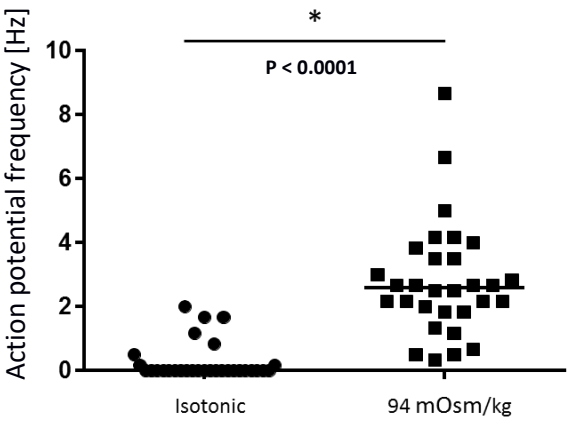

Figure 22: averaged action potential frequency in the three recording periods after application of an isotonic or a hypotonic solution in cells defined as responders (N=7/15/30). Shapiro-Wilk test revealed a non-Gaussian distribution of the values. Wilcoxon rank sum test revealed a significant difference in action potential firing frequency between the two applications (P < 0.0001).

In the vast majority of osmosensitive neurons the discharge of action potentials did not start immediately after the hypoosmolar solution was applied but with a delay of several seconds (Figure 23). 26 (87%) of the 30 cells classified as responders showed the highest action potential frequency in the second recording period (10-12 seconds after the stimulus was applied). Osmosensitive neurons fired 13.0 [5.5/ 18.5] action potentials during the whole recording period, resulting in a maximum frequency of 6.5 [2.8/ 9.3] Hz. In comparison, the maximum frequency after isotonic application was 0.0 [0.0/ 0.0] Hz. Comparison of the baseline activity with every other recording period under isoosmolar as well as hypoosmolar conditions (Friedman Test) revealed that the action potential frequency in none of the recording periods after the isoosmolar application differed significantly from basal activity. After the hypoosmolar application, nevertheless action potential frequencies of the second and the third recording period were significantly different from basal activity (Figure 24).

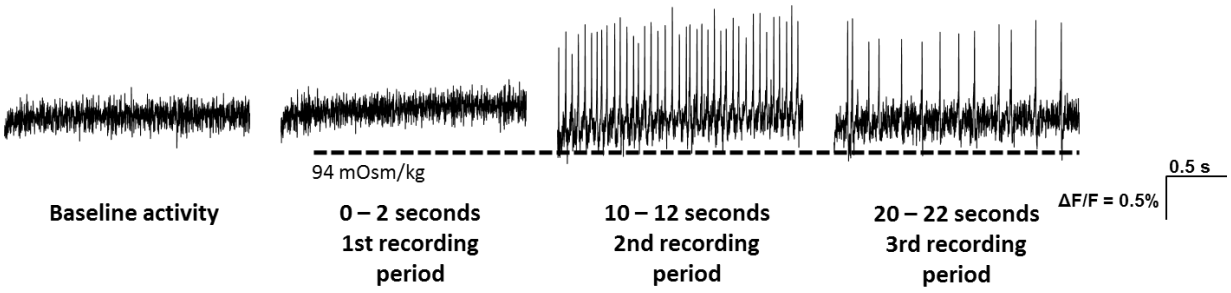

Figure 23: representative neuronal response in a VSD experiment after application of a hypoosmolar solution. Between each of the recording periods a pause of 8 seconds without illumination is adhered. The broken line indicates the time where the cells were under hypoosmolar conditions. The highest action potential frequency can be detected in the recording period from 10-12 seconds after application of the hypoosmolar HEPES solution.

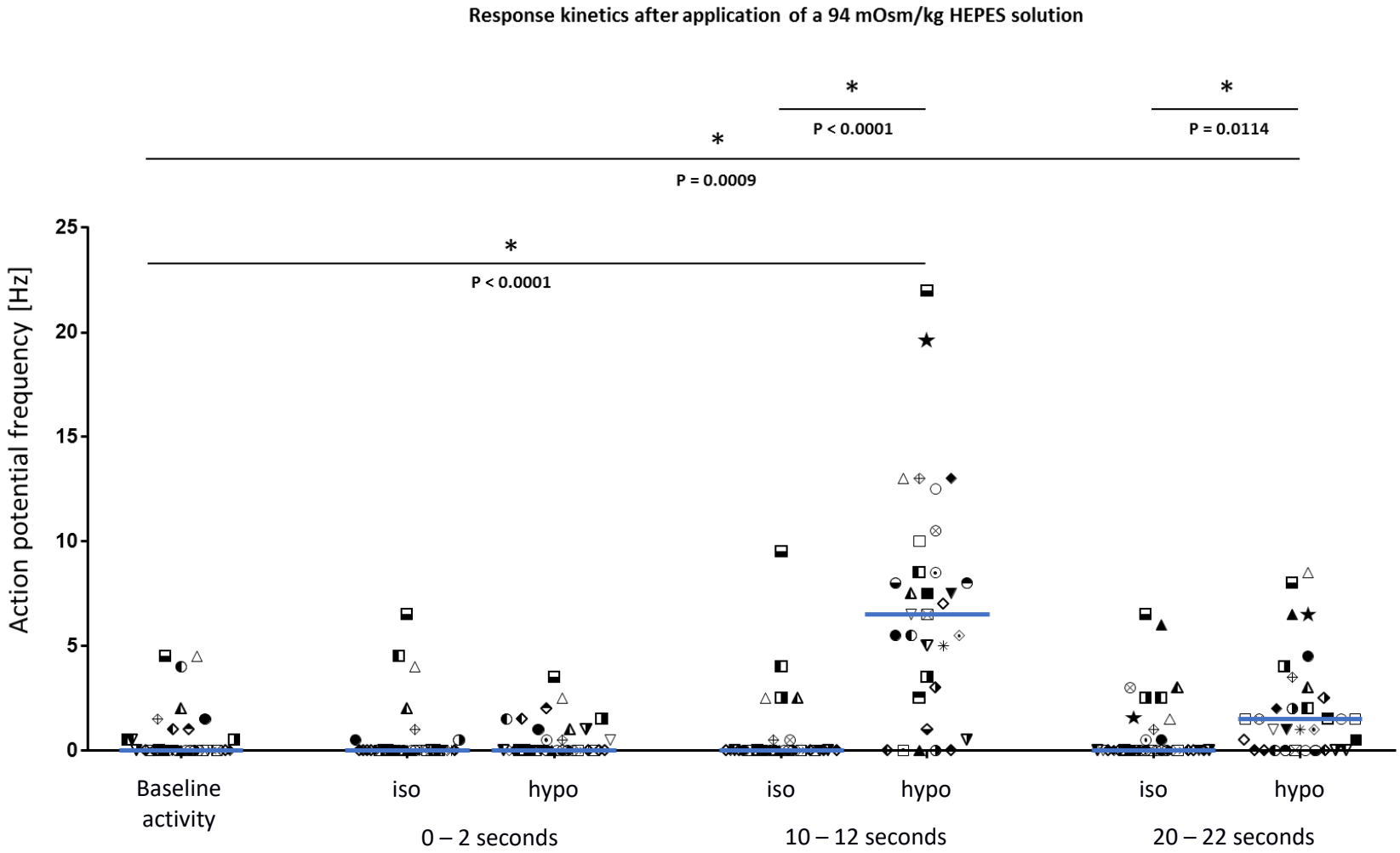

Figure 24: temporal distribution of action potential frequencies after application of an isoosmolar or hypoosmolar solution. Each symbol represents a certain neuron. Baseline activity was compared to every other recording period under isoosmolar as well as hypoosmolar conditions (Friedman test). For the last two recording periods activity under isoosmolar and hypoosmolar conditions was compared.

Response kinetics after application of 144 mOsm/kg HEPES solution

Out of a total number of 123 neurons that were investigated in this series of experiments, 29 neurons were considered responders (23.6 %). Comparison of the firing frequencies of the responsive cells with the baseline action potential firing frequencies revealed no difference between baseline activity and the first recording period (0-2 seconds after the stimulus). Firing frequencies during the second and the third recording period (5.0 [2.8/ 8.5] Hz and 2.5 [0.3/ 5.3] Hz respectively) however differed significantly from baseline activity (Figure 25).

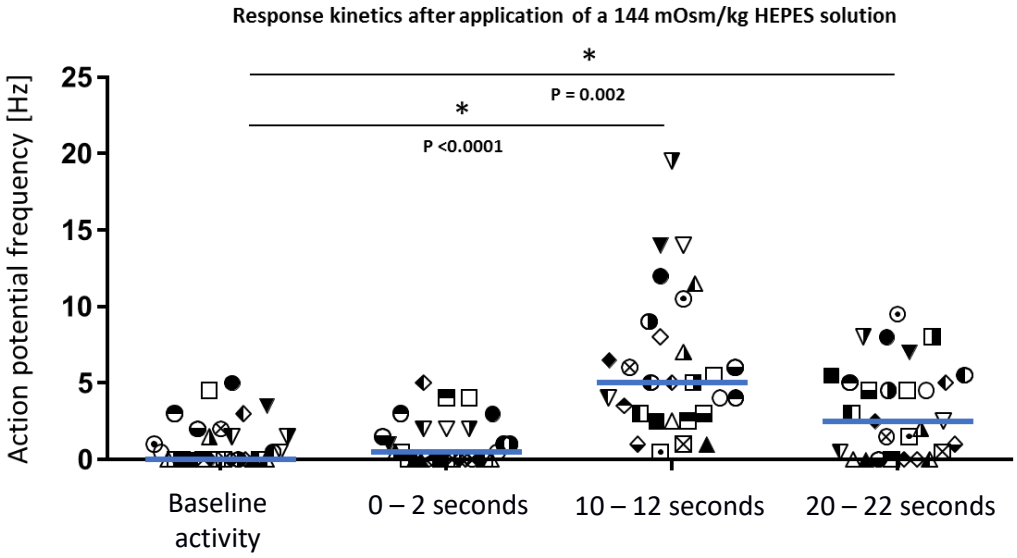

Figure 25: response kinetics after application of a 150 mOsm/kg solution. Shapiro-Wilk test revealed a non-Gaussian distribution for all four data sets. Action potential frequencies of each recording period under hypoosmolar conditions were tested for significance against the baseline activity with Friedman test. Adjusted P values were calculated with Dunn´s multiple comparison test. Frequencies of the second and the third recording period under hypoosmolar conditions were found to be significantly different from baseline activity levels with P values of < 0.0001 and 0.002.

Response kinetics after application of 394 mOsm/kg

Out of the 102 neurons only 4 (3.9%) fulfilled the criteria for responders. Nevertheless, not even for these cells a significant increase in action potential firing frequency was evident. When the median frequency after the application of an isoosmolar solution 1.0 [0.2/2.6] Hz was compared to that of a hyperosmolar solution 1.8 [0.7/3.9] Hz no significant difference was found (p = 0.1250). Comparison of the action potential frequencies of each trial under isoosmolar conditions with the action potential frequencies of each trial under hyperosmolar conditions revealed that neither under isoosmolar nor under hyperosmolar conditions the action potential frequency of any trial differed significantly from baseline activity. The only significant difference could be found between the action potential frequency

of the 10-12 second recording period under isoosmolar conditions and that of the same period after application of the hyperosmolar solution (Figure 26).

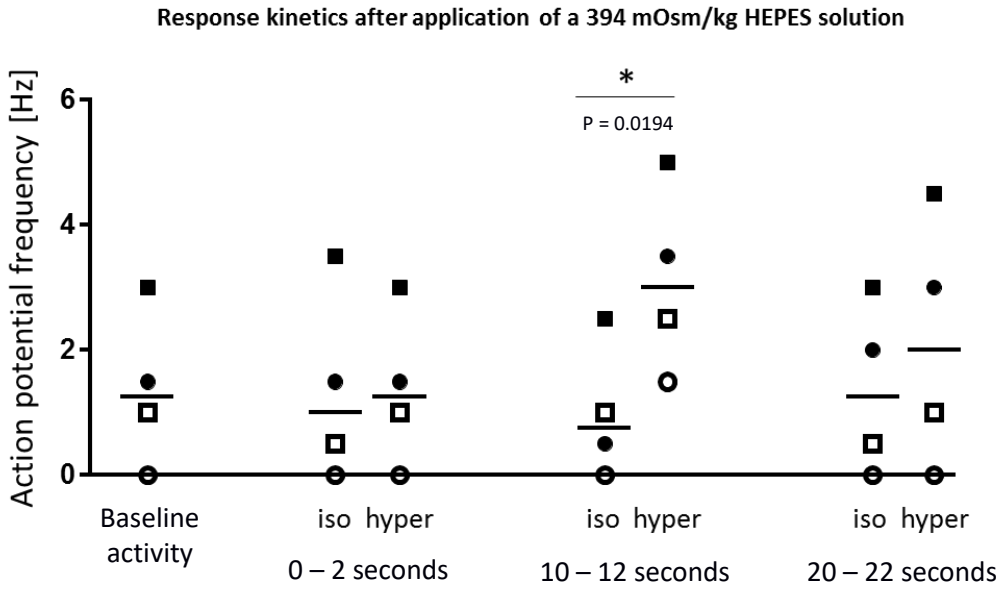

Figure 26: response kinetics after application of a 394 mOsm/kg solution. Shapiro-Wilk test revealed a non-Gaussian distribution for all four data sets. Action potential frequencies of each recording period under hyperosmolar conditions were tested for significance against the baseline activity with Friedman test. Adjusted P values were calculated with Dunn´s multiple comparison test. The only significant difference was found in the second recording period after the hyperosmolar stimulus was applied. There the action potential frequency was significantly higher after the hyperosmolar stimulus, than it was after the isoosmolar application (P = 0.0194).

Response kinetics after application of 494 mOsm/kg

Out of 190 neurons treated with the stimulus 20 neurons (10.5%) in 10 ganglia originating from 4 tissues fulfilled the criteria to be classified as responders. The average frequencies over the three recording periods after the stimulus and after application of an isoosmolar HEPES solution were found to be significantly different. After application of an isoosmolar stimulus this frequency was 0.0 [0.0/0.9] Hz while it was 1.0 [0.5/2.5] Hz after the application of the hyperosmolar HEPES solution ($P < 0.0001$). Comparison of the action potential frequencies of each trial under isoosmolar conditions with the action potential frequencies of each trial under hyperosmolar conditions revealed that the action potential frequency after the application of the isoosmolar solution was increased in none of the recording periods, while it was significantly increased after the application of the hyperosmolar HEPES solution in the second and third recording period after the stimulus was applied (Figure 27)($P < 0.0001$ for both recording periods). Further the action potential frequency in the second and third recording

period was also increased significantly after the application of the hyperosmolar HEPES compared to the application of the isoosmolar HEPES solution (P = 0.0070 and P = 0.0047 respectively).

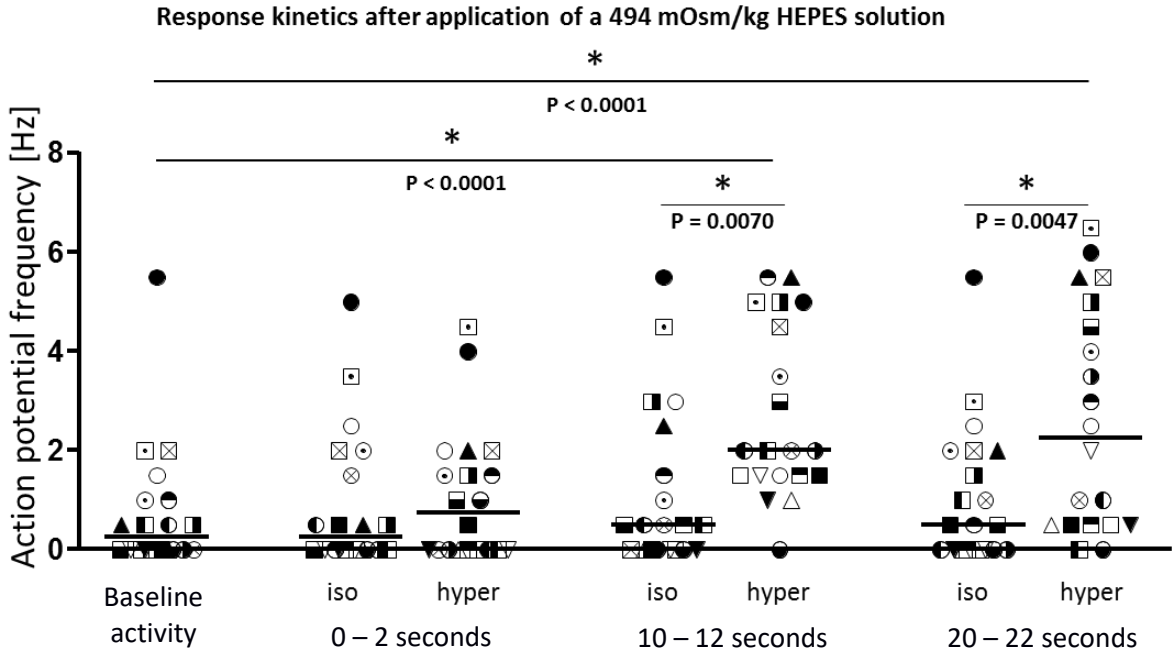

Figure 27: response kinetics after application of a 494 mOsm/kg solution. Shapiro-Wilk test revealed a non-Gaussian distribution for all four data sets. Action potential frequencies of each recording period under hyperosmolar conditions were tested for significance against the baseline activity with Friedman test. Adjusted P values were calculated with Dunn´s multiple comparison test. The action potential frequencies in the 10-12 seconds recording period after the hyperosmolar HEPES solution was applied were found to be significantly different from baseline activity. The same holds true for the action potential frequencies in the last recording period (P < 0.0001 for both data sets). Further, the action potential frequency in the second trial was significantly higher after application of the hyperosmolar HEPES compared to the action potential frequency after application of the isoosmolar solution in the same recording period (P = 0.0070). The same holds true for the action potential frequency in the last recording period (P = 0.0047).

3.10 Reproducibility of the neuronal response to osmotic shifts

Reproducibility of the neuronal response to 94 mOsm/kg HEPES

A total number of 218 cells in 12 ganglia originating from 4 different animals was investigated. Out of those cells 40 (18.3 %) responded to the first application of the hypoosmolar stimulus. After the second application of the stimulus only 13 (6.0 %) were activated, resulting in a reproducibility rate of 32.5 % (Figure 28). There was no cell that was only activated after the second application. The mean action potential firing frequency of the 13 cells that responded to both application was 3.4 ± 1.9 Hz after the first application. After the second application, it was significantly lower with 1.9 ± 1.5 Hz (Figure 29). Noteworthy the baseline activity was higher before the stimulus was applied a second time. The action potential frequency of the baseline activity was subtracted from the action potential frequency after the application of the hypoosmolar solution to normalise activity levels. Therefore, the resulting frequency after activation by the stimulus was lowered as an effect of increased baseline activity.

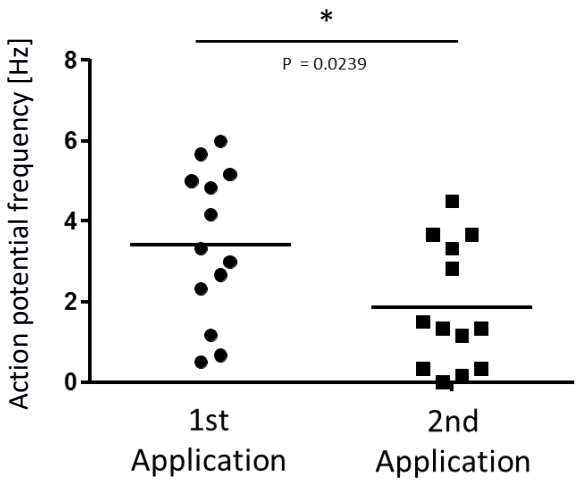

Figure 28: comparison of the response frequencies after two applications of a hypoosmolar solution. Each dot represents one neuron. Shapiro-Wilk test revealed a Gaussian distribution of the data. A paired t-test showed a significantly lower action potential frequency after the second application of the hypoosmolar stimulus (two tailed p value = 0.0239).

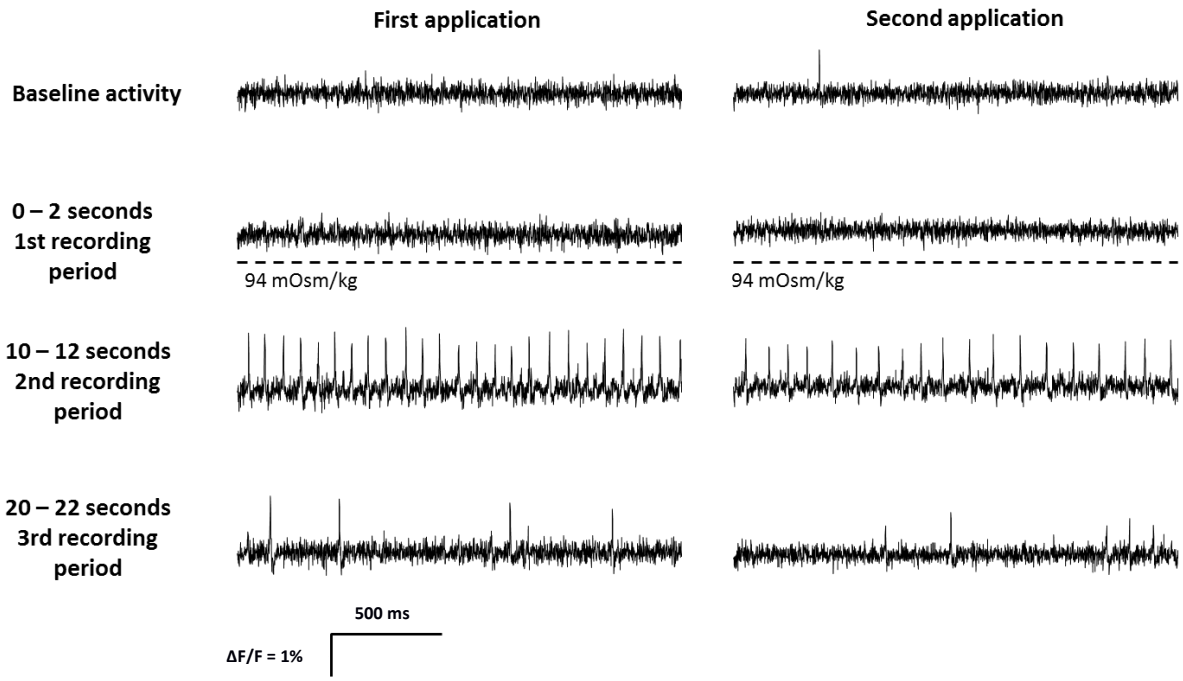

Figure 29: response patterns after a repeated hypoosmolar stimulus. In-between the two stimulations an interval of 20 minutes was adhered. Data filtered with highpass filter at 9.9 Hz.

Reproducibility of the neuronal response to 144 mOsm/kg HEPES

In this series of experiments a total number of 123 neurons in 9 ganglia coming from 4 tissues was investigated. Out of those cells 29 (23.5 %) responded to the first application of the hypoosmolar solution. To the second application 13 neurons (10.6 %) responded, resulting in a reproducibility rate of 44.8 % which is slightly higher than the 32.5 % reproducibility rate of the 94 mOsm/kg stimulus. Firing frequencies of the 13 cells that responded to both stimuli did not differ significantly being 2.7 [0.9/ 4.3] Hz after the first application and 1.3 [1.0/ 4.7] Hz after the second application (Figure 30).

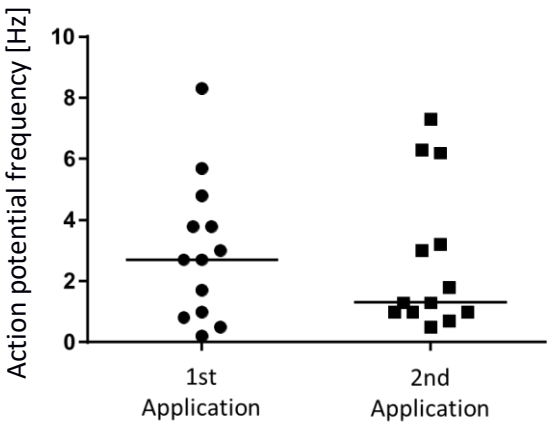

Figure 30: comparison of firing frequencies after two applications of 144 mOsm/kg HEPES solution. Displayed are only cells that responded to both applications. Each dot represents one cell. Shapiro-Wilk test for normality revealed a non-Gaussian distribution of the data. Wilcoxon rank sum test revealed no significant difference in action potential frequency between the two applications (P = 0.4441).

3.11 Influence of the concentration of NaCl on the neuronal response to osmotic shifts

A total of 109 neurons in 7 ganglia coming from 7 tissues were treated with a hypoosmolar low NaCl HEPES as well as with a HEPES solution where the osmolality was reduced by diluting it with distilled water. Out of the 109 neurons 19 (17%) showed action potential discharge after the low NaCl HEPES solution was applied while 14 neurons (13%) showed action potential discharge after 94 mOsm/kg HEPES solution diluted with distilled water was applied. 78% of the neurons responding to the solution diluted with water responded also to the low NaCl hypoosmolar solution. The other way around, 57% of the neurons responding to the low NaCl solution responded to the HEPES solution diluted with water. Comparison of the action potential firing frequency as well as the latency of the neuronal response in all neurons responding to both stimuli revealed no significant difference (Figure 31). The action potential frequency was 3.6 ± 2.2 Hz after the application of the low NaCl solution and 4.2 ± 2.1 Hz after application of HEPES solution which was diluted with water. The latencies of the neuronal responses were also not significantly different being 7.3 [4.2/ 7.9] s after application of the low NaCl solution and 5.3 [4.5/ 7.5] s after the application of the HEPES solution which was diluted with water.

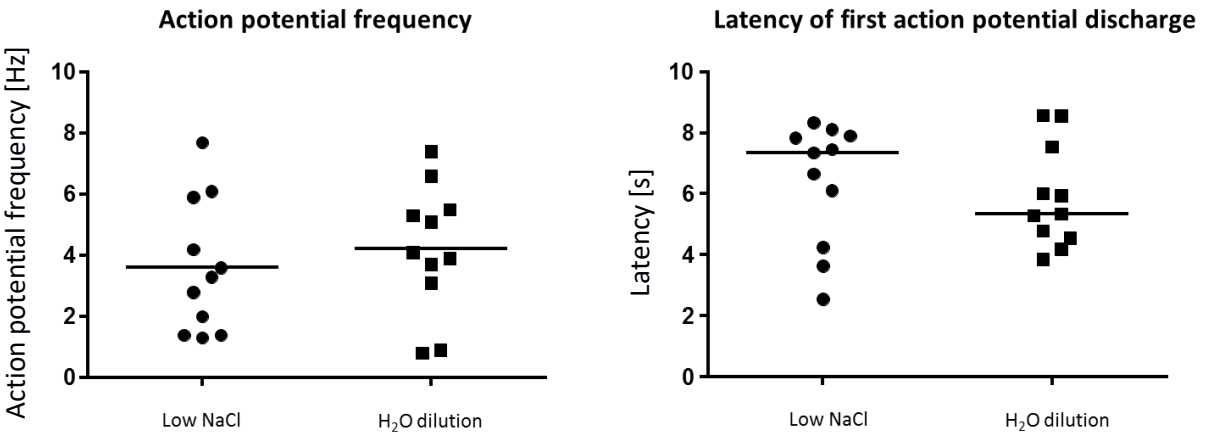

Figure 31: response frequency and latency after application of the low NaCl solution and the full dilution. Each dot represents one neuron. Left: action potential frequency after hypoosmolar stimulation. Shapiro-Wilk test showed normal distribution of both datasets. Paired t-test revealed no significant difference in action potential frequency (P = 0.4318); Right: latency of response onset after hypoosmolar stimulation. Shapiro-Wilk test revealed a non-Gaussian distribution of the data. Wilcoxon rank sum test showed no significant difference in latency of response onset (P = 0.4648).

3.12 Changes in $[Ca^{2+}]_{in}$ after osmotic stimulation

Changes in $[Ca^{2+}]_{in}$ after hypoosmolar stimulation of submucosal ganglia

A series of Ca^{2+}- imaging experiments was conducted to investigate intracellular Ca^{2+}- levels after stimulation with a hypoosmolar solution. 6 ganglia coming from 3 animals were analysed using the Ca^{2+} sensitive probe Fluo-4 AM. The exact number of cells in these ganglia could not be determined due to the fact that in contrast to Di-8-ANEPPS, Fluo-4 does not incorporate into the cell membrane but rather stains the whole cytoplasm, not allowing the distinction of single cells in stained ganglia. Therefore, single cells can only be distinguished in case of a change in $[Ca^{2+}]_{in}$ which is displayed as a change in fluorescence intensity. Per ganglion 5.2 ± 2.9 cells showed an increase in $[Ca^{2+}]_{in}$ after stimulation with a 94 mOsm/kg solution, which is more than double the number of cells showing action potential discharge after treatment with the same stimulus (1.6 ± 1.1 neurons per ganglion). Noteworthy no change in $[Ca^{2+}]_{in}$ was detectable after application of an isoosmolar solution.

The peak ΔRLI after application of the hypoosmolar stimulus was 97.2 ± 39.1 % and was reached after a period of 14.3 ± 5.2 seconds (Figure 32). The increase in $[Ca^{2+}]$ started with a latency of 2.7 ± 0.9 seconds (Figure 33), significantly earlier as the action potential discharge observed in experiments using the VSD technique.

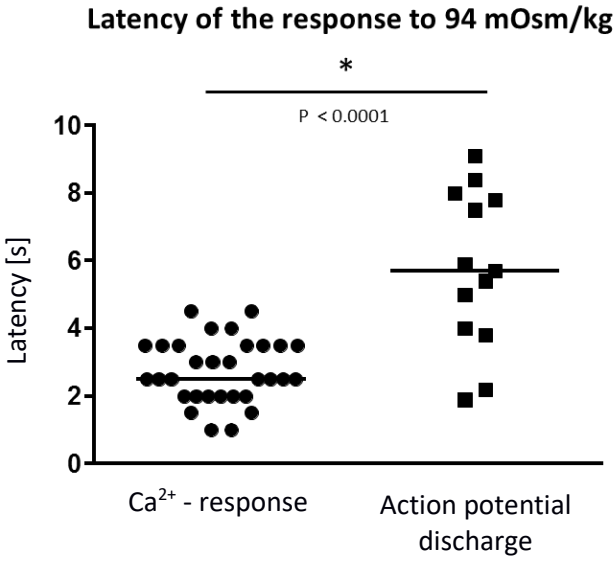

Figure 32: latency of Ca^{2+}- responses and action potential discharge after hypoosmolar stimulation (94 mOsm/kg) of enteric neurons. Shapiro-Wilk test revealed a Gaussian distribution for both datasets. Unpaired t-test revealed a significant difference of the latency of the response onset (P < 0.0001).

Table 2: responses to hypoosmolar stimulation in VSD- imaging and Ca^{2+}- imaging experiments. In Ca^{2+}-imaging experiments more cells respond to the stimulus and the response starts significantly earlier.

	Ca^{2+}- imaging	*VSD- imaging*
Responding cells per ganglion	5.2 ± 2.9	1.6 ± 1.1
Latency [s]	2.7 ± 0.9	5.7 ± 2.2
Peak of response [s]	14.3 ± 5.2	10 – 12

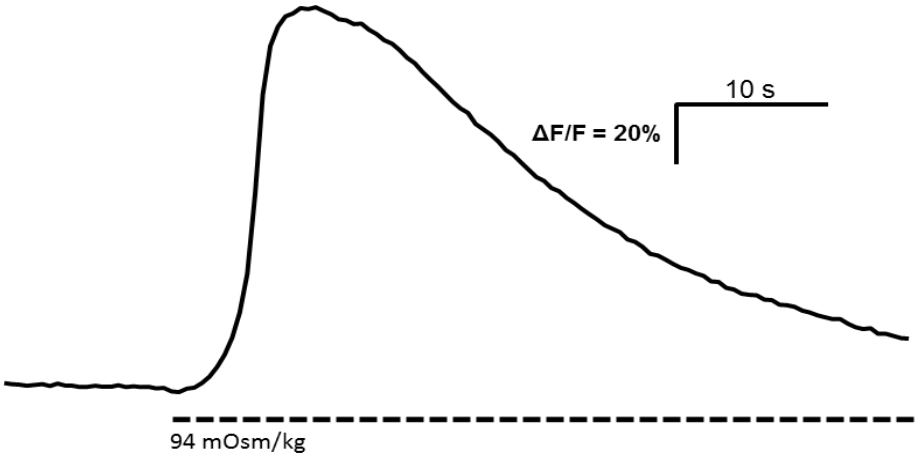

Figure 33: Ca^{2+} - response after application of a hypoosmolar solution recorded with a framerate of 2 Hz. The broken line indicates the time at which the osmotic stimulus was applied.

Changes in $[Ca^{2+}]_{in}$ after hyperosmolar stimulation of submucosal ganglia

Application of a hyperosmolar HEPES solution with an osmolality of 494 mOsm/kg to five different ganglia originating from two animals did not provoke any detectable changes in $[Ca^{2+}]_{in}$.

3.13 Changes in cell volume after hypoosmolar stimulation

Application of a 94 mOsm/kg HEPES solution caused rapid and transient swelling in the majority of submucosal enteric neurons. High resolution images of 3 ganglia originating from 3 animals revealed changes of visible cell surface area in the range of 5-19% within the first 2 seconds after the extracellular osmolality was decreased (Figure 34). The mean change in visibly cytoplasmic area after hypoosmolar stimulation was 10.4 ± 5.6 % (n = 5 cells). Within 4 to 5 seconds after the stimulus was given visible cytoplasmic area decreased again to its initial size, although the hypoosmolar conditions in the extracellular space still prevailed. Noteworthy, not all cells showed an increase in visible cytoplasmic area after hypoosmolar stimulation and in a number of cells the visible cytoplasmic area even decreased under hypoosmolar conditions. Due to the limitations of the two-dimensional imaging

method which was used, no definite claims can be made toward changes in cytoplasmic volume after hypoosmolar stimulation.

The next step was to measure specifically the changes in cytoplasmic area of cells that responded to a hypoosmolar stimulus. Interestingly measurements of the cytoplasmic area of 7 cells identified as osmosensitive showed a decrease of 8.5 ± 4.2 % under hypoosmolar conditions. In all of those cells the maximum change in visible cytoplasmic area was reached within the first seconds under hypoosmolar conditions. After application of an isoosmolar solution, no change in cell size nor in cell shape could be observed.

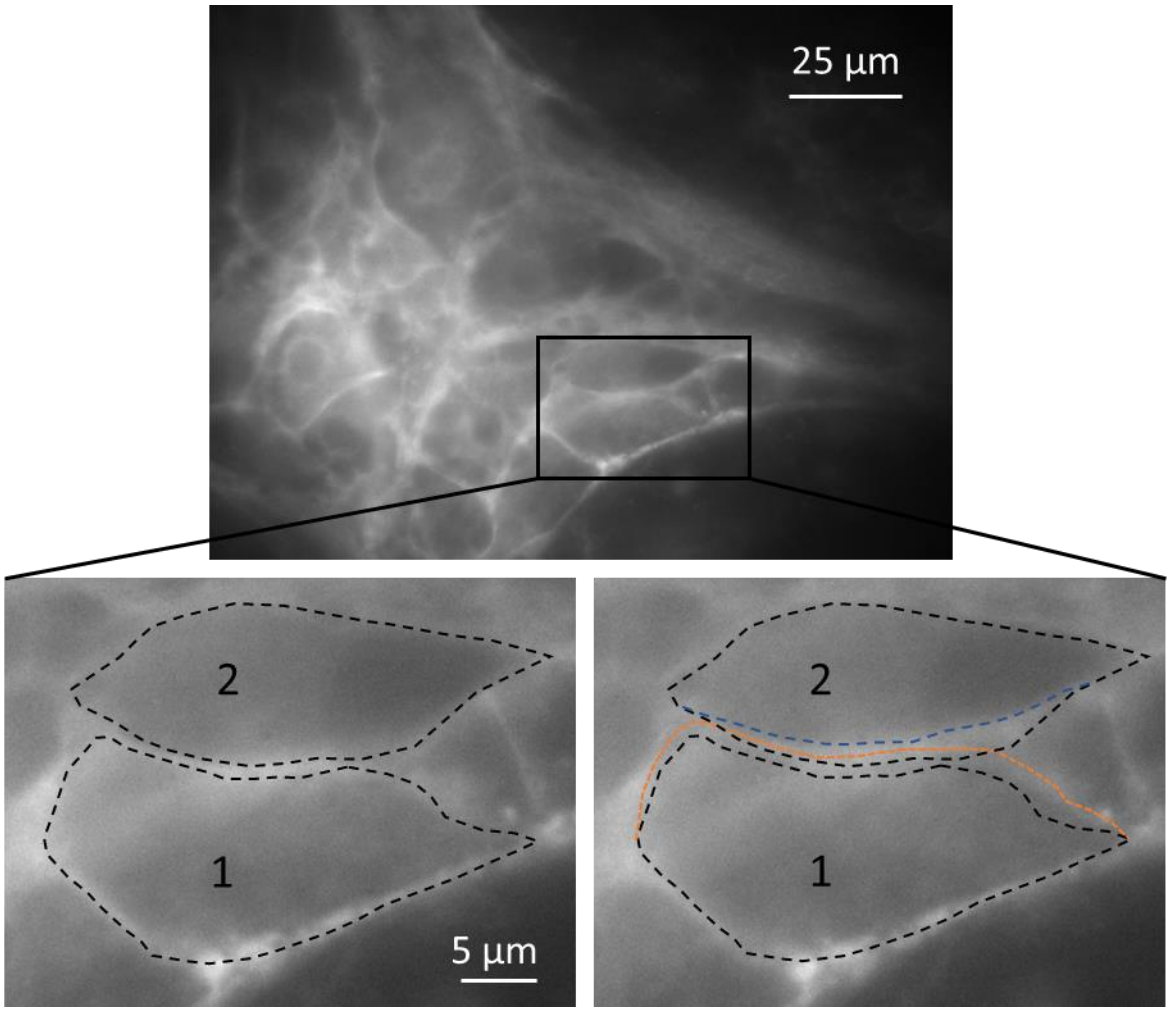

Figure 34: example of cell volume changes under hypoosmolar conditions. The upper image shows a ganglion in a VSD experiment stained with Di-8-ANEPPS. The two lower pictures are excerpts of the first picture. The left picture shows a group of cells at a time point before the hypoosmolar HEPES solution was applied. The picture on the right side shows the same cells after 8 seconds under hypoosmolar conditions. To visualise changes in cell volume the outline of the cells before stimulation have been marked with a broken line in black. The orange line indicates the altered shape of cell 1 after the stimulation while the blue line indicates the altered shape of cell 2 after the stimulation. While the visible surface area of cell 1 clearly is increased after the application of the hypoosmolar HEPES solution, the area of cell two is decreased.

3.14 Effect of ruthenium red on the Ca^{2+}- response to hypoosmolar stimuli

The number of cells per ganglion which responded to a hypoosmolar stimulus of 94 mOsm/kg, did not change significantly by adding 10 µM ruthenium red to the perfusion HEPES solution. Prior to the addition of ruthenium red on average 4.0 [3.0/ 7.8] cells per ganglion responded to the hypoosmolar stimulus. Under the influence of 10 µM ruthenium red this number decreased to 3.0 [2.3/ 4.0] *(P = 0.58)* and remained stable at 3.0 [0.0/ 4.8] *(p = 0.58)* even after the washout which took at least 30 minutes (Figure 35). Extension of the washout period to 1 hour did not increase the number of responsive cells after washout.

The maximum change in RLI was also affected by ruthenium red (Figure 36). When taking all responding cells into account there was a significant difference in maximum RLI between the hypoosmolar stimulation and the hypoosmolar stimulation in combination with ruthenium red. The change in RLI after hypoosmolar stimulation without ruthenium red was 99.0 [68.6/ 121.8] % and was decreased to 5.5 [0.0/ 55.9] % during the perfusion with 10 µM ruthenium red. After a 30-minute washout period with HEPES solution the RLI in response to hypoosmolar stimulation was still significantly reduced compared to the first application (4.8 [0.0/ 31.8] %). Due to the fact that not all cells responded to the third application the dataset was reanalysed taking only cells into account that showed increase in $[Ca^{2+}]_{in}$ in the last recording after the washout (reproducible responses). These cells showed an RLI increase of 112.3 [73.5/ 130.0] % after the first stimulation. Under the influence of ruthenium red, the RLI was significantly decreased to 42.3 [5.5/ 71.3] % and stayed significantly decreased at 31.0 [10.7/ 63.3] % after the washout period.

The latency of the onset of the response did not differ significantly, neither between the first stimulation (3.5 [2.5/ 3.5] sec) and the stimulation under the influence of ruthenium red (3.5 [1.6/ 5.5] sec), nor between the stimulation under the influence of ruthenium red and the one after the washout period (3.0 [1.8/ 4.3] seconds) (Figure 37).

The same applied for the time the response took to reach the maximum change in RLI (Figure 38). After the first hypoosmolar stimulation, it took 12.6 ± 3.5 sec until the maximum change in RLI was reached. This period was not significantly longer under the influence of ruthenium red (13.7 ± 4.5 sec) and also did not change significantly after the washout period (12.0 ± 3.4 seconds).

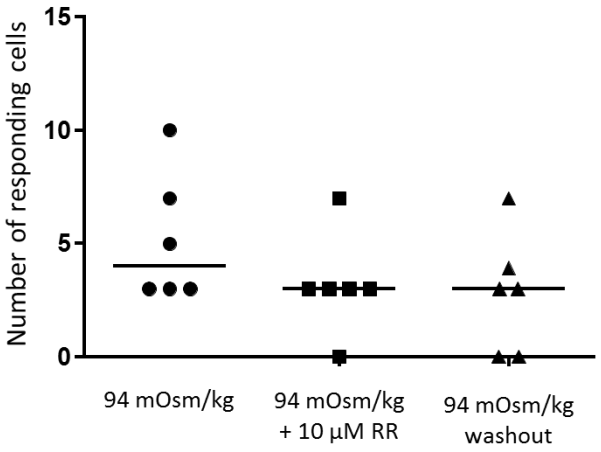

Figure 35: influence of ruthenium red on number of responding cells. Left: without ruthenium red in the perfusion solution. Middle: 10 µM ruthenium red in the perfusion solution. Right: after 30 minutes washout period with standard HEPES. Shapiro-Wilk test revealed no Gaussian distribution for the datasets. Friedman test showed no significant differences between the groups.

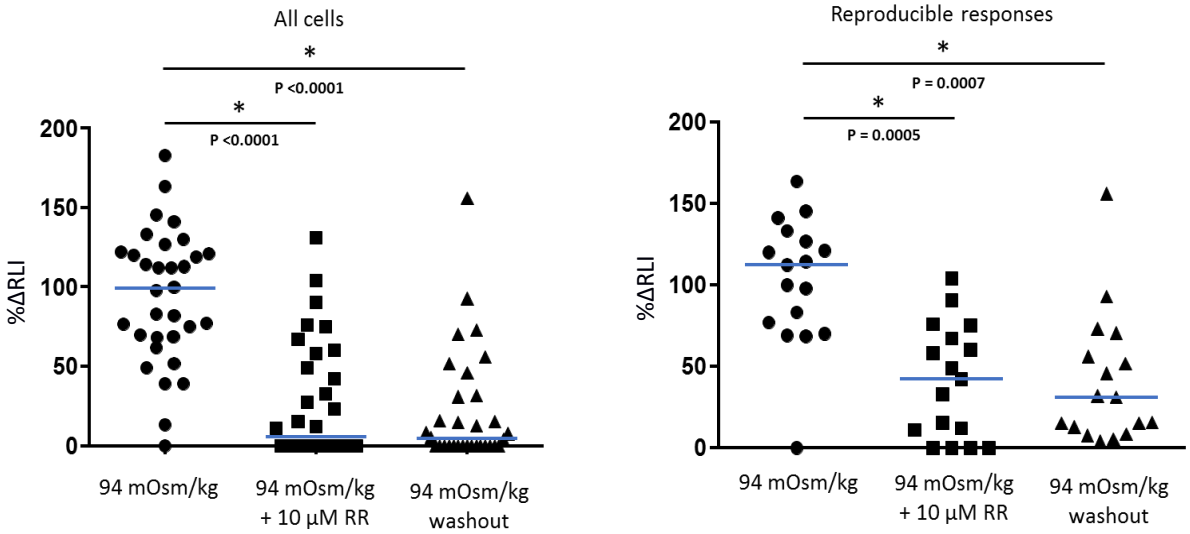

Figure 36: influence of ruthenium red on max. ΔRLI. Left: all cells that showed a Ca^{2+}- response in any of the applications. Right: all cells that showed reproducible Ca^{2+}- responses. Shapiro-Wilk test showed a non-Gaussian distribution for all datasets. Friedman test was used to test for significant difference between the datasets. When comparing all responding cells ruthenium red significantly reduced the Ca^{2+}- response after hypoosmolar stimulation (P < 0.001). Also after the washout the Ca^{2+}- response stayed significantly lower than after the initial stimulation. When only taking the cells into account that responded reproducibly to the hypoosmolar stimulus, the Ca^{2+}- response was also significantly reduced by ruthenium red (P = 0.0005) and stayed significantly reduced after the washout (P = 0.0007).

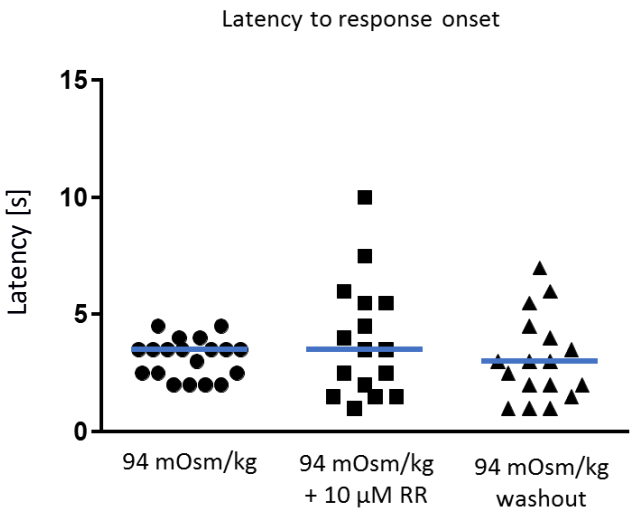

Figure 37: influence of ruthenium red on the latency of the Ca^{2+}- response to hypoosmolar stimuli. Left: hypoosmolar stimulation without ruthenium red in the perfusion solution. Middle: hypoosmolar stimulation with 10 µM ruthenium red added to the perfusion solution. Right: again, hypoosmolar stimulation without ruthenium red in the perfusion buffer after 30 minutes washout. For this analysis, only cells that showed a Ca^{2+}- response in the recording after the washout were included. Shapiro-Wilk test revealed a non-Gaussian distribution for the Datasets. Kruskal-Wallis test showed no significant difference between the three groups.

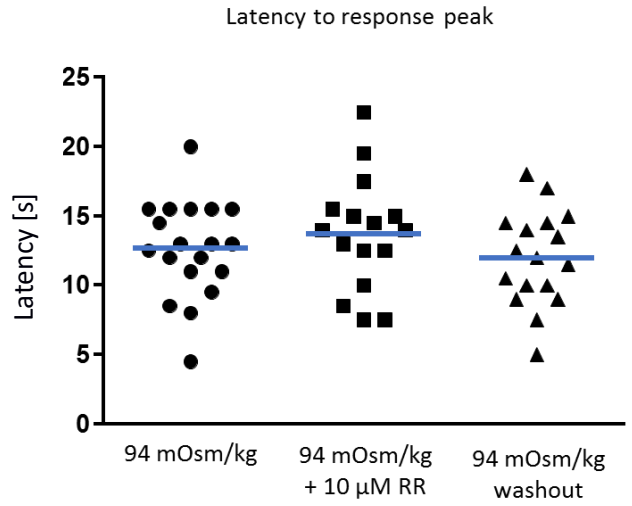

Figure 38: influence of ruthenium red on the latency to the maximum Ca^{2+}- response after hypoosmolar stimulation. Left: hypoosmolar stimulation without ruthenium red in the perfusion solution. Middle: hypoosmolar stimulation with 10 µM ruthenium red added to the perfusion solution. Right: again, hypoosmolar stimulation without ruthenium red in the perfusion buffer after 30 minutes washout. For this analysis, only cells that showed a Ca^{2+}- response in the recording after the washout were included. Shapiro-Wilk test revealed a Gaussian distribution in all three datasets. One-way ANOVA showed no significant difference in latency to the maximum increase in $[Ca^{2+}]_{in}$ between the three groups.

3.15 Effect of HC-067047 on neuronal responses after hypoosmolar stimulation

Experiments, using the antagonist HC-067047 were conducted in an unpaired experimental design. The TPRV4 antagonist was added already to the perfusion solution before the first application of hypoosmolar stimulation. The responses of 156 cells in 10 ganglia originating from 3 animals were investigated under the influence of the antagonist and compared to the responses of 8 ganglia originating from 3 animals which were stimulated without the addition of HC-067047.

150 nM HC-067047 had no effect on the EPSP (Figure 39). The ΔRLI of the EPSP in response to electrical stimulation was 0.6 [0.4/ 0.8] % before the blocker was added to the perfusion solution and 0.5 [0.3/ 0.8] % after the blocker was added to the solution (P = 0.3125).

In the experiments without the antagonist 18.0 [13.3/ 20.8] % of the neurons responded to the hypoosmolar stimulus. In the experiments in which the antagonist was added to the perfusion solution the percentage of responding neurons per ganglion was significantly lower with 0.0 [0.0/ 6.3] % (P = 0.0005) (Figure 40 upper left).

Noteworthy the action potential frequency in cells that responded to the osmotic stimulus did not differ significantly (P = 0.5052). The average action potential frequency in responding cells after stimulation was 2.2 [0.7/ 3.8] Hz in the group without antagonist. When 150 nM HC-067047 was added to the perfusion solution the action potential frequency in responding cells was 2.8 [1.7/ 5.3] Hz and therefore not significantly different compared to the control group (Figure 40 upper right right). Likewise, also the neuroindex was decreased significantly from 30.6 [8.9/72.4] to 0.0 [0.0/23.8] (P = 0.0070) (Figure 40 low).

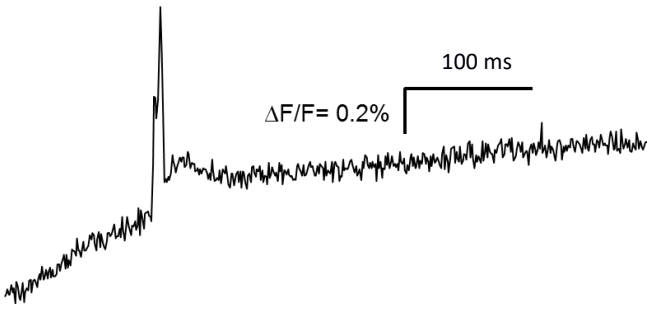

Figure 39: fEPSP under the influence of 150 nM HC-067047.

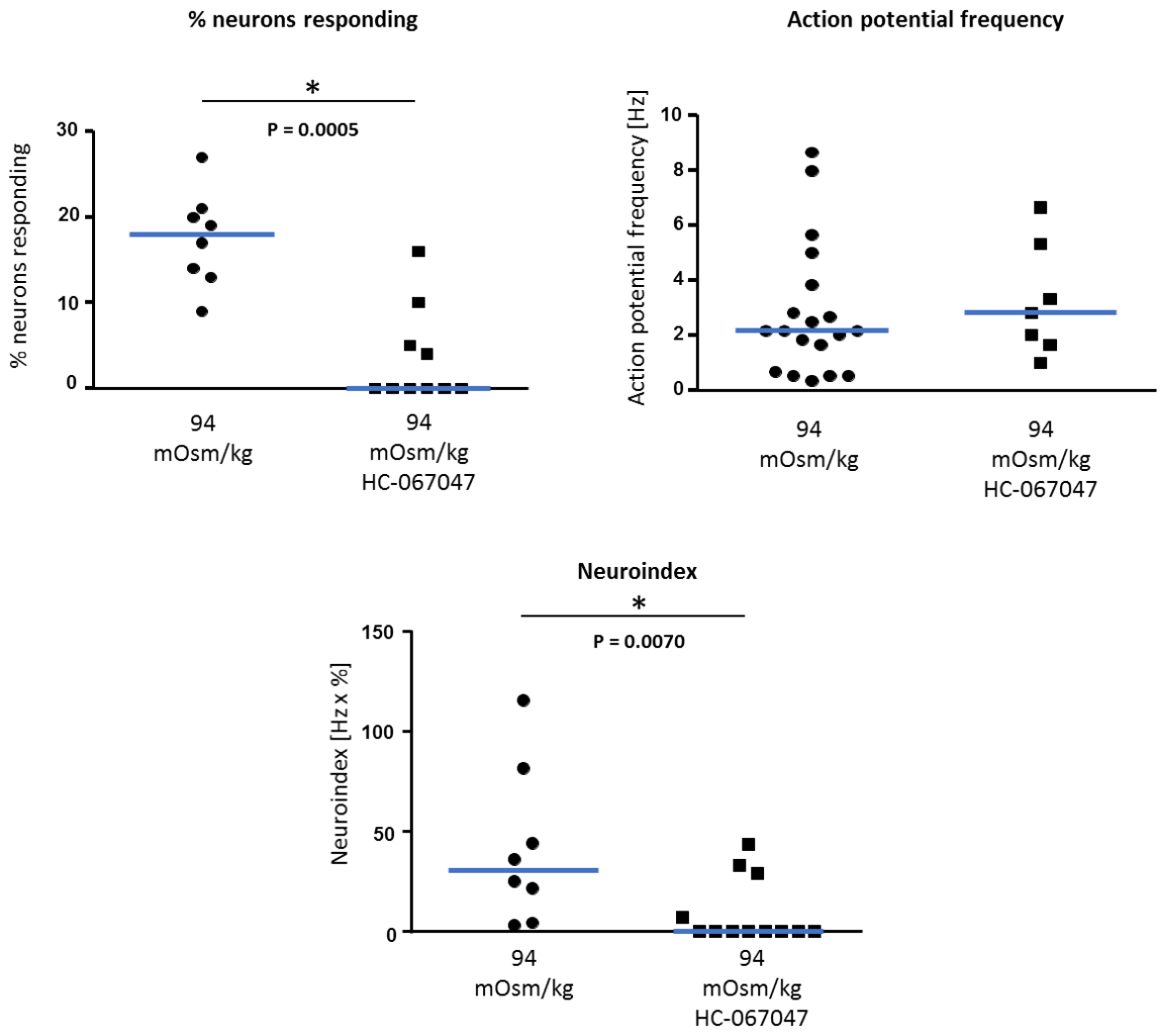

Figure 40: effects of HC-067047 on the response to hypoosmolar stimulation. Shapiro-Wilk test showed no Gaussian distribution of the data. Upper left: comparison of the percentage of responding cells after hypooosmolar stimulation with and without HC-067047. Mann Whitney test showed a significant difference in the percentage of responding cells (P = 0.0005). Upper right: comparison of the action potential frequency in responding cells after hypoosmolar stimulation with and without HC-067047. Mann Whitney test here showed no significant difference between the two groups. Lower: comparison of the neuroindex. Mann Whitney test here showed a significant difference between the two groups (P = 0.0070).

3.16 Effects of GSK1016790A on cells of the SMP

Action potential discharge in submucosal neurons

The effect of two different concentrations of the TRPV4 agonist GSK1016790A on the neurons of the SMP was tested. In a concentration of 10 µM the agonist was applied to a total number of 235 cells in 13 ganglia originating from 4 different animals. The 20 µM concentration was applied to 397 neurons in 22 ganglia from 9 different animals. To the 10 µM GSK1016790A solution 39 neurons responded with action potential discharge while 84 cells were activated by the 20 µM solution. There was no significant difference in the percentage of responding cells per ganglion between the two concentrations. Per ganglion 3.0 ± 2.0 (15.0 [7.5/ 24.5] %) neurons responded to the 10 µM concentration and 3.8 ± 2.9 (21.0 [10.5/ 29.8] %) to the 20 µM concentration (Figure 41).

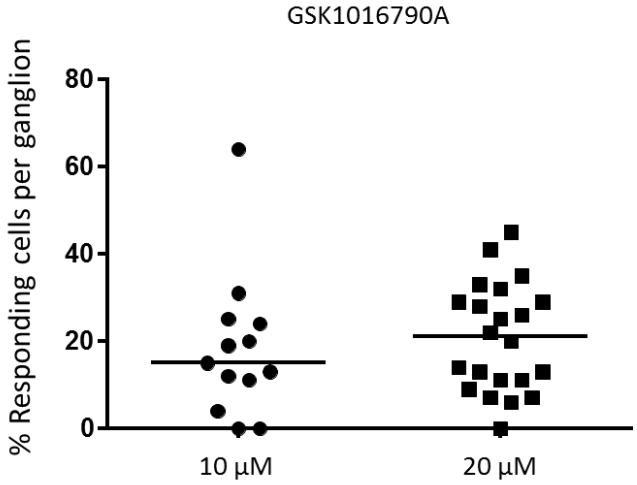

Figure 41: percentage of responding cells to different concentrations of the TRPV4 agonist GSK1016790A. Shapiro-Wilk test revealed a non-Gaussian distribution. Mann-Whitney test resulted in a P- value of 0.384.

The median frequency of action potentials that neurons fired after being treated with 10 µM of the TRPV4 activator was 1.8 [1.3/ 2.3] Hz. The action potential frequency after stimulation with 20 µM of the TRPV4 activator was 1.3 [0.5/ 2.3] Hz and not significantly different to the response to 10 µM (Figure 42).

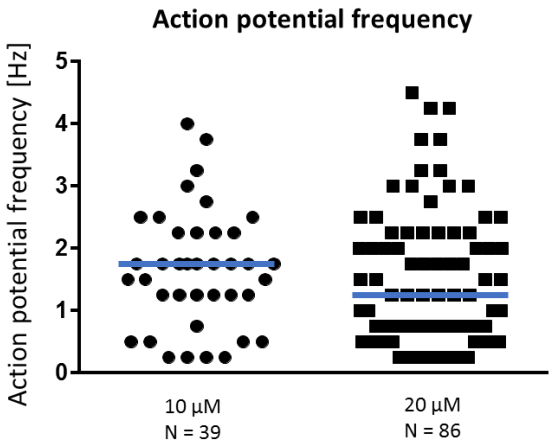

Figure 42: action potential frequencies after application of 10 µM and 20 µM GSK1016790A. Shapiro-Wilk test revealed a non-Gaussian distribution of data. Mann Whitney test showed no significant difference between the two groups (P = 0.203).

The latency of the response was also not significantly different being 1.1 [0.5/ 1.7] seconds after 10 µM and 1.0 [0.4/ 0.9] seconds after 20 µM GSK1016790A (Figure 43).

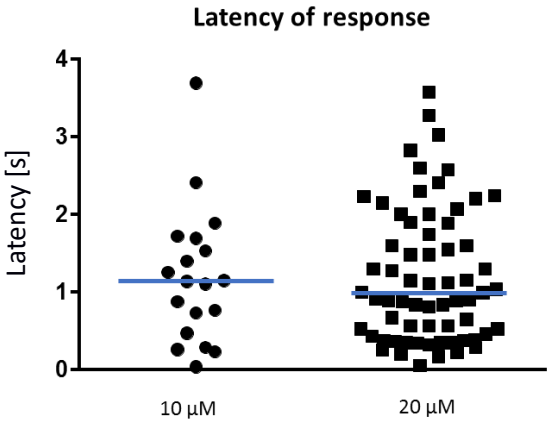

Figure 43: latency of the response to 10 µM and 20 µM GSK1016790A. All cells which displayed spontaneous action potential discharge were left out of the analysis. Shapiro-Wilk test showed a non-Gaussian distribution of data. Mann Whitney test resulted in a P value of 0.918.

To validate the reproducibility of the response the same stimulus was applied two times to the ganglia of interest. 46.5 % of the cells that responded to 20 µM GSK1016790A in a first application also responded to a second application with the same concentration. No cell responded only to the second application of the agonist. 53.8 % of the cells that responded to a 10 µM concentration of the activator responded also to a second stimulation (Figure 44). One cell showed no response to the first application of GSK1016790A but responded after the activator was applied a second time.

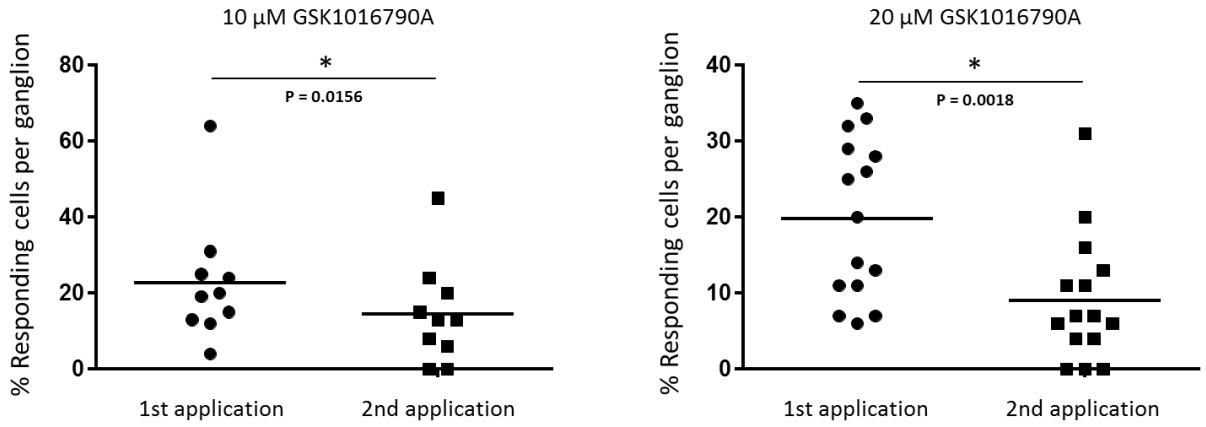

Figure 44: reproducibility of responses to GSK1016790A. Left: percentage of responding cells after 10 µM GSK106790A in a repeated application. The percentage of responding cells was significantly lower (Wilcoxon rank sum test) after the second application (P = 0.0156). Right: percentage of responding cells after 20 µM GSK1016790A. Shapiro-Wilk test here showed a Gaussian distribution of the data. The percentage of responding cells was significantly lower after the second application (paired t-test) (P = 0.0018).

For the 10 µM as well as for the 20 µM application of the agonist, the frequencies of the responses were not significantly different between the two applications (Figure 45). After the first 10 µM application the cells fired with a mean frequency of 1.8 [1.3/ 2.3] Hz while the frequency was 1.5 [0.9/ 2.1] Hz after the second application *(P = 0.546).* The first application of 20 µM activator resulted in a firing frequency of 1.7 ± 1.1 Hz while the second application evoked action potentials with a frequency of 1.7 ± 1.5 Hz (Figure 45).

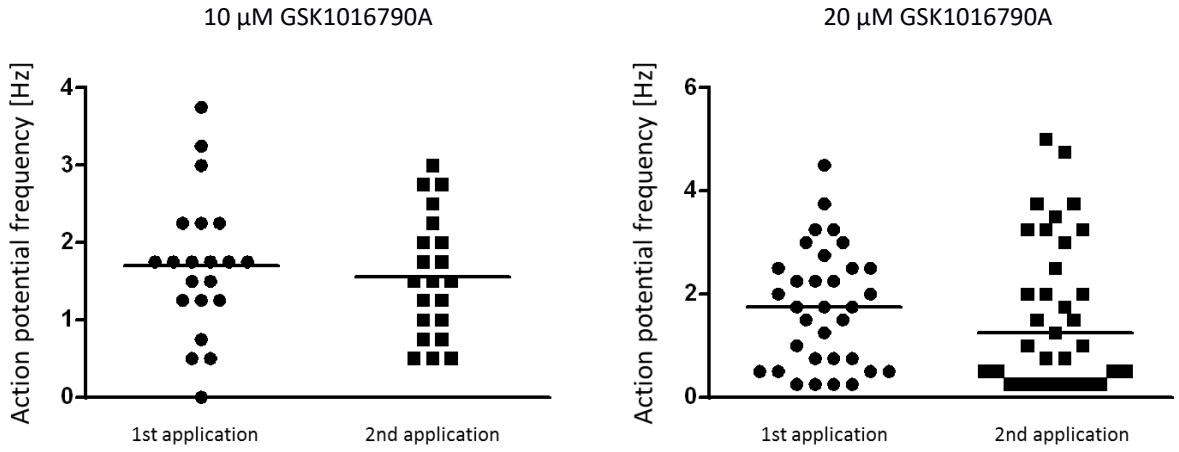

Figure 45: comparison of the action potential frequency of the first and second response to GSK1016790A. Left: 10 µM GSK1016790A. Shapiro-Wilk test revealed a Gaussian distribution of the data. Paired t-test resulted in a two-tailed p value of 0.546; Right: 20 µM GSK1016790A. Shapiro-Wilk test revealed a non-Gaussian distribution of the data. Wilcoxon signed rank test resulted in a p value of 0.962.

Ca^{2+} - responses after application of GSK1016790A

In addition to the VSD experiments, the effects of GSK1016790A were also investigated using the Ca^{2+}-imaging method. Changes in $[Ca^{2+}]_{in}$ were measured in 12 ganglia coming from 4 animals. GSK1016790A was applied in a concentration of 20 µM. To the first application of the activator 3.0 ± 1.4 cells per ganglion responded. The number of cells per ganglion responding to the activator in the Ca^{2+} - imaging experiment was not significantly different from the number of cells responding to the agonist in the VSD experiment (P = 0.3433). 53% of the responses could be reproduced with a second application. The median RLI change after the initial application of the activator was 8.1 [5.3/ 13.5] % and the response started with a latency of 2.0 [1.0/ 5.5] seconds.

In cells that responded reproducibly ΔRLI stayed the same for both recordings (9.0 ± 3.3% and 7.6 ± 3.1%) (Figure 46).

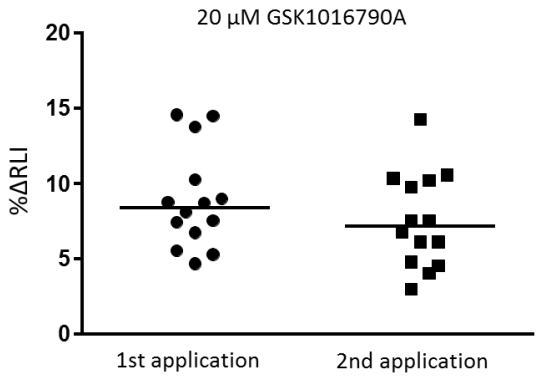

Figure 46: comparison of the Ca^{2+}- responses to repeated stimulation with 20 µM GSK1016790A. For this analysis, only cells with reproducible responses were taken into account (N = 3 tissues / 8 ganglia / 14 cells). Shapiro-Wilk test showed a Gaussian distribution for both datasets. Paired t-test resulted in a two-tailed P value of 0.176.

The latency of the response was 1.8 [1.0/ 3.4] seconds after the first application and with 1.5 [0.5/ 3.8] seconds not significantly different after the second application *(P = 0.898)* (Figure 47 left side). The same was true for the latency to the maximum change in RLI, which was 7.8 [7.0/ 10.1] seconds after the first application and 8.8 [7.3/ 9.9] seconds after the second application of the activator (Figure 47 right side) *(P = 0.143)*.

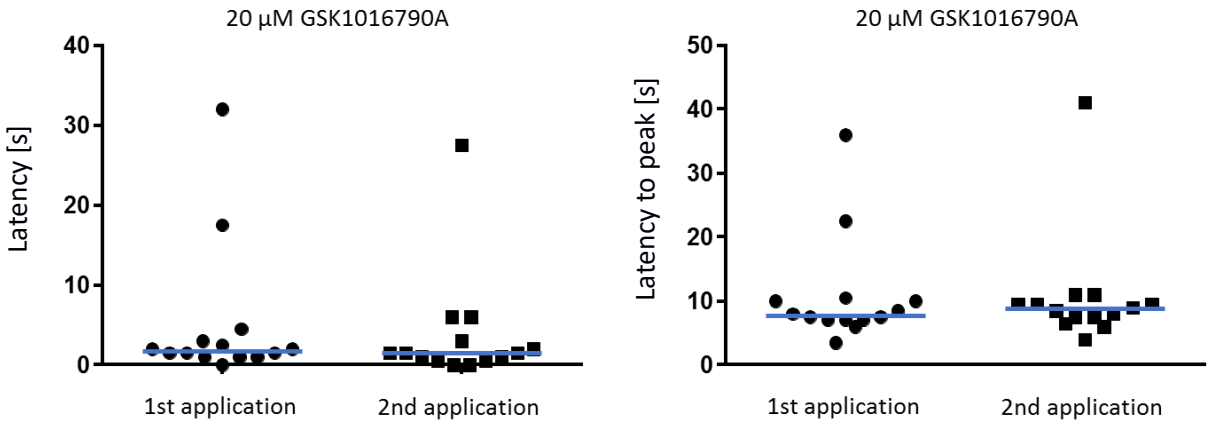

Figure 47: latency and latency to max. ΔRLI after GSK1016790A. left: comparison of response latency between first and second stimulation with GSK1016790A. Shapiro-Wilk test showed a non-Gaussian distribution of the data. After both applications, the responses started with the same delay (P = 0.898) (Wilcoxon rank sum test). Right: comparison of latency to the maximum $[Ca^{2+}]_{in.}$ Data was also not distributed normally. Here again no difference between both applications was detectable (P = 0.143) (Wilcoxon rank sum test). For this analysis, only cells that showed reproducible Ca^{2+}- responses were used (N = 14 cells, 8 ganglia, 3 animals).

3.17 Effects of HC-067047 on neuronal responses to GSK1016790A

To investigate the effects of the TRPV4 antagonist HC-067047 on the action potential discharge of enteric neurons stimulated with the selective TRPV4 agonist GSK1016970A a set of 99 neurons was initially stimulated with GSK1016790A. To this stimulus 18.0 [10.0/ 25.0] % of the neurons in each ganglion responded. In the next step, the antagonist was perfused and after an incubation time of 20 minutes another stimulation with GSK1016790A was performed. The percentage of responding neurons was significantly decreased to 6.0 [0.0/12.0] % *(P = 0.0324)*. After a washout period of 30 minutes GSK1016790A was applied a third time. The percentage of responding cells per ganglion was 0.0 [0.0/ 6.0] % and therefore still significantly decreased compared to the initial stimulation *(P = 0.0027)* (Figure 48). After the washout, an electrical stimulation of the ganglion was performed to evaluate its viability based on the fEPSPs of the neurons. In all analysed neurons fEPSPs could be evoked after the final stimulation with the activator.

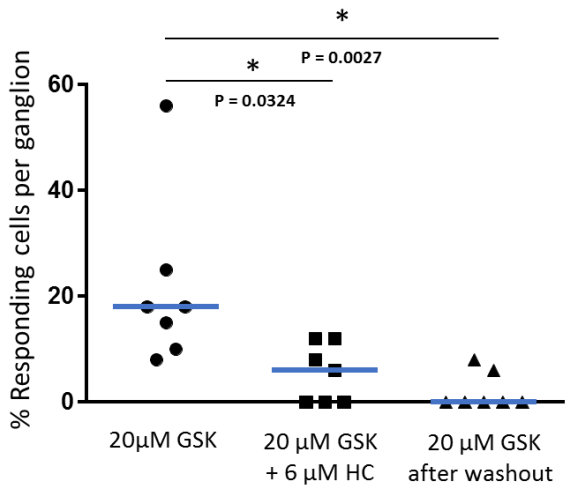

Figure 48: influence of HC-067047 on the percentage of cells responding to GSK1016790A. Shapiro-Wilk test revealed a non-Gaussian distribution of data. Friedman test with Dunn´s multiple comparison resulted in P values of 0.0324 and 0.0027.

The action potential frequency was also significantly reduced from the initial stimulation (1.0 [0.5/ 2.1] Hz) to the stimulation under the influence of HC-067047 (0.0 [0.0/ 0.25] Hz) and also did not recover after the washout period (0.0 [0.0/ 0.0] Hz) (Figure 49).

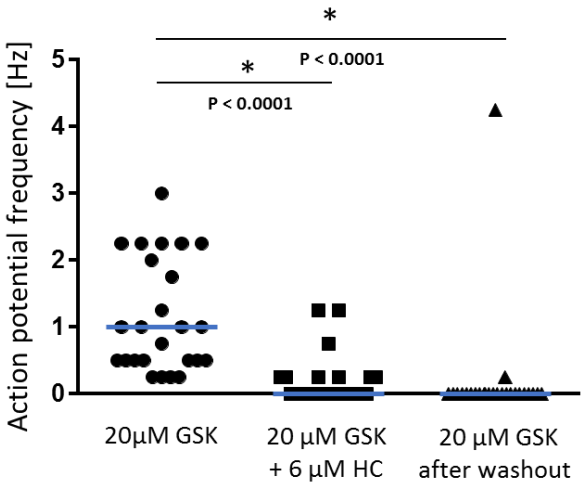

Figure 49: influence of HC-067047 on action potential frequencies after GSK1016790A application. All cells that responded to the initial application of the agonist were included in the analysis. Shapiro-Wilk test revealed a non-Gaussian distribution of the data. Friedman test with Dunn´s multiple comparison resulted in P values < 0.0001 for both groups compared to the initial stimulation.

Due to the fact that the response did not recover after the washout of the blocker, a series of experiments was conducted in an unpaired design. In these experiments in each case the response to the first stimulation with GSK1016790A was investigated. One group of ganglia was perfused with normal Krebs solution while the other was perfused with Krebs solution containing 6 µM HC-067047. This experimental design made sure that the reduction in response after the second application of the agonist was not due to desensitisation. For the experiments without the antagonist the responses of 103 cells in 7 ganglia originating from 5 animals were analysed. 31 cells showed action potential discharge after treatment with GSK1016790A. To another group of 6 ganglia originating from 3 animals the agonist was applied under the influence of the antagonist. In this constellation, only 17 cells fired action potentials after the stimulation. Nevertheless, neither the percentage of responding cells (20 [15/ 31] % and 15 [9.8/ 22.3] %) *(P = 0.250)*, nor the action potential frequency of responding cells (1.0 [0.5/ 2.3] Hz and 0.5 [0.3/ 1.4] Hz) *(P = 0.097)* was reduced significantly in the experiments in which the blocker was added (Figure 50).

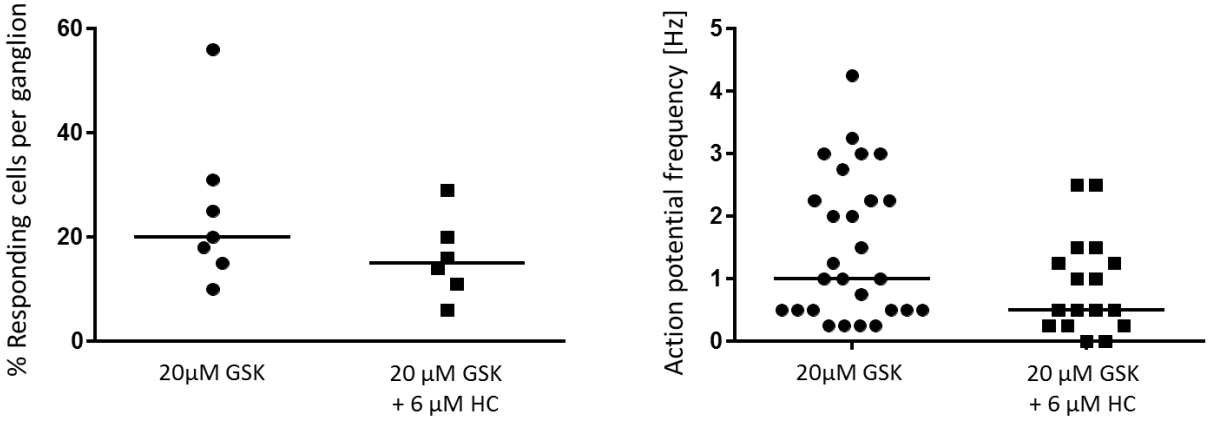

Figure 50: influence of HC-067047 on the responses to GSK1016790A in an unpaired design. Shapiro-Wilk test revealed a non-Gaussian distribution of the data. Left: percentage of responding cells per ganglion. Mann Whitney test showed no significant difference between the two goups (P = 0.250). Right: action potential frequency of responding cells. Mann Whitney test showed no significant difference between the two groups (P = 0.097).

3.18 Overlap of osmosensitive and GSK1016790A sensitive neurons

GSK1016790A and a hypoosmolar stimulus of 94 mOsm/kg were applied consecutively onto the same cells to check whether both stimuli were able to activate the same neurons.

The activation caused by the osmotic shift was measured in a period 10-12 sec after the stimulus was applied. Activation by GSK1016790A was measured in the 4 seconds following the agonist application (Figure 51). In this set of experiments a total number of 235 cells in 13 ganglia coming from 4 animals was investigated. 40 of those cells responded to hypoosmolar stimulation (17.0 %) but only 15 to application of the TRPV4 agonist (6.4 %). The order of applications was randomised.

Out of the 40 cells that have been shown to be osmosensitive, 11 responded to the TRPV4 agonist (27.5%). Out of the 15 cells that were sensitive to GSK1016790A, 11 cells were also osmosensitive (73.3%) (Figure 52). For cells that responded to both stimuli, the action potential frequencies were compared. After the hypoosmolar stimulation those neurons fired with an action potential frequency of 8.0 [7.0/14.0] Hz. Being 2.0 [1.3/2.5] Hz the action potential frequency after application of GSK1016790A was significantly lower *(P = 0.0020).*

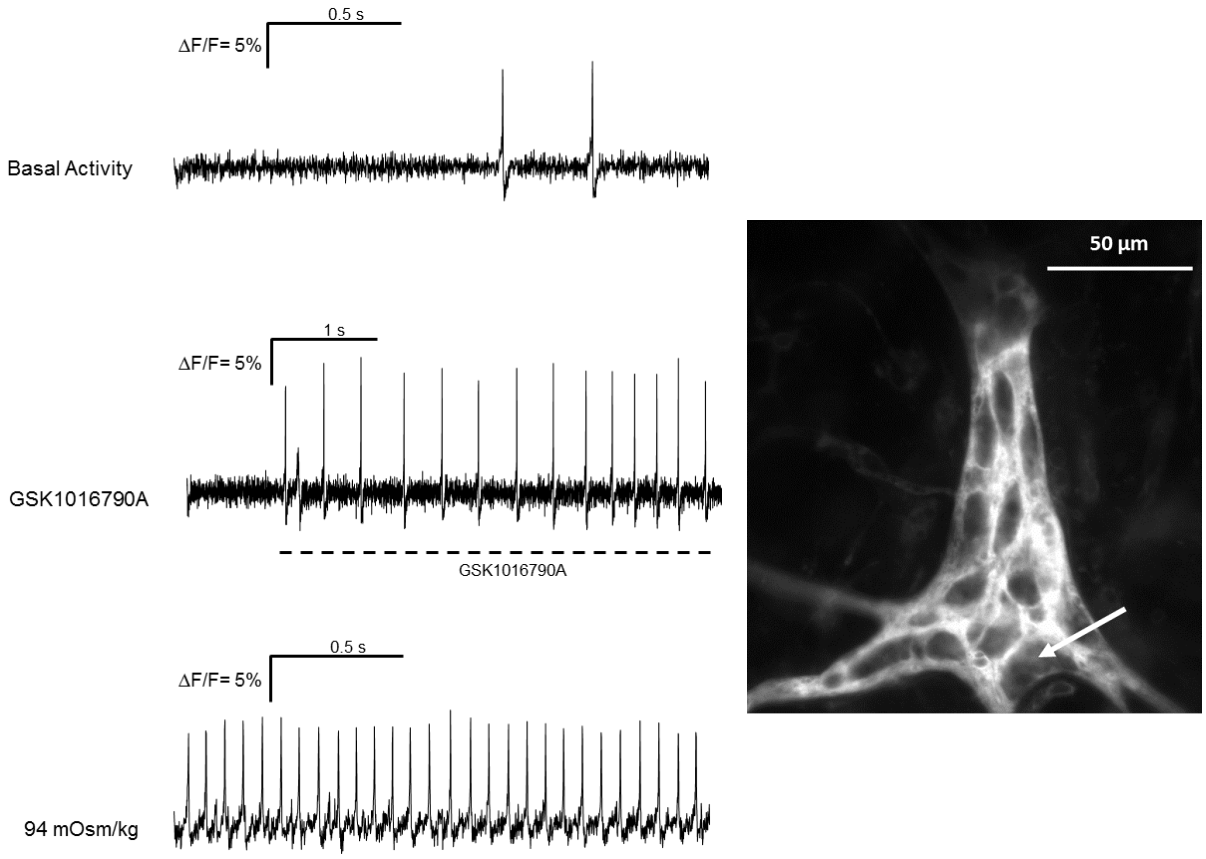

Figure 51: activity pattern after GSK1016790A and after hypoosmolar stimulation. Upper trace: neuronal activity under baseline conditions. Middle trace: response to the application of 20 µM GSK1016790A. Lower trace: action potential discharge in the period 10-12 seconds after a hypoosmolar stimulus of 94 mOsm/kg was applied. Right side: ganglion stained with Di-8-ANEPPS. White arrow indicates the cell from which the traces originated.

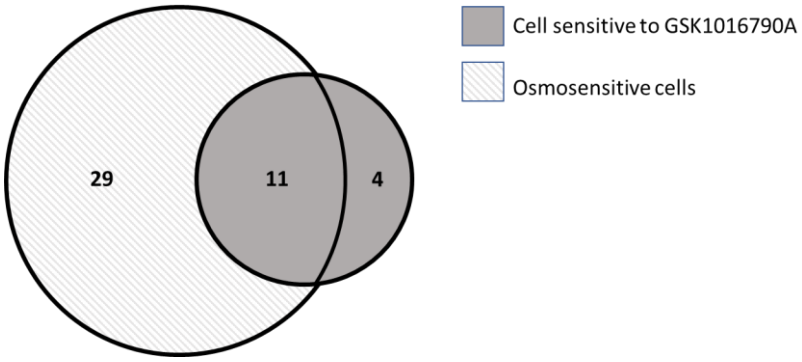

Figure 52: submucosal neurons responding to hypoosmolality, GSK1016790A or both. It has to be taken into account that all of these cells are just a subpopulation of the whole number of investigated neurons which were 235 in this series of experiments.

3.19 Influence of ω-conotoxin on responses to hypoosmolar stimuli

The influence of ω-conotoxin GVIA on neuronal responses to a 94 mOsm/kg stimulus was tested in 60 neurons in 4 ganglia coming from 3 tissues. Due to the fact that ω-conotoxin GVIA leads to an irreversible block of synaptic transmission, experiments were performed in an unpaired design (McCleskey et al., 1987). To ensure the complete blockade of synaptic transmission by ω-conotoxin GVIA, an electrical stimulation was carried out before and after the perfusion of 200 nM ω-conotoxin GVIA. In all of the 3 tissues fEPSPs were detectable prior to the perfusion with ω-conotoxin GVIA. No fEPSPs were detectable after 20 minutes of perfusion with ω-conotoxin GVIA. Out of the 60 neurons investigated, 8 neurons responded to the stimulus under the influence of ω-conotoxin GVIA. Being 13.9 [10.6/17.5] % the percentage of responding neurons per ganglion was not significantly different under the influence of 200 nM ω-conotoxin GVIA compared to a 94 mOsm/kg stimulus without ω-conotoxin GVIA where it was 11.0 [7.0/17.0] % (P = 0.5060). The same applies for the frequency of action potential discharge, which was 3.1 [1.8/5.0] Hz under the influence of ω-conotoxin GVIA and not significantly different from the average action potential frequency after the same stimulus without ω-conotoxin GVIA, which was 2.2 [0.8/3.4] Hz (P = 0.1662). The neuroindex after stimulation with 94 mOsm/kg HEPES solution under the influence of ω-conotoxin GVIA was 45.0 [24.7/56.7] and also not significantly different from the neuroindex after the same stimulation without ω-conotoxin GVIA, which was 21.7 [3.3/44.0] (P = 0.2133) (Figure 53).

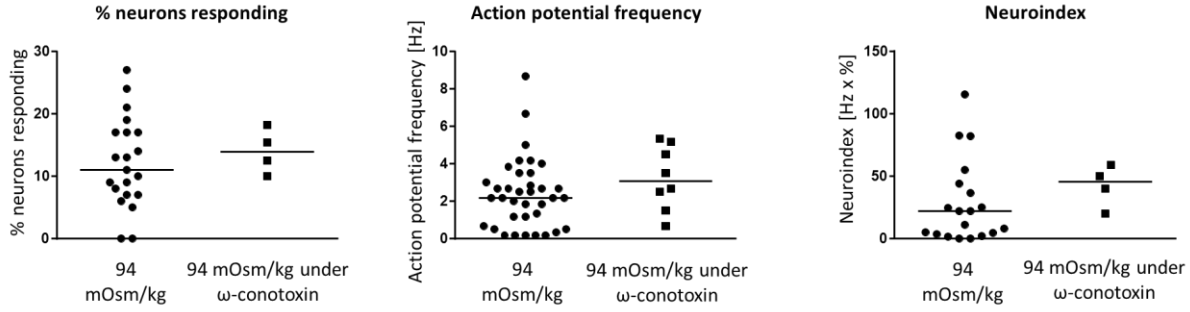

Figure 53: influence of ω-conotoxin on the neuronal response to hypoosmolar stimuli. Shapiro-Wilk test revealed a non-Gaussian distribution for all datasets. Left: the percentage of responding neurons was not significantly different under the influence of ω-conotoxin. Mann-Whitney test resulted in a p-value of 0.5060. Middle: action potential frequency in responding cells also was not changed. Mann-Whitney test resulted in a p-value of 0.1662. Right: neuroindex was not changed significantly under the influence of 200 nM ω-conotoxin. Mann-Whitney test here resulted in a p-value of 0.2133.

3.20 Expression of TRPV4 in the submucosal plexus of the guinea pig

RIN values of the collected RNA samples were determined and found to be in the range from 6.6 to 10.0 which was considered sufficient for expression analysis using qRT-PCR.

In all investigated tissue TRPV4 expression could be confirmed on mRNA level. The highest expression of TRPV4 was found in kidney tissue where mRNA levels of TRPV4 were 5.87 [4.96/ 6.27] times as high as the mRNA levels for beta-actin. In whole- wall bladder sections the normalised mRNA levels of TRPV4 were 0.70 [0.70/ 0.81]. Lowest levels of TRPV4 mRNA were found in samples of skeletal muscle, where normalised TRPV4 levels were 0.13 [0.08/ 0.17]. TRPV4 expression in the SMP was 0.36 [0.19/ 0.71]. This was not significantly different compared to all other tissues. Nevertheless, the expression was well in the range between the values for bladder and skeletal muscle (Figure 54).

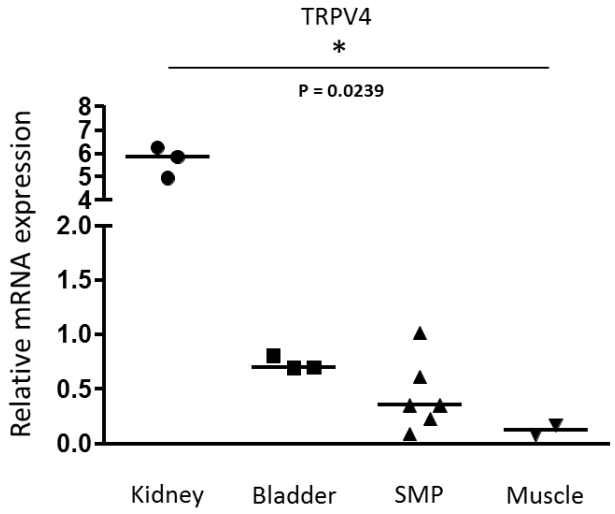

Figure 54: relative expression levels of TRPV4 in kidney, bladder, SMP and muscle tissue. Data was normalized to the expression of beta-actin for each tissue. Shapiro-Wilk test showed no Gaussian distribution of the data. Kruskal-Wallis test revealed no difference in expression levels between SMP and the other tissues. The only significant difference was found between the relative TRPV4 expression in kidney and muscle tissue (P = 0.0239).

3.21 Immunofluorescence based evidence for TRPV4 in the SMP

To investigate whether TRPV4 in the SMP is expressed in neurons immunohistochemistry with fluorescence labelled antibodies was performed. 9 ganglia of the SMP of 3 animals were co-stained with rabbit derived polyclonal anti TRPV4 antibody and human derived ANNA-1 antibody, a specific marker of enteric neurons (Li et al. 2016).

Surprisingly all cells which were positive for ANNA-1 also showed fluorescence labelling of TRPV4. Nevertheless, the amount of TRPV4 staining varied strongly from neuron to neuron. TRPV4 staining was in all cells localised in the neuronal cytoplasm or in the cell membrane but never in the nucleus. Despite the lower sequence identity in guinea pig, the antibody stained the same cellular structures as it did in human. Incubation without the primary antibody led to a complete absence of the fluorescence signal (Figure 55).

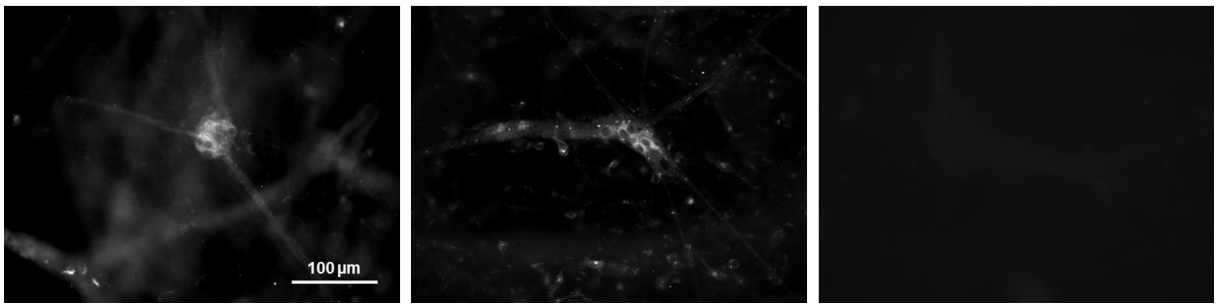

Figure 55: validation of the primary antibody against TRPV4. Left: human submucosal plexus incubated with 1:500 rabbit derived anti TRPV4. Middle: guinea pig SMP treated in the same way. Right: guinea pig SMP incubated without the primary antibody. Fluorescence labelling was done with donkey anti rabbit Cy3 labelled antibody in all three tissues.

3.22 Chemical coding of osmosensitive enteric neurons

To investigate the chemical coding of the neurons identified as osmosensitive immunofluorescent staining of 3 tissues was performed using primary antibodies against ChAT and VIP. A total of 20 neurons in 7 ganglia, which showed action potential discharge after hypoosmolar stimulation in the VSD experiment, could be re-identified after the immunohistochemical staining. 13 (65%) of those neurons were positive for ChAT while 7 (35%) were positive for VIP (Figure 56).

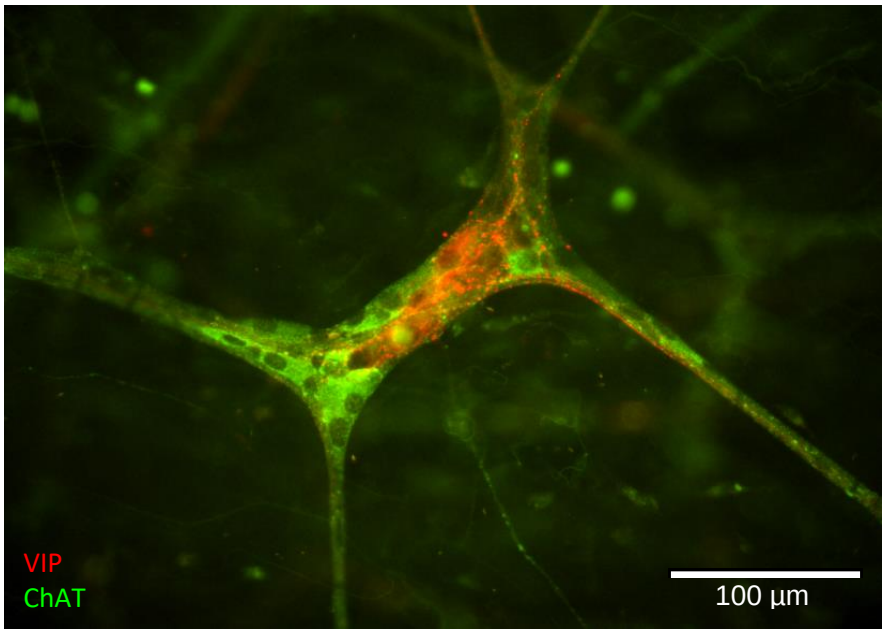

Figure 56: immunofluorescent staining of a SMP ganglion. Red: VIP positive cells, Green: ChAT positive cells.

4. DISCUSSION

This study was the first to describe osmosensitivity in neurons of the SMP. Furthermore, it provided valuable mechanistic insight into the process of osmotransduction in the ENS by pharmacological experiments where we tested a specific agonist and antagonists of a candidate receptor. Moreover, the expression of the channel proposed to be involved in the osmosensory process, TRPV4, was investigated in the SMP for the first time. Furthermore, in the course of this study a self-made application device for fluid quantities in the range of 10-20 µl was tested. This device was found to be reliable, cost-effective and easy to rebuild in any laboratory.

4.1 Plasma osmolality of the guinea pig in relation to other small rodents

The mean plasma osmolality was found to be 293.5 ± 2.1 mOsm/kg. This finding fits well into existing values known for other small rodents including 294 ± 1 mOsm/kg for rats (Dunn et al., 1973), 311 ± 1 mOsm/kg for mice (Sharif Naeini et al., 2006) and 281 ± 1 mOsm/kg for rabbits (Badoer et al., 2003). The plasma osmolality of humans is 288 ± 1 mOsm/kg (Zerbe and Robertson, 1983). With a plasma osmolality between that of a rat and a human, the guinea pig therefore seems to be a suitable model to study the effects of changes in extracellular osmolality on enteric neurons.

In this context, it has to be noted that in this study water and food was provided *ad libitum* to the guinea pigs. This implies that the measured values for plasma osmolality are the values in a state of normal hydration and satiety.

4.2 Physiological relevance of the used stimuli and region

Looking at the changes in plasma osmolality that occur under physiological conditions, the stimulus used in this study appears to be rather drastic. For example in humans the extracellular osmolality is monitored closely and kept in a narrow range between 280 and 295 mOsm/kg despite intake of food and water as well as changes in activity level (Baylis, 1983; Gill et al., 1985). Ingestion of 13 g of salt increases plasma osmolality in healthy humans by 5 mOsm/kg within 30 minutes (Andersen et al., 2000), while drinking of 850 ml of water lowers the plasma osmolality by about 6 mOsm/kg in the same period (Geelen et al., 1996). Under extreme conditions (in this case an acute water intoxication caused by compulsive intake of large amounts of water) a drop in plasma osmolality down to 208 mOsm/kg has been measured in a human subject (Maruyama et al., 1991). In the mentioned studies only systemic osmolality was taken into account. It has to be mentioned that fluctuations in osmolality after food or water intake might be much higher on a local level in the walls of the gastrointestinal tract.

Shifts in plasma osmolality of the portal vein might be much more meaningful when investigating shifts in gastrointestinal osmolality. In experiments that measured systemic plasma osmolality and portal

plasma osmolality simultaneously after gastric infusion of water, the reduction of portal vein plasma osmolality was significantly larger than the drop in systemic plasma osmolality (292.7±4.7 mOsm/kg and 304.4±6.9 mOsm/kg, respectively, p = 0.002) (McHugh et al., 2010). Taking into account that the SMP is located between the lumen of the intestine and the blood vessels transporting absorbed nutrients as well as water from the gut lumen towards the liver, shifts in osmolality after food or water uptake here might be even higher than in the portal vein. Yet, it is still unknown what changes in osmolality the ENS experiences after food or water intake. For the future, one could design Ussing-chamber experiments in which the osmolality on the luminal side of the epithelium is altered while changes in osmolality on the basolateral side of the epithelium are measured. Another, rather complex way of learning about the osmotic shifts that the ENS experiences under physiological conditions, could be the system which uses mesenterial perfusion. Until now, this elegant experimental approach has been used to measure the absorbance of pharmaceuticals in the rat intestine (Schreiber et al., 2014) but there are chances that it could be utilised to monitor fluctuations in mesenterial blood osmolality.

In the CNS MNCs of the SON respond to a 10-15 mOsm/kg increase in extracellular osmolality (Brimble and Dyball, 1977). Neurons of the OVLT were shown to be sensitive to a 25 mOsm/kg increase in extracellular osmolality (Ciura and Bourque, 2006) and inhibited by application of a hypoosmolar solution (Oliet and Bourque, 1993). A reduction of osmolality by 70 mOsm/kg activated 60 % of vestibular neurons in rats (Kamakura et al., 2016). Unfortunately, in none of those studies the authors make comments on why they choose to use a particular stimulus strength.

Peripheral osmoreceptors have been described to be activated by hypoosmolar and hyperosmolar stimuli. One study conducted in guinea pig liver afferent nerve fibres, showed activation by an increase of only 17 mOsm/kg extracellular osmolality (Niijima, 1969). With stimuli ranging from 110 mOsm/kg to 200 mOsm/kg another group showed that one type of vagal liver afferents in rats was activated by hypoosmolar stimuli, while another type was activated by hyperosmolar stimuli (Adachi, 1984). Thoracic DRG neurons of mice could be activated by perfusing them with a 230 mOsm/kg solution for 20 seconds (Lechner et al., 2011). Unfortunately, as in the case of peripheral osmoreception, authors fail to provide physiological evidence for the stimuli used in the experiments.

In heterologous expression systems TRPV4 dependent hypotonic activation of cells could be achieved by reducing the extracellular osmolality by 25 % (240 mOsm/kg) (Vriens et al., 2004). Another experiment conducted in Chinese hamster ovary (CHO) cells transfected with TRPV4 showed that these cells could be activated by a 1% reduction in extracellular osmolality (Liedtke et al., 2000). One possible explanation for the high sensitivity in those experiments probably is that receptor density in a heterologous expression system might be much higher than in the neurons investigated in the presented study and therefore a much smaller stimulus is sufficient to trigger responses.

One study, which in terms of investigated cell type comes closest to the presented work, investigated mechanosensitivity in cultured rat esophageal myenteric neurons (Dong et al., 2015). The authors used a hypoosmolar solution as an entity of mechanical stimulation and perfused the cells with a 170 mOsm/kg solution. This led to volume increase in all investigated neurons and an immediate and transient increase in $[Ca^{2+}]_{in}$ in 64% of the investigated cells (Dong et al., 2015).

Independent from whether the used stimulus is exactly in the physiological range or not, it has to be kept in mind that this study aimed to investigate the principle excitability of enteric neurons by osmotic stimuli, which it adequately did. The disadvantage of a less salient stimulus, which might be closer to the physiological range, is that it would possibly take longer to trigger a neuronal response and therefore would be easily missed in the VSD imaging experiments. One possible way to assess changes in neuronal activity after subtler osmotic stimulation could be to gradually change the osmolality of the perfusion buffer and perform short intermitting recordings with several minute-long intervals in between. By doing so phototoxic effects can be minimised and the number of recordings increased. In a similar way, changes in $[Ca^{2+}]_{in}$ following a gradual change in osmolality could be investigated.

Another unanswered question is whether prolonged deviation from the set-point of plasma osmolality, caused by restriction of water intake, would influence neuronal excitability after a sudden osmotic shift. Like most membrane bound proteins, TRP channels are not statically integrated into the plasma membrane but are in a constant cycle of translation, exocytosis, endocytosis, recycling or proteolysis in the proteasome (Ferrandiz-Huertas et al., 2014). Therefore, it is possible that a prolonged shift in plasma osmolality could influence neuronal excitability through altering receptor density. Another way of influencing the excitability of cells to osmotic shifts would be due to changes in cytoskeletal architecture. To test this hypothesis, it would be necessary to test the excitability of enteric neurons to osmotic stimuli after the animals experienced restricted intake of drinking water over several hours.

The focus of the present study on hypoosmolality is justified by the finding that the stomach has a strong damping function on osmotic fluctuations after food intake. Interestingly the luminal osmolality of the jejunum of fed dogs was only significantly different for one out of three measured time periods from that of unfed dogs (Ferraris et al., 1990). In contrast to that, liquids pass the stomach much faster and therefore can lower the intestinal osmolality (Hinder and Kelly, 1977).

It has to be kept in mind that for this study only colonic preparations were used. Although the general architecture and characteristics of the ENS are conserved throughout the gastrointestinal tract, the exact properties and functions of enteric neurons vary between the regions of the gut (Furness, 2006). Therefore, it cannot be ruled out completely that the osmosensitive properties described in this thesis are specific for the colon, and differ in other regions of the gastrointestinal tract. One reason for

choosing the guinea pig colon for this experiment was that the method for preparation of colonic SMP is well established, and as such can be performed more quickly, and with less stress for the tissue, than the preparation of other gut regions. Another important reason is that the colon is the region of the gastrointestinal tract where large amounts of water are reabsorbed from the faecal matter, against a high osmotic gradient (Ma and Verkman, 1999). Nevertheless, in the future further experiments are needed to compare the osmosensitive properties of different gut regions and also investigate interspecies differences.

4.3 Suitability of the used stimulation method

For precise osmotic stimulation in a distinct area of the preparation a method for local application of multi-microliter volumes was developed and tested. The tests performed with Fast Green resulted in a high accordance of the expected and the measured resting light intensity for all tested concentrations of Fast Green. Because of the linear relationship between RLI and Fast Green concentration the high accordance between the measured and expected value suggests that the same concentrations of the dye are present at the site of application and in the syringe lumen. For the investigation of osmotic stimuli this finding implies that the same osmotic concentration inside the syringe lumen is at the site of application. The small deviation between expected and measured RLI most likely was caused by the stray light of Fast Green molecules which were not exactly in the focal plane during the measurement. This stray light amount only exists in the calibration measurements, in which the whole chamber was filled with dye. In contrast to that, in the application measurements the dye is only injected in a certain area lying in the focus layer and stray light from other layers is nearly non-existent.

4.4 Spontaneous action potential discharges of submucosal neurons

On average 1.0 [0.0/2.0] neurons per ganglion showed spontaneous action potential discharge with a median frequency of 1.0 [0.5/3.0] Hz. These findings slightly differ from the values described by other authors (e.g. 3.7 neurons per ganglion firing with a frequency of 0.32 Hz (Obaid et al., 1999)). Spontaneous activity in the SMP could be influenced by a variety of factors. Moreover, it has to be kept in mind that the tissue was subjected to a pre- tension when it was pinned to the Sylgard® ring and that this could have led to the activation of tension-sensitive mechanosensitive enteric neurons (MEN) (Mazzuoli-Weber and Schemann, 2015a). While the majority of MEN adapt relatively fast to deformation (in the range from several hundred milliseconds to seconds) a smaller amount of MEN keeps on firing action potentials throughout a sustained deformation without any sign of adaptation. These neurons have been termed ultra-slowly adapting mechanosensitive enteric neurons (USAMEN) (Mazzuoli-Weber and Schemann, 2015b). The percentage of neurons defined as USAMEN is highly dependent on the species and the region of the gastrointestinal tract, and ranges from 2 % in the ileum to up to 21 % in the colon of mice (Mazzuoli-Weber and Schemann, 2015a). It has to be taken into

account that all the data about MEN was obtained from neurons of the MP and, therefore, no definite claims can be made about the percentage of MEN or even USAMEN in the SMP. Nevertheless, the presence of USAMEN in the SMP in combination with variations in pre-tension of the tissue on the Sylgard® ring during the experiment could account for variations in spontaneous activity from one experiment to another.

Before the second application of the stimulus, the basal spontaneous action potential discharge frequency was reduced. One possible cause of this phenomenon might be found in the phototoxic effects that accompany all photometric dye measurements. The cause of this phototoxic effects is the formation of singlet molecular oxygen which interferes with intracellular physiological processes (Kalyanaraman et al., 1987). Phototoxicity is one of the main obstacles in VSD imaging as it largely limits the recording duration. Different measures have been tried to reduce phototoxicity e.g. reduction of the oxygen tension (Obaid et al., 1999). However, the easiest way of limiting phototoxicity is a strict reduction of continuous illumination duration. One possibility to reduce illumination time, while still investigating neuronal responses over a larger period of time, is to perform interval recordings, as done in the majority of the experiments in this study.

A considerable number of neurons (between 3.6 and 7.0 %, depending on the experiment) in the SMP showed an increase in action potential discharge frequency after application of an isoosmolar solution. Although this increase was not significant, one may ask what caused it. Unfortunately, at the moment no satisfying answer can be given to that question. Among the possible factors influencing the activity after application of an isoosmolar solution is the temperature of the applied solution, the pH as well as the oxygen concentration in the applied solution. While changes in pH are already known to trigger responses in enteric neurons (Bertrand et al., 1997; Furness et al., 1998) the effect of the other factors on enteric neurons is still unknown. Although those factors were controlled as precisely as possible, small fluctuations cannot be ruled out completely. To keep the pH of the applied solution stable and independent from the supply of carbogen, a HEPES buffered Krebs solution was used instead of the standard bicarbonate buffered Krebs solution for all experiments investigating osmosensitivity. Nevertheless, the most satisfying explanation for this effect is a mechanical activation of the enteric neurons by the application of the stimulus. Although the UltraMicroPump III was already used for other studies of our group, the combination with the self- manufactured application device as well as the pump settings used were not tested before. Therefore, no claims can be made whether the application of a solution with the reported methodology causes mechanical stimulation of enteric neurons.

One might ask why the action potential frequency after application of the isoosmolar solution was different for different sets of experiments. In general patterns of spontaneous activity of enteric neurons are not constant but rather fluctuate (Obaid et al., 1999).

4.5 Submucosal neurons are osmosensitive

The main finding of this thesis is that changes in extracellular osmolality are able to provoke neuronal responses in the SMP of the guinea pig. This study is the first one to provide evidence for osmosensitivity in submucosal neurons.

This work showed clear evidence for the neuronal sensitivity to different hypoosmolar stimuli: action potential frequency and neuroindex are increased after application of the hypoosmolar solution. At the moment, no statement about the sensitivity of enteric neurons to hyperosmolar stimuli can be made. While the application of a mild hyperosmolar stimulus compared to the application of an isoosmolar solution led to a reduction of the action potential firing frequency, the application of a higher hyperosmolar stimulus led to an increase in action potential firing frequency. The percentage of responding neurons was increased only after the strong hyperosmolar stimulus. Neither the mild, nor the strong hyperosmolar stimulus led to changes in the neuroindex.

Until now the only study investigating responses of enteric neurons to hypoosmolar as well as to hyperosmolar stimuli (170 mOsm and 430 mOsm) was performed in cultured myenteric neurons of rats (Dong et al., 2015). The authors report 10 % increase in cell volume under hypoosmolar and 5 % decrease in cell volume under hyperosmolar conditions in all investigated cells (Dong et al., 2015). In contrast, our experiments showed only cell swelling under hypoosmolar conditions, but never cell shrinkage under hyperosmolar conditions. Nevertheless, the range of cell volume change was similar in our experiments, being 8.5 ± 4.2 %. Further, the authors report a 38 % increase in intracellular Ca^{2+} levels in 64 % of the investigated neurons after hypoosmolar stimulation (Dong et al., 2015). Due to technical limitations, the absolute number of investigated neurons in our Ca^{2+}- imaging experiments could not be determined and therefore no percentage of responding neurons can be given. Dong and colleagues also report that after hyperosmolar stimulation, Ca^{2+} increase was evident but much weaker than after hypoosmolar stimulation (personal communication of Mr. Dong). In the present work we could not evidence any Ca^{2+}- response to hyperosmolar stimuli, which was described in cultured myenteric neurons of rats. In parts, these results do fit well with the results found in the present study. Differences in the volume changes of cells after osmotic shifts might be due to the fact that the study of Dong and colleagues was conducted in cultured neurons while this study is based on experiments in intact tissues. Further, Dong et al. used rats for their experiments while our experiments were performed in guinea pigs.

Culturing has been shown to alter chemical coding and signalling cascades in sensory neurons. In cultured DRG neurons the amount of VIP was altered and calcitonin gene- related peptide was downregulated compared to the situation *in vivo*, supposedly caused by the fetal bovine serum added to the culture medium (Delrée et al., 1993). Due to fast trafficking of possible candidate channels

(Ferrandiz-Huertas et al., 2014), it cannot be ruled out that the culturing of the neurons led to changes in sensitivity to hyperosmolar stimuli.

Variation of the stimulus strength of the hypoosmolar stimulus from 94 mOsm/kg to 144 mOsm/kg did not lead to a change in number of cells activated. Furthermore, activation by a strong hypoosmolar stimulus did not result in a higher action potential discharge frequency than activation by a moderate hypoosmolar stimulus. Likewise, the neuroindex also was not altered. The strength of the hypoosmolar stimulus also had no effect on the latency of the response. This strongly indicates that the hypoosmolar stimulus of 144 mOsm/kg led to a maximal activation of the osmosensory pathway.

4.6 Possible causes for the low reproducibility of neuronal responses to osmotic stimuli

Enteric neurons that displayed a response when a hypoosmolar solution was applied did not in all cases respond to a second stimulation of the same strength. The reproducibility rate of the responses to hypoosmolar stimulation was similar for both, the mild and the strong hypoosmolar stimulus. For the mild hypoosmolar stimulus (150 mOsm/kg below the physiological set point for plasma osmolality) it was 44.8 % while it was only 32.5 % for the strong hypoosmolar stimulus (200 mOsm/kg below the physiological set point). The spike discharge frequency in cells that showed reproducible responses was also reduced after the second stimulation with the strong hypoosmolar stimulus, while repeated stimulation with the moderate hypoosmolar stimulus did not reduce action potential firing frequency after the second application.

There are several possible explanations for the low reproducibility rate of the responses. One reason for the low reproducibility of the response could be caused by a de-sensitizing effect of the stimulus. Such an effect for example could be due to desensitisation of the receptors as reported in the SMP after a repeated stimulation with 5-HT (Michel et al., 2005) or due to changes in receptor density (Ferrandiz-Huertas et al., 2014). The RVD which is observed after hypoosmolar stimulation of cells could have a long-term effect on the neurons which leads to a desensitisation to the stimulus. The first phase of RVD is the expulsion of ions from the cytoplasm which has a direct effect on the membrane potential and possibly leads to inactivity of the cells (Fisher et al., 2008; Lang et al., 1998b; Strange and Jackson, 1995). Nevertheless, one would expect that the 20-minute period between two stimulations with the hypoosmolar stimulus would be enough to normalise cytoplasmic ion levels. More likely is the influence of neuroactive small organic molecules, which are secreted from cells in the second phase of RVD (e.g. taurine and myo-inositol) (Pasantes-Morales and Tuz, 2006; Pasantes-Morales et al., 1990). Their accumulation is mediated by energy dependent transport and by their rate of synthesis and therefore more time consuming than the accumulation of ions (McManus et al., 1995).

Another reason for the low reproducibility of the response could be due to neuronal damage induced by the stimulus itself. Other authors described neuronal cell damage not only by hypoosmolar stimulation in the CNS, but also the release of neurotransmitters from the affected cells and hyperexcitability (Kimelberg et al., 1990; Pasantes-Morales and Tuz, 2006). An overshooting release of those excitatory amino acids (EAAs) such as L-glutamate and L-aspartate has been widely known to have a neurotoxic effect (Olney, 1969) presumably mediated through the NMDA receptor (Faden et al., 1989). A third explanation could be due to an experimental artefact induced by the phototoxicity of the dye molecules. This is a well-known phenomenon in live cell imaging applications but can hardly be overcome (Kalyanaraman et al., 1987; Obaid et al., 1999).

4.7 Kinetics of responses to hypoosmolar stimuli

Action potential discharges after hypoosmolar stimuli did not occur instantaneously after the cells were treated with the hypo- or hyperosmolar solution, but appeared with a considerable delay. The peak frequency was reached in the recording period 10-12 sec after the stimulus was delivered. This suggests that the mechanism of activation after osmotic stimulation of neurons is not mediated directly by ligand binding to ionotropic receptors, as in this case a much faster response would be expected comparable to the activation of neurons through nicotinic acetylcholine receptors (Obaid et al., 1999). Interestingly the latency of the increase in $[Ca^{2+}]_{in}$ after hypoosmolar stimulation was significantly shorter than the latency of spike discharge. There are mainly two reasons that would explain this. Firstly, this could be due to the fact that subthreshold activation, in terms of $[Ca^{2+}]_{in}$ increase could take place before depolarisation occurs. In contrast to the VSD imaging technique, the Ca^{2+}- imaging technique allows detection of those subthreshold Ca^{2+} - events, which take place before depolarisation is detectable with electrophysiological methods (Michel et al., 2011). Cell swelling in response to hypoosmolar stimulation has been shown to trigger Ca^{2+} influx into the cytoplasm (Strotmann et al., 2000). This increase in $[Ca^{2+}]_{in}$ might be mediated by proposed SAC which are presumed to play a role in RVD (Fisher et al., 2008; Kanzaki et al., 1999; McManus et al., 1995; Pasantes-Morales and Tuz, 2006). One of those Ca^{2+} permeable channels is TRPV4 (Liedtke et al., 2000; Strotmann et al., 2000). This channel in particular has been demonstrated to facilitate Ca^{2+} influx in peripheral sensory neurons after hypoosmolar stimulation (Lechner et al., 2011).

4.8 Responses to hypoosmolar stimuli might be transduced mechanically

The effect of a HEPES solution whose hypoosmolality was established by specifically reducing the concentration of Na^+ and Cl^- ions, was not different from the effect of a HEPES solution whose hypoosmolality was established by reducing the concentration of all solutes equally (the so called “full dilution”). The fact that neither in response latency, nor in action potential frequency any difference between the low NaCl and the “full dilution” HEPES was detectable suggests that osmosensitive neurons do not sense the concentrations of single ion types in the extracellular fluid, but rather the total concentration of solutes as a whole. In a very recent study it was demonstrated that the activation of TRPV4 after hypoosmolar stimulation is dependent on changes in cell volume, rather than changes in the solute concentration (Toft-Bertelsen et al., 2017). This finding is in accordance to the results of the present study. In addition, osmosensitivity in the CNS has been shown to be a mechanical process (Prager-Khoutorsky and Bourque, 2015). This was demonstrated by applying hydrostatic pressure of the same strength but with the opposite orientation of the osmotic pressure to the cells. Under this conditions cells did not respond to the induced hyperosmolality (Ciura and Bourque, 2006). In peripheral neurons, the demonstration of a functional link between cell volume changes and activation after osmotic shifts is still missing. Nevertheless, swelling and neuronal activation also appear

simultaneously in peripheral neurons after hypoosmolar stimulation (Dong et al., 2015; Lechner et al., 2011).

4.9 Changes in cell volume after hypoosmolar stimulation

Changes in cell volume were observed in submucosal neurons after application of a hypoosmolar solution, whilst application of an isoosmolar solution did not lead to any visible changes in cell volume or shape. Due to the laws of physics and to membrane properties increase in cell volume is the expected consequence of hypoosmolar stimulation (Friedrich et al., 2006; Hoffmann et al., 2009; Lang, 2007; Mongin and Orlov, 2001). Strikingly all investigated neurons which showed increased action potential discharge after hypoosmolar stimulation displayed decrease in visible cell surface area in response to the application of the hypoosmolar solution. With the methods used only changes in visible cell surface area could be measured while changes in the thickness of cells (z-axis) were not detectable. Therefore, it is still possible, that also those cells after application of a hypoosmolar stimulation experienced an increase in cell volume but did not expand in the X-Y-plane but rather in the Z-axis. It is highly unlikely that a decrease in extracellular osmolality per se would lead to a decrease in cell volume as it has not been described in any cell type, and further would conflict with common principles of cell physiology (Friedrich et al., 2006, 2006; McManus et al., 1995; Mongin and Orlov, 2001). Neurons in the ENS are densely packed in ganglia which are surrounded by a rather rigid envelope (Gabella 1972; Gershon and Bursztajn 1978). Therefore, possibilities for neurons to increase their volume are limited inside the ganglion. While some neurons swell, others might be compressed due to the volume increase of the neighbouring cells. Nevertheless, the consistency in the decrease of visible cell surface area by cells sensitive to hypoosmolar stimuli is astonishing. This could lead to the assumption that the activation of osmosensitive cells is mediated by mechanical compression rather than by mechanical stretch. This assumption is supported by the recent finding that mechanical deformation of cultured myenteric neurons triggers action potential discharge (Kugler et al., 2015). Although this study describes activation of neurons by von Frey hairs in myenteric neurons only, submucosal neurons might share this characteristic.

Unfortunately, the question whether osmosensitive cells are compressed, swell or just change their morphology after osmotic shifts has to remain unanswered for the moment. Experimental techniques suitable to tackle this question are for example Ca^{2+}- imaging at the isosbestic point of the Ca^{2+}-indicator, as described by a previous study conducted in cultured myenteric neurons (Dong et al., 2015). Another elegant but rather expensive way of measuring changes in cell volume after changes in osmolality would be the use of confocal live cell microscopy in order to obtain 3-dimensional images of cells under iso- and hypoosmolar conditions.

4.10 Blocking of synaptic transmission does not reduce osmosensitivity

Due to the delayed action potential discharge after hypoosmolar stimulation it was necessary to test whether all responses to the hypoosmolar stimulus were due to direct activation of the neurons or whether part of them was mediated by synaptic transmission. 200 nM ω-conotoxin GVIA effectively blocks synaptic transmission by inhibition of the N-type voltage gated calcium channel and therefore was used for these experiments (Cruz and Olivera, 1986; Olivera et al., 1985). Performing electrical stimulation on the ganglia before and after application of ω-conotoxin revealed an absence of fEPSPs in the presence of ω-conotoxin GVIA and, therefore, effective blockade of synaptic transmission. Under the influence of ω-conotoxin GVIA, neither the percentage of responding neurons, or the action potential firing frequency after hypoosmolar stimulation, were significantly reduced. This leads to the conclusion that all recorded responses to hypoosmolality are a direct effect and not transduced synaptically by other neurons.

4.11 Ruthenium red reduces increase $[Ca^{2+}]_{in}$ after hypoosmolar stimulus

10 µM of ruthenium red significantly reduced the increase in $[Ca^{2+}]_{in}$ after hypoosmolar stimulation. It is noteworthy that the number of responding cells per ganglion was not reduced. This finding strongly indicates involvement of TRP channels in enteric osmotransduction. Due to the fact that hypoosmolar stimulation with and without the blocker was tested in a paired design, the decrease in response could possibly be traced back to a lack of reproducibility. The concentration of the blocker was chosen based on a study in which a near complete block of osmotically induced responses was achieved by this concentration in rat vestibular organ (Kamakura et al., 2016). Due to the rather non-specific effect of the drug, no other concentrations were tested. Nevertheless, the reduction of the calcium response provided evidence that was strong enough to test more specific blockers of TRP channels.

4.12 HC-067047 reduces the number of cells responding to a hypoosmolar stimulus

Through the experiments with ruthenium red the group of possible candidates for the osmosensory structure in the ENS could be narrowed down. As TRPV4 was the most promising candidate, the effect of HC-067047, a specific and potent blocker of TRPV4 (Everaerts et al., 2010), on the response to hypoosmolar stimuli was investigated.

150 nM of HC-067047 effectively reduced the percentage of responding neurons per ganglion as well as the neuroindex after stimulation with a 94 mOsm/kg HEPES solution. It is noteworthy that the action potential frequency remained unchanged in cells that responded despite the presence of the antagonist. These findings are strong evidence that TRPV4 is involved in enteric osmosensitivity. Nevertheless, there were osmosensitive enteric neurons which were not blocked by the compound which strongly suggests that there might be other channels involved in enteric osmosensitivity. The

concentration of 150 nM HC-067047 was based on another study which reports IC_{50} values for human, rat and mouse to be 48 nM, 133 nM and 17 nM respectively (Everaerts et al., 2010). The fact that fEPSPs were not altered by 150 nM HC-067047 indicates that the antagonist does not have any unspecific effects on sodium channels. Although at this rather low concentration HC-067047 is described to be a specific antagonist of TRPV4, off-target have been described in higher concentrations of 5 µM (Xia et al., 2013a).

4.13 TRPV4 agonist GSK1016790A activates enteric neurons

In order to find out whether TRPV4 plays a physiological role in the ENS, the responses of enteric neurons to the potent and specific TRPV4 agonist GSK1016790A were investigated (Thorneloe et al., 2008). Concentrations of 10 µM and 20 µM reliable led to action potential discharge in neurons of the SMP. Concentrations were chosen based on literature data from experiments where 10 µM of the drug were infused into the bladder lumen of mice and led to a significant reduction of the voiding volume (Thorneloe et al., 2008). In our experiments both concentrations of the agonist led to action potential discharge in a subset of SMP neurons. Neither in the percentage of responding neurons, nor in the spike discharge frequency, was there a significant difference between the two concentrations. Therefore, the assumption can be made that 10 µM of the agonist already lead to maximum activation of TRPV4 on enteric neurons.

When the agonist was applied a second time the number of cells responding was significantly reduced. This reduction was higher when the 20 µM concentration of the agonist was used, strongly indicating a desensitisation effect of GSK1016790A on enteric neurons. This was similar to the behaviour of the neurons after a second application of a hypoosmolar stimulus. For future experiments the 10 µM can be considered to be sufficient for reliable TRPV4 activation in enteric neurons. GSK1016790A reportedly has no off-target effects especially in regards to TRPV1 which in terms of sequence homology is the closest TRP family member of TRPV4 (Willette et al., 2008). In addition 20 µM of the agonist also has no effect on TRPM8 and TRPA1 (Thorneloe et al., 2008).

Furthermore a 20 µM application of GSK1016790A led to a transient $[Ca^{2+}]_{in}$ increase in 3.0 ± 1.4 cells per ganglion. 53% of the responses were reproducible in terms of ΔRLI. Interestingly the number of neurons per ganglion activated by the same concentration of the agonist in the VSD experiments was not significantly different. This indicates that GSK1016790A predominantly activates neurons in the SMP and stands in contrast to the findings of Rajasekhar and colleagues who describe solely activation of non-neuronal cells in the SMP by GSK1016790A (Rajasekhar et al., 2017). Another indicator that the concentration of the agonist used in our experiments was excessively high is that even 6 µM of HC-067047 could not block the agonist action on SMP neurons. This might be due to competitive receptor

binding of the antagonist and agonist. Unfortunately, no comparative data about the affinity of HC-067047 and GSK1016790A to TRPV4 is available at the moment.

The decision to use a much higher concentration of the agonist than other authors was based on the difference in how the drug was applied to the cells. While other groups use bath incubation, in these experiments local pressure application of the drugs was used. In former studies a dilution factor of 1:10 was estimated for this application method (Breunig, 2006). Observations on the action of other drugs indicate an even higher dilution factor. For example, a 1 µM nicotine concentration applied via bath incubation was enough to trigger responses in enteric neurons (Patel et al., 2008) while for the pressure application 100 µM has been necessary to elucidate neuronal responses (Kugler et al., 2015).

In contrast to our results, another study found no direct neuronal activation by 100 nM GSK1016790A in the SMP of mice but report increase in $[Ca^{2+}]_{in}$ in a subset of glia cells. These responses could be blocked effectively by 10 µM of HC-067047 and were absent in $trpv4^{-/-}$ mice (Rajasekhar et al., 2017). The fact that we did see neuronal activation while it was absent in the experiments of Rajasekhar et al. is most likely due to the large difference in concentration of GSK1016790A. Neurons as well as glia cells might express TRPV4, but the expression level might be different.

Neuronal activation by 100 nM GSK1016790A has been described in the MP of mice, where 48 % of the investigated neurons displayed an increase in $[Ca^{2+}]_{in}$ in response to an application of the TRPV4 agonist (Fichna et al., 2015). These responses could be blocked by 10 µM HC-067047 and were absent in $trpv4^{-/-}$ animals.

In order to find out whether neurons that are sensitive to GSK1016790A are osmosensitive and vice versa, a series of paired experiments was performed, in which both stimuli were applied consecutively onto the same ganglia. 27.5 % of the cells that were osmosensitive were also activated by the TRPV4 agonist. On the other hand, 73.3 % of the cells sensitive to GSK1016790A were also osmosensitive. In cells that responded to both, the hypoosmolar stimulus and the TRPV4 activator, the action potential frequency was significantly higher after the hypoosmolar stimulation compared to the application of the activator. When comparing those values to the results of the unpaired experiments it becomes obvious, that the frequencies after application of GSK1016790A are quite similar (2.0 Hz in the paired experiments and 1.7 Hz in the unpaired experiments). Nevertheless, the frequencies after application of the hypoosmolar stimulus were much higher in the paired experiments (8.0 Hz) than in the unpaired experiments (2.6 Hz). It has to be kept in mind that the order of applications was randomised. Nevertheless, this behaviour could be due to a sensitising effect of GSK1016790A on osmosensitive enteric neurons.

The majority of neurons functionally expressing TRPV4 are osmosensitive while only around one fourth of all osmosensitive neurons expresses functional TRPV4. On the first view this seems to be contradictory to the findings obtained with HC-067047. In case only 27.5% of the osmosensitive responses are TRPV4 dependent, then an inhibition of TRPV4 should only reduce the responses to osmotic shifts by this percentage. This means that even under influence of 150 nM HC-067047 13.5 % of the submucosal neurons are expected to respond to the hypoosmolar stimulus. The numbers found in the experiments using paired application of the agonist and the osmotic stimulus nevertheless were much lower being 0.0 [0.0 / 6.3] %. There are two possible reasons for this discrepancy.

On one hand HC-067047 could affect other osmosensitive channels due to off-target effects. Although studies suggest that HC-067047 is a highly selective blocker for TRPV4 (Everaerts et al., 2010) of course not all channels with a possible relevance for osmosensitivity were investigated. For example, there is no literature published on the action of HC-067047 on piezo proteins. As Xia and colleagues reported HC-067047 has off-target effects in smooth muscle cells of the pulmonary artery at high concentrations (Xia et al., 2013b). Therefore off-target effects in other cell types cannot be ruled out, even when lower concentrations of the blocker are used. On the other hand, the discrepancy could be explained by the lack in reproducibility that was evident after the hypoosmolar stimulation. Assuming that the osmotic stimulus and GSK1016790A both activate TRPV4 a desensitisation of TRPV4 would also reduce the response to GSK1016790A when applied after the hypoosmolar stimulus.

4.14 Expression levels of TRPV4 in the SMP

mRNA levels of TRPV4 in the SMP

This study was the first to evaluate the relative expression of TRPV4 in the SMP by using qRT-PCR. TRPV4 mRNA-levels were normalised to ß-actin (Kreuzer et al., 1999) and compared to the expression levels in skeletal muscle, kidney sections and whole wall bladder samples. As expected the highest mRNA levels were found in the kidney (Tian, 2004) followed by bladder (Birder et al., 2007). To evaluate the expression levels of TRPV4 a tissue sample with no or low expression of TRPV4 was required. Due to the fact that no data is published concerning this issue in guinea pig it was decided to choose a tissue based on “The Human Protein Atlas” (Uhlén et al., 2015). Interestingly mRNA levels of TRPV4 in the SMP were not significantly different from any other tissue. The only significant difference was found between the expression in the kidney and skeletal muscle. TRPV4 expression has been shown in macrophages (Hamanaka et al., 2010), endothelial cells (Vriens et al., 2005) and astrocytes (Benfenati et al., 2007). All of these cell types are present in the enteric submucosal layer and therefore this result cannot be taken as an indicator for the importance of TRPV4 in the ENS (Boesmans et al., 2013; Furness, 2006; Reichardt et al., 2013). An elegant but technically demanding method to investigate expression of TRPV4 specifically in osmosensitive cells would be the use of single cell qRT-PCR as described by (Zaelzer et al., 2015). Interestingly the variance in TRPV4 expression between the samples

was higher in the SMP, than it was in bladder and muscle tissue. Unfortunately, it was not possible to perform RT-PCR and neuroimaging experiments on the same tissues due to technical limitations, as it would be interesting to investigate whether tissues with a higher expression of TRPV4 show higher activity after hypoosmolar stimulation than tissues with a lower expression.

Immunohistochemical evidence for TRPV4 on enteric neurons

Quantitative RT-PCR demonstrated the presence of mRNA coding for TRPV4 in the colonic SMP. Nevertheless, this finding does not proof the expression of TRPV4 on protein level in neurons. Co-staining of tissues with human derived anti ANNA-1 antibodies and rabbit derived polyclonal anti TRPV4 antibodies were performed to test whether TRPV4 was located on enteric neurons. Like the majority of commercial antibodies, the TRPV4 antibody used in this study was only validated in human, mouse and rat tissue. It is noteworthy that the staining of human and guinea pig tissue with the same concentration of the antibody resulted in a similar staining pattern. In guinea pig tissue, nevertheless the vast majority (97 %) of ANNA-1 positive cells showed binding of the anti TRPV4 antibody. Due to the fact that pharmacological experiments revealed physiological relevance of TRPV4 in a much lower number of enteric neurons unspecific binding of the TRPV4 antibody has to be estimated. Incubation without the primary antibody ruled out unspecific binding of the secondary antibody. In a recent study, performed in mouse colonic and ileal MP preparations, immunofluorescent staining with TRPV4 antibodies is described (Fichna et al., 2015). Although the authors do not state the percentage of TRPV4 positive neurons it is evident from the example images that only a small population of myenteric neurons shows TRPV4 positive staining. Nevertheless, due to the fact that this study was performed in mouse and a different antibody was used its comparability with our study is limited (Fichna et al., 2015).

4.15 Chemical coding of neurons sensitive to hypoosmolar stimuli

Immunohistochemical co-staining with antibodies against ChAT and VIP after VSD imaging revealed that 65 % of the neurons sensitive to a hypoosmolar stimulus were positive for ChAT while 35 % were positive for VIP. The distribution of ChAT and VIP positive neurons in the colonic SMP of the guinea pig is described to be roughly 50 % each (Neunlist et al., 1998). This allows the assumption that the responses to hypoosmolar stimuli in the colonic SMP of the guinea pig are predominantly mediated through cholinergic pathways. In the SMP of the guinea pig distal colon VIP has been shown to serve as an activator of chloride secretion (Reddix et al., 1994). Therefore, it seems counter intuitive that only a minority of VIP secreting neurons are sensitive to hypoosmolar stimuli, as increased chloride secretion would counteract hypoosmolality in the lumen. Further experiments are needed to investigate the chemical coding of osmosensitive enteric neurons in detail.

4.16 A possible role of enteric glia cells in enteric osmosensitivity

The number of cells responding to a hypoosmolar stimulus was significantly higher in the Ca^{2+}-imaging experiments compared to the experiments using the VSD technique. This, in combination with the fact that the latency to the onset of the response after hypoosmolar stimulation was significantly higher in the VSD experiments than in the Ca-imaging experiments, strongly indicates that in addition to neurons glia cells are activated by hypoosmolar stimuli. Due to technical limitations, no reliable immunohistochemical staining could be performed after Ca^{2+} - imaging experiments and the cell type of responding cells remained unclear.

The findings of Rajasekhar and coleagues who reported activation of enteric glia cells after 100 nM of GSK1016790A (Rajasekhar et al., 2017) are in accordance to our results in which we found $[Ca^{2+}]_{in}$ responses in neurons as well as supposedly in enteric glia cells. Enteric glia cells are known to share several features with astrocytes (Boesmans et al., 2013; De Giorgio et al., 2012; Gabella, 1981). These features include morphological similarities as well as similarities in the expression of several antigens (Gabella, 1981). Osmosensitivity is a well-known feature of astrocytes. In the process of RVD after hypoosmolar stimulation astrocytes release organic molecules from their cytoplasm (Pasantes-Morales et al., 1990). Amongst those molecules are taurine, glutamate and aspartate (Kimelberg et al., 1990). Although RVD may be the primary purpose of those molecules, they also have neuroactive effects (Kimelberg et al., 1990). Besides its function as an non-perturbing osmolyte, taurine also acts on glycine receptors (Betz, 1992). Because glycine as well as glutamate receptors are expressed on enteric neurons (Galligan, 2002) and are also shown to have functional relevance (Neunlist et al., 2001) it is possible that the activity of enteric neurons is modulated by the release of neuroactive amino acids from enteric glia cells after osmotic stimulation.

4.17 Final conclusion and future perspectives

This study was the first to describe osmosensitivity in enteric submucosal neurons. It revealed that enteric neurons possess all the components necessary to sense changes in extracellular osmolality. Furthermore, it revealed valuable mechanistic insights in terms of the molecular structures involved in enteric osmosensitivity by showing that TRPV4 plays a role in enteric osmosensitivity. Now that the ability of enteric neurons to respond to osmotic shifts has been demonstrated, it is important to evaluate the physiological relevance of this finding. Unfortunately, the range of osmotic fluctuations that enteric neurons experience under physiological or pathophysiological conditions is still unknown. To prove the physiological relevance of TRPV4 in enteric osmosensitivity, we are planning to conduct experiments in $TRPV^{-/-}$ mice in the future.

LIST OF REFERENCES

Adachi, A. (1984). Thermosensitive and osmoreceptive afferent fibers in the hepatic branch of the vagus nerve. J. Auton. Nerv. Syst. *10*, 269–273.

Alessandri-Haber, N., Joseph, E., Dina, O.A., Liedtke, W., and Levine, J.D. (2005). TRPV4 mediates pain-related behavior induced by mild hypertonic stimuli in the presence of inflammatory mediator. Pain *118*, 70–79.

Andersen, L.J., Jensen, T.U., Bestle, M.H., and Bie, P. (2000). Gastrointestinal osmoreceptors and renal sodium excretion in humans. Am. J. Physiol. Regul. Integr. Comp. Physiol. *278*, R287-294.

Apperly, F.L. (1926). Duodenal Regulation and the Control of the Pylorus. British Journal of Experimental Pathology.

Auerbach, L. (1862). Über einen Plexus myentericus.

Badoer, E., Ng, C.-W., and De Matteo, R. (2003). Glutamatergic input in the PVN is important in renal nerve response to elevations in osmolality. Am. J. Physiol. Renal Physiol. *285*, F640-650.

Baertschi, A.J., and Pence, R.A. (1995). Gut-brain signaling of water absorption inhibits vasopressin in rats. Am. J. Physiol. *268*, R236-247.

Baertschi, A.J., and Vallet, P.G. (1981). Osmosensitivity of the hepatic portal vein area and vasopressin release in rats. J. Physiol. *315*, 217–230.

Bandell, M., Story, G.M., Hwang, S.W., Viswanath, V., Eid, S.R., Petrus, M.J., Earley, T.J., and Patapoutian, A. (2004). Noxious cold ion channel TRPA1 is activated by pungent compounds and bradykinin. Neuron *41*, 849–857.

Baylis, P.H. (1983). Posterior pituitary function in health and disease. Clin. Endocrinol. Metab. *12*, 747–770.

Bayliss, W., and Starling, E. (1899). The movements and innervation of the small intestine. J. Physiol. *24*.

Benfenati, V., Amiry-Moghaddam, M., Caprini, M., Mylonakou, M.N., Rapisarda, C., Ottersen, O.P., and Ferroni, S. (2007). Expression and functional characterization of transient receptor potential vanilloid-related channel 4 (TRPV4) in rat cortical astrocytes. Neuroscience *148*, 876–892.

Berridge, M.J. (1998). Neuronal calcium signaling. Neuron *21*, 13–26.

Bertrand, P.P., Kunze, W.A., Bornstein, J.C., Furness, J.B., and Smith, M.L. (1997). Analysis of the responses of myenteric neurons in the small intestine to chemical stimulation of the mucosa. Am. J. Physiol. *273*, G422-435.

Betz, H. (1992). Structure and function of inhibitory glycine receptors. Q. Rev. Biophys. *25*, 381–394.

Birder, L., Kullmann, F.A., Lee, H., Barrick, S., de Groat, W., Kanai, A., and Caterina, M. (2007). Activation of Urothelial Transient Receptor Potential Vanilloid 4 by 4 -Phorbol 12,13-Didecanoate Contributes to Altered Bladder Reflexes in the Rat. J. Pharmacol. Exp. Ther. *323*, 227–235.

Blackshaw, l. a., Brookes, s. j. h., Grundy, d., and Schemann, M. (2007). Sensory transmission in the gastrointestinal tract. Neurogastroenterol. Motil. *19*, 1–19.

Boesmans, W., Owsianik, G., Tack, J., Voets, T., and Vanden Berghe, P. (2011). TRP channels in neurogastroenterology: opportunities for therapeutic intervention. Br. J. Pharmacol. *162*, 18–37.

Boesmans, W., Martens, M.A., Weltens, N., Hao, M.M., Tack, J., Cirillo, C., and Vanden Berghe, P. (2013). Imaging neuron-glia interactions in the enteric nervous system. Front. Cell. Neurosci. *7*.

Bohnen, N., Terwel, D., Markerink, M., Ten Haaf, J.A., and Jolles, J. (1992). Pitfalls in the measurement of plasma osmolality pertinent to research in vasopressin and water metabolism. Clin. Chem. *38*, 2278–2280.

Borgnia, M., Nielsen, S., Engel, A., and Agre, P. (1999). Cellular and molecular biology of the aquaporin water channels. Annu. Rev. Biochem. *68*, 425–458.

Bornstein, J.C., Furness, J.B., and Kunze, W.A. (1994). Electrophysiological characterization of myenteric neurons: how do classification schemes relate? J. Auton. Nerv. Syst. *48*, 1–15.

Boujard, D., Anselme, B., Cullin, C., Raguénès-Nicol, C. (2014). Zell- und Molekularbiologie im Überblick., Springer Spektrum, Wiesbaden

Bourque, C.W. (2008). Central mechanisms of osmosensation and systemic osmoregulation. Nat. Rev. Neurosci. *9*, 519–531.

Breunig, E. (2006). Die Wirkung von Histamin auf die Nervenaktivität im humanen Plexus submucosus. Technische Universität München.

Brierley, S.M., Hughes, P.A., Page, A.J., Kwan, K.Y., Martin, C.M., O'Donnell, T.A., Cooper, N.J., Harrington, A.M., Adam, B., Liebregts, T., et al. (2009). The Ion Channel TRPA1 Is Required for Normal Mechanosensation and Is Modulated by Algesic Stimuli. Gastroenterology *137*, 2084–2095.e3.

Brimble, M.J., and Dyball, R.E. (1977). Characterization of the responses of oxytocin- and vasopressin-secreting neurones in the supraoptic nucleus to osmotic stimulation. J. Physiol. *271*, 253–271.

Buhner, S., Braak, B., Li, Q., Kugler, E.M., Klooker, T., Wouters, M., Donovan, J., Vignali, S., Mazzuoli-Weber, G., Grundy, D., et al. (2014). Neuronal activation by mucosal biopsy supernatants from irritable bowel syndrome patients is linked to visceral sensitivity. Exp. Physiol. *99*, 1299–1311.

Burnstock, G. (1972). Purinergic nerves. Pharmacol. Rev. *24*, 509–581.

Campbell, G., and Burnstock, G. (1968). Comparative physiology of gastrointestinal motility. In Comparative Physiology of Gastrointestinal Motility, pp. 2213–2266.

Carlson, S.H., Beitz, A., and Osborn, J.W. (1997). Intragastric hypertonic saline increases vasopressin and central Fos immunoreactivity in conscious rats. Am. J. Physiol. *272*, R750-758.

Choi-Kwon, S., and Baertschi, A.J. (1991). Splanchnic osmosensation and vasopressin: mechanisms and neural pathways. Am. J. Physiol. *261*, E18-25.

Ciura, S., and Bourque, C.W. (2006). Transient Receptor Potential Vanilloid 1 Is Required for Intrinsic Osmoreception in Organum Vasculosum Lamina Terminalis Neurons and for Normal Thirst Responses to Systemic Hyperosmolality. J. Neurosci. *26*, 9069–9075.

Cohen, L.B., Salzberg, B.M., and Grinvald, A. (1978). Optical methods for monitoring neuron activity. Annu. Rev. Neurosci. *1*, 171–182.

Colbert, H.A., Smith, T.L., and Bargmann, C.I. (1997). OSM-9, a novel protein with structural similarity to channels, is required for olfaction, mechanosensation, and olfactory adaptation in Caenorhabditis elegans. J. Neurosci. Off. J. Soc. Neurosci. *17*, 8259–8269.

Cruz, L.J., and Olivera, B.M. (1986). Calcium channel antagonists. Omega-conotoxin defines a new high affinity site. J. Biol. Chem. *261*, 6230–6233.

Cunningham, S.M., Mihara, S., and Higashi, H. (1998). Presynaptic calcium channels mediating synaptic transmission in submucosal neurones of the guinea-pig caecum. J. Physiol. *509 (Pt 2)*, 425–435.

De Giorgio, R., Giancola, F., Boschetti, E., Abdo, H., Lardeux, B., and Neunlist, M. (2012). Enteric glia and neuroprotection: basic and clinical aspects. AJP Gastrointest. Liver Physiol. *303*, G887–G893.

Delrée, P., Ribbens, C., Martin, D., Rogister, B., Lefebvre, P.P., Rigo, J.M., Leprince, P., Schoenen, J., and Moonen, G. (1993). Plasticity of developing and adult dorsal root ganglion neurons as revealed in vitro. Brain Res. Bull. *30*, 231–237.

Denker, B.M., Smith, B.L., Kuhajda, F.P., and Agre, P. (1988). Identification, purification, and partial characterization of a novel Mr 28,000 integral membrane protein from erythrocytes and renal tubules. J. Biol. Chem. *263*, 15634–15642.

Dogiel, A.S. (1895). Zur Frage über die Ganglien der Darmgeflechte bei den Säugetieren. Anat. Anz.

Dong, H., Jiang, Y., Dong, J., and Mittal, R.K. (2015). Inhibitory motor neurons of the esophageal myenteric plexus are mechanosensitive. Am. J. Physiol. Cell Physiol. *308*, C405-413.

Dunn, F.L., Brennan, T.J., Nelson, A.E., and Robertson, G.L. (1973). The role of blood osmolality and volume in regulating vasopressin secretion in the rat. J. Clin. Invest. *52*, 3212–3219.

Epstein, F.H., Goyal, R.K., and Hirano, I. (1996). The Enteric Nervous System. N. Engl. J. Med. *334*, 1106–1115.

Everaerts, W., Zhen, X., Ghosh, D., Vriens, J., Gevaert, T., Gilbert, J.P., Hayward, N.J., McNamara, C.R., Xue, F., Moran, M.M., et al. (2010). Inhibition of the cation channel TRPV4 improves bladder function in mice and rats with cyclophosphamide-induced cystitis. Proc. Natl. Acad. Sci. U. S. A. *107*, 19084–19089.

Faden, A., Demediuk, P., Panter, S., and Vink, R. (1989). The role of excitatory amino acids and NMDA receptors in traumatic brain injury. Science *244*, 798–800.

Fahrenkrug, J. (1979). Vasoactive intestinal polypeptide: measurement, distribution and putative neurotransmitter function. Digestion *19*, 149–169.

Ferrandiz-Huertas, C., Mathivanan, S., Wolf, C.J., Devesa, I., and Ferrer-Montiel, A. (2014). Trafficking of ThermoTRP Channels. Membranes *4*, 525–564.

Ferraris, R.P., Yasharpour, S., Lloyd, K.C., Mirzayan, R., and Diamond, J.M. (1990). Luminal glucose concentrations in the gut under normal conditions. Am. J. Physiol. *259*, G822-837.

Fichna, J., Poole, D.P., Veldhuis, N., MacEachern, S.J., Saur, D., Zakrzewski, P.K., Cygankiewicz, A.I., Mokrowiecka, A., Małecka-Panas, E., Krajewska, W.M., et al. (2015). Transient receptor potential vanilloid 4 inhibits mouse colonic motility by activating NO-dependent enteric neurotransmission. J. Mol. Med. *93*, 1297–1309.

Fisher, S.K., Cheema, T.A., Foster, D.J., and Heacock, A.M. (2008). Volume-dependent osmolyte efflux from neural tissues: regulation by G-protein-coupled receptors. J. Neurochem. ???-???

Fluhler, E., Burnham, V.G., and Loew, L.M. (1985). Spectra, membrane binding, and potentiometric responses of new charge shift probes. Biochemistry (Mosc.) *24*, 5749–5755.

Friedrich, B., Matskevich, I., and Lang, F. (2006). Cell Volume Regulatory Mechanisms. In Contributions to Nephrology, F. Lang, ed. (Basel: KARGER), pp. 1–8.

Furness, J.B. (2000). Types of neurons in the enteric nervous system. J. Auton. Nerv. Syst. *81*, 87–96.

Furness, J.B. (2006). The enteric nervous system (Malden, Mass: Blackwell Pub).

Furness, J.B., and Costa, M. (1973). The nervous release and the action of substances which affect intestinal muscle through neither adrenoreceptors nor cholinoreceptors. Philos. Trans. R. Soc. Lond. B. Biol. Sci. *265*, 123–133.

Furness, J.B., Kunze, W.A., Bertrand, P.P., Clerc, N., and Bornstein, J.C. (1998). Intrinsic primary afferent neurons of the intestine. Prog. Neurobiol. *54*, 1–18.

Furness, J.B., Jones, C., Nurgali, K., and Clerc, N. (2004). Intrinsic primary afferent neurons and nerve circuits within the intestine. Prog. Neurobiol. *72*, 143–164.

Gabella, G. (1972). Fine structure of the myenteric plexus in the guinea-pig ileum. J. Anat. *111*, 69–97.

Gabella, G. (1981). Ultrastructure of the nerve plexuses of the mammalian intestine: The enteric glial cells. Neuroscience *6*, 425–436.

Galligan, J.J. (2002). Ligand-gated ion channels in the enteric nervous system. Neurogastroenterol. Motil. Off. J. Eur. Gastrointest. Motil. Soc. *14*, 611–623.

Ganfornina, M.D., Sánchez, D., and Bastiani, M.J. (1996). Embryonic development of the enteric nervous system of the grasshopper Schistocerca americana. J. Comp. Neurol. *372*, 581–596.

Gee, K.R., Brown, K.A., Chen, W.-N.U., Bishop-Stewart, J., Gray, D., and Johnson, I. (2000). Chemical and physiological characterization of fluo-4 Ca2+-indicator dyes. Cell Calcium *27*, 97–106.

Geelen, G., Greenleaf, J.E., and Keil, L.C. (1996). Drinking-induced plasma vasopressin and norepinephrine changes in dehydrated humans. J. Clin. Endocrinol. Metab. *81*, 2131–2135.

Gershon, M.D. (1999). The second brain: a groundbreaking new understanding of nervous disorders of the stomach and intestine (New York, NY: HarperPerennial).

Gershon, M.D., and Bursztajn, S. (1978). Properties of the enteric nervous system: Limitation of access of intravascular macromolecules to the myenteric plexus and muscularis externa. J. Comp. Neurol. *180*, 467–487.

Gill, G.V., Baylis, P.H., Flear, C.T., and Lawson, J.Y. (1985). Changes in plasma solutes after food. J. R. Soc. Med. *78*, 1009–1013.

Gomis, A., Soriano, S., Belmonte, C., and Viana, F. (2008). Hypoosmotic- and pressure-induced membrane stretch activate TRPC5 channels. J. Physiol. *586*, 5633–5649.

Grimm, C., Kraft, R., Sauerbruch, S., Schultz, G., and Harteneck, C. (2003). Molecular and Functional Characterization of the Melastatin-related Cation Channel TRPM3. J. Biol. Chem. *278*, 21493–21501.

Grinvald, A., Frostig, R.D., Lieke, E., and Hildesheim, R. (1988). Optical imaging of neuronal activity. Physiol. Rev. *68*, 1285–1366.

Hamanaka, K., Jian, M.-Y., Townsley, M.I., King, J.A., Liedtke, W., Weber, D.S., Eyal, F.G., Clapp, M.M., and Parker, J.C. (2010). TRPV4 channels augment macrophage activation and ventilator-induced lung injury. Am. J. Physiol. Lung Cell. Mol. Physiol. *299*, L353-362.

Hansen, M.B. (2003). The enteric nervous system I: organisation and classification. Pharmacol. Toxicol. *92*, 105–113.

Hinder, R.A., and Kelly, K.A. (1977). Canine gastric emptying of solids and liquids. Am. J. Physiol. *233*, E335-340.

Hirst, G.D., Holman, M.E., and Spence, I. (1974). Two types of neurones in the myenteric plexus of duodenum in the guinea-pig. J. Physiol. *236*, 303–326.

Hoffmann, E.K., Lambert, I.H., and Pedersen, S.F. (2009). Physiology of cell volume regulation in vertebrates. Physiol. Rev. *89*, 193–277.

Holzer, P. (2011). TRP channels in the digestive system. Curr. Pharm. Biotechnol. *12*, 24–34.

Huang, P.L., Dawson, T.M., Bredt, D.S., Snyder, S.H., and Fishman, M.C. (1993). Targeted disruption of the neuronal nitric oxide synthase gene. Cell *75*, 1273–1286.

Hunt, J.N., MacDonald, I., and Spurrell, W.R. (1951). The gastric response to pectin meals of high osmotic pressure. J. Physiol. *115*, 185–195.

Jänig, W. (2006). The integrative action of the autonomic nervous system: neurobiology of homeostasis (Cambridge, UK ; New York: Cambridge University Press).

Kalyanaraman, B., Feix, J.B., Sieber, F., Thomas, J.P., and Girotti, A.W. (1987). Photodynamic action of merocyanine 540 on artificial and natural cell membranes: involvement of singlet molecular oxygen. Proc. Natl. Acad. Sci. U. S. A. *84*, 2999–3003.

Kamakura, T., Kondo, M., Koyama, Y., Hanada, Y., Ishida, Y., Nakamura, Y., Yamada, T., Takimoto, Y., Kitahara, T., Ozono, Y., et al. (2016). Functional Expression of an Osmosensitive Cation Channel, Transient Receptor Potential Vanilloid 4, in Rat Vestibular Ganglia. Audiol. Neurotol. *21*, 268–274.

Kandel, E.R. (1996). Neurowissenschaften: eine Einführung (Heidelberg [u.a.]: Spektrum, Akad. Verl.).

Kanzaki, M., Nagasawa, M., Kojima, I., Sato, C., Naruse, K., Sokabe, M., and Iida, H. (1999). Molecular identification of a eukaryotic, stretch-activated nonselective cation channel. Science *285*, 882–886.

Keinke, O., Schemann, M., and Ehrlein, H.-J. (1984). Mechanical Factors Regulating Gastric Emptying of Viscous Nutrient Meals in Dogs. Q. J. Exp. Physiol. *69*, 781–795.

Kimelberg, H.K. (1995). Current concepts of brain edema. Review of laboratory investigations. J. Neurosurg. *83*, 1051–1059.

Kimelberg, H.K., Goderie, S.K., Higman, S., Pang, S., and Waniewski, R.A. (1990). Swelling-induced release of glutamate, aspartate, and taurine from astrocyte cultures. J. Neurosci. Off. J. Soc. Neurosci. *10*, 1583–1591.

Kreuzer, K.A., Lass, U., Landt, O., Nitsche, A., Laser, J., Ellerbrok, H., Pauli, G., Huhn, D., and Schmidt, C.A. (1999). Highly sensitive and specific fluorescence reverse transcription-PCR assay for the

pseudogene-free detection of beta-actin transcripts as quantitative reference. Clin. Chem. *45*, 297–300.

Kugler, E.M., Michel, K., Zeller, F., Demir, I.E., Ceyhan, G.O., Schemann, M., and Mazzuoli-Weber, G. (2015). Mechanical stress activates neurites and somata of myenteric neurons. Front. Cell. Neurosci. *9*, 342.

Kuramochi, G., and Kobayashi, I. (2000). Regulation of the urine concentration mechanism by the oropharyngeal afferent pathway in man. Am. J. Nephrol. *20*, 42–47.

Lang, F. (2007). Mechanisms and Significance of Cell Volume Regulation. J. Am. Coll. Nutr. *26*, 613S–623S.

Lang, F., Busch, G.L., Ritter, M., Völkl, H., Waldegger, S., Gulbins, E., and Häussinger, D. (1998a). Functional significance of cell volume regulatory mechanisms. Physiol. Rev. *78*, 247–306.

Lang, F., Busch, G.L., and Völkl, H. (1998b). The diversity of volume regulatory mechanisms. Cell. Physiol. Biochem. Int. J. Exp. Cell. Physiol. Biochem. Pharmacol. *8*, 1–45.

Lechner, S.G., Markworth, S., Poole, K., Smith, E.S.J., Lapatsina, L., Frahm, S., May, M., Pischke, S., Suzuki, M., Ibañez-Tallon, I., et al. (2011). The Molecular and Cellular Identity of Peripheral Osmoreceptors. Neuron *69*, 332–344.

Li, Q., Michel, K., Annahazi, A., Demir, I.E., Ceyhan, G.O., Zeller, F., Komorowski, L., Stöcker, W., Beyak, M.J., Grundy, D., et al. (2016). Anti-Hu antibodies activate enteric and sensory neurons. Sci. Rep. *6*, 38216.

Liedtke, W. (2006). Transient receptor potential vanilloid channels functioning in transduction of osmotic stimuli. J. Endocrinol. *191*, 515–523.

Liedtke, W. (2007). Role of TRPV ion channels in sensory transduction of osmotic stimuli in mammals. Exp. Physiol. *92*, 507–512.

Liedtke, W., and Friedman, J.M. (2003). Abnormal osmotic regulation in trpv4-/- mice. Proc. Natl. Acad. Sci. U. S. A. *100*, 13698–13703.

Liedtke, W., Choe, Y., Martí-Renom, M.A., Bell, A.M., Denis, C.S., Sali, A., Hudspeth, A.J., Friedman, J.M., and Heller, S. (2000). Vanilloid receptor-related osmotically activated channel (VR-OAC), a candidate vertebrate osmoreceptor. Cell *103*, 525–535.

Lieu, T., Kollarik, M., Myers, A.C., and Undem, B.J. (2011). Neurotrophin and GDNF family ligand receptor expression in vagal sensory nerve subtypes innervating the adult guinea pig respiratory tract. AJP Lung Cell. Mol. Physiol. *300*, L790–L798.

Lin, H.C., Elashoff, J.D., Kwok, G.M., Gu, Y.G., and Meyer, J.H. (1994). Stimulation of duodenal motility by hyperosmolar mannitol depends on local osmoreceptor control. Am. J. Physiol. *266*, G940-943.

Lippi, A., Santicioli, P., Criscuoli, M., and Maggi, C.A. (1998). Depolarization evoked co-release of tachykinins from enteric nerves in the guinea-pig proximal colon. Naunyn. Schmiedebergs Arch. Pharmacol. *357*, 245–251.

Liu, S., Qu, M.-H., Ren, W., Hu, H.-Z., Gao, N., Wang, G.-D., Wang, X.-Y., Fei, G., Zuo, F., Xia, Y., et al. (2008). Differential expression of canonical (classical) transient receptor potential channels in guinea pig enteric nervous system. J. Comp. Neurol. *511*, 847–862.

Ma, T., and Verkman, A.S. (1999). Aquaporin water channels in gastrointestinal physiology. J. Physiol. *517 (Pt 2)*, 317–326.

Maggi, C.A. (1995). The mammalian tachykinin receptors. Gen. Pharmacol. *26*, 911–944.

Maruyama, T., Tabata, K., Nakagawa, S., and Yanagisawa, N. (1991). [A case of acute water intoxication showing triphasic waves on EEG]. Rinsho Shinkeigaku *31*, 523–527.

Mazzuoli, G., and Schemann, M. (2009). Multifunctional rapidly adapting mechanosensitive enteric neurons (RAMEN) in the myenteric plexus of the guinea pig ileum. J. Physiol. *587*, 4681–4694.

Mazzuoli, G., and Schemann, M. (2012). Mechanosensitive enteric neurons in the myenteric plexus of the mouse intestine. PloS One *7*, e39887.

Mazzuoli, G., Liao, D., Gregersen, H., and Schemann, M. (2008). Mechanosensitive neurons in the enteric nervous system (Lucerne, Switzerland).

Mazzuoli-Weber, G., and Schemann, M. (2015a). Mechanosensitive enteric neurons in the guinea pig gastric corpus. Front. Cell. Neurosci. *9*, 430.

Mazzuoli-Weber, G., and Schemann, M. (2015b). Mechanosensitivity in the enteric nervous system. Front. Cell. Neurosci. *9*, 408.

McCleskey, E.W., Fox, A.P., Feldman, D.H., Cruz, L.J., Olivera, B.M., Tsien, R.W., and Yoshikami, D. (1987). Omega-conotoxin: direct and persistent blockade of specific types of calcium channels in neurons but not muscle. Proc. Natl. Acad. Sci. U. S. A. *84*, 4327–4331.

McConalogue, K., Lyster, D.J., and Furness, J.B. (1995). Electrophysiological analysis of the actions of pituitary adenylyl cyclase activating peptide in the taenia of the guinea-pig caecum. Naunyn. Schmiedebergs Arch. Pharmacol. *352*, 538–544.

McHugh, J., Keller, N.R., Appalsamy, M., Thomas, S.A., Raj, S.R., Diedrich, A., Biaggioni, I., Jordan, J., and Robertson, D. (2010). Portal osmopressor mechanism linked to transient receptor potential vanilloid 4 and blood pressure control. Hypertension *55*, 1438–1443.

McManus, M.L., Churchwell, K.B., and Strange, K. (1995). Regulation of cell volume in health and disease. N. Engl. J. Med. *333*, 1260–1266.

Meissner, G. (1857). Über die Nerven der Darmwand. Z. Für Ration. Med. 364–366.

Michel, K., Zeller, F., Langer, R., Nekarda, H., Kruger, D., Dover, T.J., Brady, C.A., Barnes, N.M., and Schemann, M. (2005). Serotonin excites neurons in the human submucous plexus via 5-HT3 receptors. Gastroenterology *128*, 1317–1326.

Michel, K., Michaelis, M., Mazzuoli, G., Mueller, K., Berghe, P.V., and Schemann, M. (2011). Fast calcium and voltage sensitive dye imaging in enteric neurons reveal calcium peaks associated with single action potential discharge. J. Physiol. no-no.

Mongin, A.A., and Orlov, S.N. (2001). Mechanisms of cell volume regulation and possible nature of the cell volume sensor. Pathophysiology *8*, 77–88.

Mortimer, C.E., and Müller, U. (2003). Chemie: das Basiswissen der Chemie ; 125 Tabellen (Stuttgart: Thieme).

Muraki, K., Iwata, Y., Katanosaka, Y., Ito, T., Ohya, S., Shigekawa, M., and Imaizumi, Y. (2003). TRPV2 is a component of osmotically sensitive cation channels in murine aortic myocytes. Circ. Res. *93*, 829–838.

Nagahama, M., Ma, N., Semba, R., and Naruse, S. (2006). Aquaporin 1 immunoreactive enteric neurons in the rat ileum. Neurosci. Lett. *395*, 206–210.

Neunlist, M., Frieling, T., Rupprecht, C., and Schemann, M. (1998). Polarized enteric submucosal circuits involved in secretory responses of the guinea-pig proximal colon. J. Physiol. *506*, 539–550.

Neunlist, M., Peters, S., and Schemann, M. (1999a). Multisite optical recording of excitability in the enteric nervous system. Neurogastroenterol. Motil. Off. J. Eur. Gastrointest. Motil. Soc. *11*, 393–402.

Neunlist, M., Reiche, D., Michel, K., Pfannkuche, H., Hoppe, S., and Schemann, M. (1999b). The enteric nervous system: region and target specific projections and neurochemical codes. Eur. J. Morphol. *37*, 233–240.

Neunlist, M., Michel, K., Reiche, D., Dobreva, G., Huber, K., and Schemann, M. (2001). Glycine activates myenteric neurones in adult guinea-pigs. J. Physiol. *536*, 727–739.

Nič, M., Jirát, J., Košata, B., Jenkins A., McNaught, A. eds. (2009). Osmolality. In IUPAC Compendium of Chemical Terminology (Research Triagle Park, NC: IUPAC), p.

Nielsen, S., Frøkiær, J., Marples, D., Kwon, T.-H., Agre, P., and Knepper, M.A. (2002). Aquaporins in the Kidney: From Molecules to Medicine. Physiol. Rev. *82*, 205–244.

Niijima, A. (1969). Afferent discharges from osmoreceptors in the liver of the guinea pig. Science *166*, 1519–1520.

Nobelprize.org (2017). Peter Agre - Facts.

North, R.A. (1973). The calcium-dependent slow after-hyperpolarization in myenteric plexus neurones with tetrodotoxin-resistant action potentials. Br. J. Pharmacol. *49*, 709–711.

Obaid, A.L., Koyano, T., Lindstrom, J., Sakai, T., and Salzberg, B.M. (1999). Spatiotemporal patterns of activity in an intact mammalian network with single-cell resolution: optical studies of nicotinic activity in an enteric plexus. J. Neurosci. Off. J. Soc. Neurosci. *19*, 3073–3093.

Oliet, S.H., and Bourque, C.W. (1993). Mechanosensitive channels transduce osmosensitivity in supraoptic neurons. Nature *364*, 341–343.

Oliet, S.H., and Bourque, C.W. (1996). Gadolinium uncouples mechanical detection and osmoreceptor potential in supraoptic neurons. Neuron *16*, 175–181.

Olivera, B.M., Gray, W.R., Zeikus, R., McIntosh, J.M., Varga, J., Rivier, J., de Santos, V., and Cruz, L.J. (1985). Peptide neurotoxins from fish-hunting cone snails. Science *230*, 1338–1343.

Olney, J.W. (1969). Brain lesions, obesity, and other disturbances in mice treated with monosodium glutamate. Science *164*, 719–721.

Papadopoulos, M.C., and Verkman, A.S. (2013). Aquaporin water channels in the nervous system. Nat. Rev. Neurosci. *14*, 265–277.

Pasantes-Morales, H., and Tuz, K. (2006). Volume changes in neurons: hyperexcitability and neuronal death. Contrib. Nephrol. *152*, 221–240.

Pasantes-Morales, H., Moran, J., and Schousboe, A. (1990). Volume-sensitive release of taurine from cultured astrocytes: properties and mechanism. Glia *3*, 427–432.

Pasantes-Morales, H., Lezama, R.A., Ramos-Mandujano, G., and Tuz, K.L. (2006). Mechanisms of Cell Volume Regulation in Hypo-osmolality. Am. J. Med. *119*, S4–S11.

Patel, B. A., Galligan, J. J., Swain, G. M., and Bian, X. (2008). Electrochemical monitoring of nitric oxide released by myenteric neurons of the guinea pig ileum. Neurogastroenterol. Motil. *20*, 1243–1250.

Pedersen, S., Lambert, I.H., Thoroed, S.M., and Hoffmann, E.K. (2000). Hypotonic cell swelling induces translocation of the alpha isoform of cytosolic phospholipase A2 but not the gamma isoform in Ehrlich ascites tumor cells. Eur. J. Biochem. *267*, 5531–5539.

Pompolo, S., and Furness, J.B. (1998). Quantitative analysis of inputs to somatostatin-immunoreactive descending interneurons in the myenteric plexus of the guinea-pig small intestine. Cell Tissue Res. *294*, 219–226.

Prager-Khoutorsky, M., and Bourque, C.W. (2015). Mechanical Basis of Osmosensory Transduction in Magnocellular Neurosecretory Neurones of the Rat Supraoptic Nucleus. J. Neuroendocrinol. *27*, 507–515.

Rajasekhar, P., Veldhuis, N.A., Nowell, C., Fichna, J., Bunett, N., and Poole, D.P. (2017). Identification of novel sites of TRPV4 expression in the mouse colon.

Ramsey, I.S., Delling, M., and Clapham, D.E. (2006). An introduction to TRP channels. Annu. Rev. Physiol. *68*, 619–647.

Randall, D.J. (1997). Eckert animal physiology: mechanisms and adaptations (New York: W.H. Freeman and Co).

Rattan, S., and Chakder, S. (1993). Inhibitory effect of CO on internal anal sphincter: heme oxygenase inhibitor inhibits NANC relaxation. Am. J. Physiol. *265*, G799-804.

Reddix, R., Kuhawara, A., Wallace, L., and Cooke, H.J. (1994). Vasoactive intestinal polypeptide: a transmitter in submucous neurons mediating secretion in guinea pig distal colon. J. Pharmacol. Exp. Ther. *269*, 1124–1129.

Reichardt, F., Baudry, C., Gruber, L., Mazzuoli, G., Moriez, R., Scherling, C., Kollmann, P., Daniel, H., Kiesling, S., Haller, D., et al. (2013). Properties of myenteric neurons and mucosal functions in the distal colon of diet-induced obese mice. J. Physiol.

Robinson, D., Besley, N.A., O'Shea, P., and Hirst, J.D. (2011). Di-8-ANEPPS Emission Spectra in Phospholipid/Cholesterol Membranes: A Theoretical Study. J. Phys. Chem. B *115*, 4160–4167.

Rühl, A. (2005). Glial cells in the gut. Neurogastroenterol. Motil. *17*, 777–790.

Salzberg, B.M., Grinvald, A., Cohen, L.B., Davila, H.V., and Ross, W.N. (1977). Optical recording of neuronal activity in an invertebrate central nervous system: simultaneous monitoring of several neurons. J. Neurophysiol. *40*, 1281–1291.

Sanders, J.I., and Kepecs, A. (2014). A low-cost programmable pulse generator for physiology and behavior. Front. Neuroengineering *7*.

Schabadasch, A. (1930). Intramurale Nervengeflechte des Darmrohrs. Z. Für Zellforsch. Mikrosk. Anat. *10*, 320–385.

Schemann, M., and Ehrlein, H.-J. (1986). Postprandial Patterns of Canine Jejunal Motility and Transit of Luminal Content. Gastroenterology *90*, 991–1000.

Schemann, M., Michel, K., Peters, S., Bischoff, S.C., and Neunlist, M. (2002). Cutting-edge technology. III. Imaging and the gastrointestinal tract: mapping the human enteric nervous system. Am. J. Physiol. Gastrointest. Liver Physiol. *282*, G919-925.

Schofield, G.C. (1960). Experimental Studies on the Innervation of the Mucous Membrane of the Gut. Brain *83*, 490–514.

Schreiber, D., Klotz, M., Laures, K., Clasohm, J., Bischof, M., and Schäfer, K.-H. (2014). The mesenterially perfused rat small intestine: A versatile approach for pharmacological testings. Ann. Anat. Anat. Anz. Off. Organ Anat. Ges. *196*, 158–166.

Seidl, H., Schmidt, T., Gundling, F., and Pfeiffer, A. (2013). The effect of osmolarity and caloric load on small bowel motility: The effect of osmolarity and caloric load on small bowel motility. Neurogastroenterol. Motil. *25*, e11–e16.

Sharif Naeini, R., Witty, M.-F., Séguéla, P., and Bourque, C.W. (2006). An N-terminal variant of Trpv1 channel is required for osmosensory transduction. Nat. Neurosci. *9*, 93–98.

Shimizu, H., Koizumi, O., and Fujisawa, T. (2004). Three digestive movements in Hydra regulated by the diffuse nerve net in the body column. J. Comp. Physiol. A *190*.

Silverman, A.J., and Zimmerman, E.A. (1983). Magnocellular Neurosecretory System. Annu. Rev. Neurosci. *6*, 357–380.

Sperelakis, N. (2012). Cell physiology sourcebook: essentials of membrance biophysics. Cell Physiol. Sourceb. Essent. Membr. Biophys.

Stach, W. (1981). [The neuronal organization of the plexus myentericus (Auerbach) in the small intestine of the pig. II. Typ II-neurone (author's transl)]. Z. Mikrosk. Anat. Forsch. *95*, 161–182.

Strange, K., and Jackson, P.S. (1995). Swelling-activated organic osmolyte efflux: a new role for anion channels. Kidney Int. *48*, 994–1003.

Strotmann, R., Harteneck, C., Nunnenmacher, K., Schultz, G., and Plant, T.D. (2000). OTRPC4, a nonselective cation channel that confers sensitivity to extracellular osmolarity. Nat Cell Biol *2*, 695–702.

Thi, M.M., Spray, D.C., and Hanani, M. (2008). Aquaporin-4 water channels in enteric neurons. J. Neurosci. Res. *86*, 448–456.

Thorneloe, K.S., Sulpizio, A.C., Lin, Z., Figueroa, D.J., Clouse, A.K., McCafferty, G.P., Chendrimada, T.P., Lashinger, E.S.R., Gordon, E., Evans, L., et al. (2008). N-((1S)-1-{[4-((2S)-2-{[(2,4-dichlorophenyl)sulfonyl]amino}-3-hydroxypropanoyl)-1-piperazinyl]carbonyl}-3-methylbutyl)-1-benzothiophene-2-carboxamide (GSK1016790A), a novel and potent transient receptor potential vanilloid 4 channel agonist induces urinary bladder contraction and hyperactivity: Part I. J. Pharmacol. Exp. Ther. *326*, 432–442.

Tian, W. (2004). Renal expression of osmotically responsive cation channel TRPV4 is restricted to water-impermeant nephron segments. AJP Ren. Physiol. *287*, F17–F24.

Toft-Bertelsen, T.L., Križaj, D., and MacAulay, N. (2017). When size matters: transient receptor potential vanilloid 4 channel as a volume-sensor rather than an osmo-sensor: TRPV4 and volume-sensing. J. Physiol.

Trendelenburg, P. (1917). Physiologische und Pharmakologische Versuhe über die Dünndarmperistaltik. Arch. Für Exp. Pathol. Pharmakol. 55–129.

Uhlén, M., Fagerberg, L., Hallström, B.M., Lindskog, C., Oksvold, P., Mardinoglu, A., Sivertsson, Å., Kampf, C., Sjöstedt, E., Asplund, A., et al. (2015). Proteomics. Tissue-based map of the human proteome. Science *347*, 1260419.

Vallet, P.G., and Baertschi, A.J. (1982). Spinal afferents for peripheral osmoreceptors in the rat. Brain Res. *239*, 271–274.

Vanden Berghe, P., Bisschops, R., and Tack, J. (2001). Imaging of neuronal activity in the gut. Curr. Opin. Pharmacol. *1*, 563–567.

Vilceanu, D., and Stucky, C.L. (2010). TRPA1 mediates mechanical currents in the plasma membrane of mouse sensory neurons. PloS One *5*, e12177.

Vriens, J., Watanabe, H., Janssens, A., Droogmans, G., Voets, T., and Nilius, B. (2004). Cell swelling, heat, and chemical agonists use distinct pathways for the activation of the cation channel TRPV4. Proc. Natl. Acad. Sci. U. S. A. *101*, 396–401.

Vriens, J., Owsianik, G., Fisslthaler, B., Suzuki, M., Janssens, A., Voets, T., Morisseau, C., Hammock, B.D., Flemig, I., Busse, R., et al. (2005). Modulation of the Ca2 Permeable Cation Channel TRPV4 by Cytochrome P450 Epoxygenases in Vascular Endothelium. Circ. Res. *97*, 908–915.

Watanabe, H., Vriens, J., Prenen, J., Droogmans, G., Voets, T., and Nilius, B. (2003). Anandamide and arachidonic acid use epoxyeicosatrienoic acids to activate TRPV4 channels. Nature *424*, 434–438.

Willette, R.N., Bao, W., Nerurkar, S., Yue, T.-L., Doe, C.P., Stankus, G., Turner, G.H., Ju, H., Thomas, H., Fishman, C.E., et al. (2008). Systemic activation of the transient receptor potential vanilloid subtype 4 channel causes endothelial failure and circulatory collapse: Part 2. J. Pharmacol. Exp. Ther. *326*, 443–452.

Xia, Y., Fu, Z., Hu, J., Huang, C., Paudel, O., Cai, S., Liedtke, W., and Sham, J.S.K. (2013a). TRPV4 channel contributes to serotonin-induced pulmonary vasoconstriction and the enhanced vascular reactivity in chronic hypoxic pulmonary hypertension. Am. J. Physiol. Cell Physiol. *305*, C704-715.

Xia, Y., Fu, Z., Hu, J., Huang, C., Paudel, O., Cai, S., Liedtke, W., and Sham, J.S.K. (2013b). TRPV4 channel contributes to serotonin-induced pulmonary vasoconstriction and the enhanced vascular reactivity in chronic hypoxic pulmonary hypertension. AJP Cell Physiol. *305*, C704–C715.

Yancey, P.H. (2004). Compatible and counteracting solutes: protecting cells from the Dead Sea to the deep sea. Sci. Prog. *87*, 1–24.

Zaelzer, C., Hua, P., Prager-Khoutorsky, M., Ciura, S., Voisin, D.L., Liedtke, W., and Bourque, C.W. (2015). ΔN-TRPV1: A Molecular Co-detector of Body Temperature and Osmotic Stress. Cell Rep. *13*, 23–30.

Zerbe, R.L., and Robertson, G.L. (1983). Osmoregulation of thirst and vasopressin secretion in human subjects: effect of various solutes. Am. J. Physiol. *244*, E607-614.

Zhang, Z., Kindrat, A.N., Sharif-Naeini, R., and Bourque, C.W. (2007). Actin Filaments Mediate Mechanical Gating during Osmosensory Transduction in Rat Supraoptic Nucleus Neurons. J. Neurosci. *27*, 4008–4013.

LIST OF FIGURES

LIST OF TABLES

APPENDIX

Thermal cycler protocols

Table 3: PCR program for cDNA synthesis

Step	*Temperature [°C]*	*Duration [min]*
Primer annealing	25	10
Reverse transcription	42	15
Inactivation	85	5
Hold	4	∞

Table 4: PCR program for qRT-PCR

Step	*Temperature [°C]*	*Duration [min]*	*Cycles*
Initial denaturation	95	420	
Denaturation	97	10	x45
Primer annealing	53	15	
Elongation	72	20	
Melting curve	60-95	0.11°C/s	

Primer Sequences

Table 5: primer sequences used in qRT-PCR

Target	**Primer forward**	**Primer reverse**	**Product length cDNA [bp]**	**Product length gDNA [bp]**
TRPV4	AGGGTGGATGAGGTGAACTG	GGCTGGAGTTCTTGTTCAGC	178	690
β-Actin	GATCTGGCACCACACCTTTT	GGGGTGTTGAAAGTCTCGAA	138	566

All primers were produced by Eurofins MWG Operon, Ebersberg,Germany. Source of ß-actin primer sequence: (Lieu et al., 2011)

DANKSAGUNG

Zunächst möchte ich Herrn Prof. Dr. Michael Schemann dafür danken, dass ich an seinem Lehrstuhl promovieren durfte. Er hat mich stets motiviert und mir eine Vielzahl wichtiger Denkanstöße gegeben. Dabei war er jedoch auch stets neuen Ideen gegenüber aufgeschlossen.

Prof. Dr. Gemma Mazzuoli-Weber danke ich, dass sie diese Arbeit so wunderbar betreut hat und trotz Elternzeit immer die nötige Zeit für mich und dieses Projekt gefunden hat. Ich danke ihr, dass sie stets erreichbar war und sich aller kleineren und größeren Probleme, die während meiner Arbeit auftraten immer ohne zu zögern angenommen hat. Liebe Gemma, es macht nach wie vor sehr viel Spaß mit dir zusammen zu arbeiten! Ich freue mich, dass du mir so viel Vertrauen entgegenbringst und weiterhin in Hannover mit mir zusammenarbeiten willst.

Ein ganz herzlicher Dank geht an Dr. Klaus Michel. Für seine scheinbar unendliche Geduld beim Erklären technischer und physikalischer Zusammenhänge und beim Lösen von allerlei technischen Problemen, die im Laufe dieser Arbeit aufgetreten sind.

Darüber hinaus möchte ich dem gesamten Team der Humanbiologie einerseits dafür danken, dass sie mich immer bei meiner Arbeit unterstützt haben und andererseits dafür, dass sie meine Zeit in der Humanbiologie zu einem Abschnitt in meinem Leben gemacht haben, auf den ich stets gerne zurückblicken werden.

Ein herzliches Dankeschön geht auch an Prof. Dr. Martin Klingenspor, der mir es sehr unbürokratisch und kurzfristig ermöglichte, an seinem Lehrstuhl die qPCR durchzuführen. In diesem Zusammenhang möchte ich mich auch sehr herzlich bei Frau Dr. Stefanie Maurer bedanken, welche mir bei der Durchführung der qPCR mit Rat und Tat zur Seite stand und trotz ihrer zahlreichen eigenen Projekte immer die Zeit gefunden hat sich um dieses Thema zu kümmern.

Abschließend möchte ich meinen Eltern danken. Dafür, dass sie während meines Studiums und meiner Promotion stets hinter mir standen und in guten wie auch in schwierigen Zeiten an mich geglaubt, und mich unterstützt haben.

CURRICULUM VITAE

May 2017 – Present	Scientific assistant at the physiological institute of the university of veterinary medicine Hannover, foundation
2014 – Present	PhD. Candidate at the chair of Human Biology of the TUM
May 2013 – Nov 2013	Master Thesis at the chair of Human Biology of the TUM
2012 - 2013	Technische Universität München: Studies in biology (M.Sc.) Final Grade 1.7 Titel of Master Thesis: “Sensitivity of enteric neurons to hyperosmolar stimuli”
Nov. 2011 - Feb. 2012	Bachelor Thesis at the chair of Human Biology of the TU Munich
2008 - 2012	Technische Universität München: Studies in biology (B.Sc.)

PUBLICATIONS

Agnieszka Pastuła, Moritz Middelhoff, Anna Brandtner, Moritz Tobiasch, Bettina Höhl, Andreas H. Nuber, Ihsan Ekin Demir, Steffi Neupert, **Patrick Kollmann**, Gemma Mazzuoli-Weber, Michael Quante Three-Dimensional Gastrointestinal Organoid Culture in Combination with Nerves or Fibroblasts: A Method to Characterize the Gastrointestinal Stem Cell Niche. *Stem cell International 2016*
DOI:10.1155/2016/3710836

Sander JM van Wanrooij, Mira M Wouters, Lukas Van Oudenhove, Winde Vanbrabant, Stephanie Mondelaers, **Patrick Kollmann**, Florian Kreutz, Michael Schemann, Guy Boeckxstaens: Sensitivity testing in Irritable Bowel Syndrome with rectal capsaicin stimulations: role of TRPV1 upregulation and sensitization in visceral hypersensitivity? *The American Journal of Gastroenterology 2013*
DOI: 10.1038/ajg.2013.371

François Reichardt, Charlotte Baudry, Lisa Gruber, Gemma Mazzuoli, Raphaël Moriez, Christian Scherling, **Patrick Kollmann**, Hannelore Daniel, Sigrid Kisling, Dirk Haller, Michel Neunlist and Michael Schemann: Properties of myenteric neurons and mucosal functions in the distal colon of diet-induced obese mice. *The Journal of Physiology 2013*
DOI: 10.1113/jphysiol.2013.262733

EIDESSTATTLICHE ERKLÄRUNG

Ich erkläre an Eides statt, dass ich die bei der Fakultät Wissenschaftszentrum Weihenstephan für Ernährung, Landnutzung und Umwelt der TUM zur Promotionsprüfung vorgelegte Arbeit mit dem Titel:

Sensitivity of enteric neurons to osmotic stimuli

am Lehrstuhl für Humanbiologie unter der Anleitung und Betreuung durch Prof. Dr. Michael Schemann ohne sonstige Hilfe erstellt und bei der Abfassung nur die gemäß § 6 Abs. 6 und 7 Satz 2 angegebenen Hilfsmittel benutzt habe.

Ich habe keine Organisation eingeschaltet, die gegen Entgelt Betreuerinnen und Betreuer für die Anfertigung von Dissertationen sucht, oder die mir obliegenden Pflichten hinsichtlich der Prüfungsleistungen für mich ganz oder teilweise erledigt.

Ich habe die Dissertation in dieser oder ähnlicher Form in keinem anderen Prüfungsverfahren als Prüfungsleistung vorgelegt.

Die vollständige Dissertation wurde noch nicht veröffentlicht.

Ich habe den angestrebten Doktorgrad noch nicht erworben und bin nicht in einem früheren Promotionsverfahren für den angestrebten Doktorgrad endgültig gescheitert.

Die öffentlich zugängliche Promotionsordnung der TUM ist mir bekannt, insbesondere habe ich die Bedeutung von § 28 (Nichtigkeit der Promotion) und § 29 (Entzug des Doktorgrades) zur Kenntnis genommen. Ich bin mir der Konsequenzen einer falschen Eidesstattlichen Erklärung bewusst.

Mit der Aufnahme meiner personenbezogenen Daten in die Alumni-Datei der TUM bin ich einverstanden.

Hannover, den 27.06.2017 _____

Patrick Kollmann